



DARLINGe – Danube Region Leading Geothermal Energy

www.interreg-danube.eu/darlinge

D.5.1.1. Identification, ranking and characterization of potential geothermal reservoirs

March 2018

D.5.4.1. Identification, ranking and characterization of potential geothermal reservoirs

Authors: Ágnes Rotár-Szalkai (MBFSZ), Gyula Maros (MBFSZ), László Bereczki (MBFSZ), Gábor Markos (MBFSZ) Edit Babinszki (MBFSZ), László Zilahi-Sebess (MBFSZ), Ágnes Gulyás (MBFSZ), Éva Kun (MBFSZ), Teodóra Szócs(MBFSZ), Tamás Kerékgyártó (MBFSZ), Annamária Nádor (MBFSZ), László Ádám (MANNVIT), Nina Rman (GeoZS), Dušan Rajver (GeoZS), Andrej Lapanje (GeoZS), Dejan Šram (GeoZS), Tamara Marković (HGI-CGS), Ana Vranješ (FMG), Radu Fărnoaga (IGR), (IGR), Albert Baltres (IGR), Ioan Cociuba (IGR), Ștefan Olah (Terratechnik), Natalija Samardžić (FZZG), Hazim Hrvatović (FZZG), Ferid Skopljak (FZZG), Boban Jolović (GSRS) with contributions from MBFSZ, Mannvit, InnoGeo, GeoZS, LEAP, HGI-CGS, ZARA, IGR, Terratechnik, FMG, FZZG, GSRS

DARLINGe project is co-funded by the European Regional Development Fund (1612249,99 €) and by the Instrument for Pre-Accession Assistance II (534646,6 €) under Grant Agreement no DTP1-099-3.2

Content

1.	Introduction.....	1
2.	Methods for the identification of geothermal reservoirs	1
3.	Geographical setting of the project area	2
4.	Geological conditions	3
4.1.	Pre-Cenozoic basement.....	9
4.1.1.	ALCAPA	9
4.1.2.	Europe derived units	10
4.1.3.	Adria derived units	11
4.1.4.	Europe-Adria derived units	12
4.1.5.	Neotethys Ocean	13
4.1.6.	Suture	13
4.1.7.	Senon cover	14
4.2.	Cenozoic	14
5.	Hydrogeological settings	17
6.	Geothermal conditions.....	19
7.	Outlining geothermal reservoirs	29
7.1.	Reservoir types.....	29
7.2.	Geological surfaces delineating potential reservoirs	30
7.3.	Construction of the isotherm surfaces.....	40
7.3.1.	Estimated temperature values in the sedimentary basins.....	40
7.3.2.	Temperature calculation in the pre-Cenozoic basement.....	47
7.4.	Reservoir delineation	49
7.4.1.	Basin fill (BF) reservoirs	49
7.4.2.	Basement (BM) reservoirs.....	55
8.	Hydrogeochemical characterisation of the geothermal reservoirs	69
8.1.	Basin fill reservoirs	70
8.2.	Basement reservoirs.....	74
8.3.	Other thermal aquifers.....	75
8.3.1.	Pliocene and Quaternary aquifers.....	75
8.3.2.	Pre-Pannonian (older Miocene) reservoirs	75
9.	Resources assessment of geothermal reservoirs.....	76

10. Summary and conclusions..... 84

List of Tables

Table 1. The main statistical values of major chemical parameters and the total dissolved solids (TDS) according to temperature categories in the basin fill reservoirs	71
Table 2. Number of hydrogeochemical water types grouped by mean depth intervals and their 10-90% percentiles and median TDS values (83 wells).....	75
Table 3. Area of the reservoirs related to selected sub-basins (km ²).....	78
Table 4. Estimated average thickness of the BF reservoirs for the selected sub-basins (m).	79
Table 5. Estimated average effective porosity in the BF reservoirs for the evaluation areas in isotherm intervals in (V/V) units.....	80
Table 6. Estimated heat content of effective porosity in the BF reservoirs related to selected sub-basins, confidence levels at P10, P50, P90 [P].....	81
Table 7. Estimated heat content of effective porosity considering recovery factor (0.1) in the BF reservoirs related to selected sub-basins, confidence levels at P10, P50, P90 [P].....	82

List of Figures

Figure 1. The DARLINGe project area	3
Figure 2. Plate tectonic setting of the research area based on Bada (1999).....	3
Figure 3. Sketch of the basin forming phases of the Pannonian Basin (Horváth 2007)	4
Figure 4. Geodynamic reconstructions of the Mediterranean area (Csontos et al. 1992)	5
Figure 5. Geodynamic model of the Early Miocene extrusion of the ALCAPA terrane (Horváth 2007, Horváth et al. 2006)	6
Figure 6. Geodynamic model Pliocene state of the Pannonian Basin (Horváth 2007, Horváth et al. 2006).....	7
Figure 7. Geodynamic model of Quaternary to recent of the Pannonian Basin and surrounding orogens (Horváth 2007, Horváth et al. 2006) 1. European foreland with Transeuropean Suture Zone (TT); 2. Foreland molasse basin; 3. Alpean orogenic wedge on the surface; 4. Tectonic window; 5. Emerging parts of the basin; 6. Sinking parts of the basin; 7. Inactive and active volcanoes; 8. Transpressional strike slip and inactive and active throust; 9. Movement direction.	8
Figure 8. Map of thickness of Neogene sediments of the Pannonian basin and surrounding regions (Horváth et al. 2015) 1. Foredeeps; 2. Flysh belt; 3. Miocene volcanoes and approximate position of explosive centres erupting rhyolitic volcanoclasts; 4. Inner Alpine, Carpathian and Dinaric mountains; 5. Penninic windows; 6. West- and East-Vardar ophiolites; 7. Detachment and normal faults; 8. Thrusts and folded anticlines; 9. Strike-slip faults; 10. Firstorder strike-slip faults; AC = Alcapa terrane; MHFZ = Mid-Hungarian Fault Zone; TD = Tisza-Dacia terrane.....	8
Figure 9. Pre-Cenozoic basement units in the DARLINGe territory (based on Haas et al. in press)9	9
Figure 10: Change of the shorelines of the Pannonian Lake from the Late Sarmatian to the Early Pliocene. On the first map the thickness of the Sarmatian is given in metres; blue – covered by water; yellow – land) (after Magyar et al. 1999).....	15
Figure 11: Block model of a prograding shelf-system in the Pannonian Basin (after Juhász 1992)	16
Figure 12. 3D seismic section in the Algyő-region (SE Hungary), showing typical transition of the relief from the shelf toward the basin (Magyar 2010)	17
Figure 13. Cross-sections with groundwater flow paths characteristic of the regional groundwater flow systems in the western part of the Pannonian Basin (Tóth et al. 2016).....	18
Figure 14. Heat flow map of the Pannonian Basin (Lenkey et al. 2002)	20
Figure 15. Geothermal areas in Bosnia and Hezegovina (Miošić et al. 2013).....	22
Figure 16. Geothermal potential of Croatia (modified after EIHP, 1998)	23
Figure 17. Known geothermal resources of Croatia (Živković et al., 2016).....	23
Figure 18. Thermal water utilization in Hungary (Nádor et al. in press).....	24
Figure 19. Geothermal map of Romania (adapted after Veliciu et al., 1985).....	25
Figure 20. Map of geothermal resources of Serbia (Milivojevic, 2001)	27
Figure 21. Main types of utilization for direct use in Slovenia (Rajver et al., 2016)	28
Figure 22. Schematic view of reservoir types.....	30
Figure 23. The depth horizon of the pre-Cenozoic basement formations (BM top)	33

Figure 24. The depth horizon of the bottom of the nearshore sandy succession deposited in the Pannonian Lake (BF bottom).....	33
Figure 25. The depth horizon between the Pannonian Lake deposits and Quaternary terrestrial sequences (BF top)	34
Figure 26. Index map of the geological cross-sections in the project area	34
Figure 27. Section 1 in Slovenia–Croatia	35
Figure 28. Section 2 in Hungary–Croatia–Bosnia-Herzegovina.....	36
Figure 29. Section 3 in Hungary–Serbia.....	37
Figure 30. Section 4 in Serbia–Hungary.....	38
Figure 31. Section 5 in Romania	39
Figure 32. Lithospheric cross-section of the central CPR before the Miocene extension (~20 Ma), immediately after the extension in the Late Miocene (~10 Ma) and in the post extensional (thermal relaxation) stage in the Pliocene (~5 Ma) (Kovács et al 2012).....	41
Figure 33. Theoretical scheme of isostatic sinking (A) and the crust fragmentation due to asthenosphere movement (B)	42
Figure 34. Temperature vs. depth and basin depth	43
Figure 35. Calculated 30 °C isotherm surface in the Neogene sediments	44
Figure 36. Calculated 50 °C isotherm surface in the Neogene sediments	44
Figure 37. Calculated 75 °C isotherm surface in the Neogene sediments	45
Figure 38. Calculated 100 °C isotherm surface in the Neogene sediments.....	45
Figure 39. Calculated 125 °C isotherm surface in the Neogene sediments.....	46
Figure 40. Calculated 150 °C isotherm surface in the Neogene sediments.....	46
Figure 41. Comparison of 50 °C isotherm surface to calculated depth of 50 °C value from measured temperature values in wells.....	47
Figure 42. Geothermal potential map of the basement reservoirs Comparison of the temperature estimated (by the conductive model) at the top of the basement to the measured temperature values which was extrapolated to the top of the basement	48
Figure 43. Top surface of the low temperature Quaternary potential geothermal reservoirs	50
Figure 44. Bottom surface of low temperature Quaternary potential geothermal reservoirs.....	50
Figure 45. Top surface of the BF30-50 reservoir	51
Figure 46. Bottom surface of the BF30-50 reservoir	51
Figure 47. Top surface of the BF50-75 reservoir	52
Figure 48. Bottom surface of the BF50-75 reservoir	52
Figure 49. Top surface of the BF75-100 reservoir	53
Figure 50. Bottom surface of the BF75-100 reservoir	53
Figure 51. Top surface of the BF100-125 reservoir.....	54
Figure 52. Bottom surface of the BF100-125 reservoir.....	54
Figure 53. Recent analogue: Interpreted fissure network of a karstified limestone plateau in cross-sections before and after the arrival of overlying sediments. The sediments are filling the top part of the fissures, but the deeper part remains unplugged. The background picture was shot near Rjavo jezero (Brown Lake) in Triglav Lakes Valley, Slovenia.	56
Figure 54. Simplified geological model of a basement reservoir characterized by increased porosity. The top part of crystalline rock was exposed to weathering, while the top part of limestone layer was karstified prior to the deposition of overlying sediments. The sub-vertical fractures within the basement are likely conductive, if they are not perpendicular on maximum stress. The upper part of the fractures, where it is bordered by fine-grained sediments, are likely	

less permeable, in those cases when faulting is approximately coeval with overlying sedimentations,. The suggested drilling targets, like faults and karstified surfaces are indicated on the figure.	57
Figure 55. View on north side of Kanin Plateau between Visoki Kanin and Prestreljenik, Slovenia. The north side of Kanin Plateau is very steep as it is depicted on the elevation profile. The loose part of wall has been eroded away in the past, and the most solid (least permeable) part of the formation is outcropping now.	58
Figure 56. Tectonic units of the pre-“Pannonian” basement in the Romanian project area (after Stănică, 1990).....	60
Figure 57. Cross-section Beba Veche – Timișoara, showing the pre-“Pannonian” basement and basin fill. For location see Figure 56.....	61
Figure 58. Structural interpretation of Battonya-Pusztaföldvár Ridge (modified after Tari et al. 1999).....	62
Figure 59. Geological map of the pre-Tertiary basement of the Pannonian basin in North Serbia according to well data. Legend: 1. Upper Cretaceous deep marine siliciclastic, carbonate and flysch formation, 2. Lower Cretaceous shallow marine and reefal formation, 3. Lower Cretaceous deep marine formation, 4. Upper Jurassic and Lower Cretaceous deep basin formation, 5. Jurassic and Lower Cretaceous deep marine formation, 6. Middle and upper Jurassic deep basin formation, 7. Lower Jurassic deep marine formation, 8. Middle and upper Triassic deep marine formations, 9. Upper Triassic platform carbonate, 10. Middle Triassic shallow marine formation, 11. Lower Triassic shallow marine siliciclastic carbonate, evaporite, 12. Carboniferous and Permian shallow marine formations, 13. Serpentinite, 14. Gabbro, 15. Basalt, 16. Rhyolite, 17. Granite, granodiorite, 18. Migmatite, 19. Crystalline schist in general. Source: Kemenci & Čanović, 1997.	63
Figure 60. Simplified pre-Cenozoic basement map of east side of Slovenia, after Rajver et al. (2015).....	64
Figure 61. Pre-Tertiary basement map of Bosnia and Hercegovina.....	65
Figure 62. Geological cross section of Dinarides (Tari, 2002)	66
Figure 63. Pre-Tertiary basement map of Croatia. Source: Pamić & Lanphere, 1991; Haas et al. 2000.	67
Figure 64. Pre-Tertiary basement map of Hungary (after Haas et al. 2010)	68
Figure 65. Location of hydro-geochemical data	70
Figure 66. The concentration distribution of some major chemical parameters and the TDS values (with their median values) shown in Box&Whiskers diagrams characteristic for the thermal waters of the 30 – 50 °C temperature range of the Upper Pannonian basin fill reservoirs	72
Figure 67. The concentration distribution of some major chemical parameters and the TDS values (with their median values) shown in Box&Whiskers diagrams characteristic for the thermal waters of the 50 – 75 °C temperature range of the Upper Pannonian basin fill reservoirs	72
Figure 68. The concentration distribution of some major chemical parameters and the TDS values (with their median values) shown in Box&Whiskers diagrams characteristic for the thermal waters of the 75 – 100 °C temperature range of the Upper Pannonian basin fill reservoirs	73
Figure 69. The concentration distribution of some major chemical parameters and the TDS values (with their median values) shown in Box&Whiskers diagrams characteristic of the	

thermal waters of the 100 – 125 °C temperature range of the Upper Pannonian basin fill reservoirs	74
Figure 70. Regions of resources estimation.....	77
Figure 71. Distribution the estimated heat content by Monte Carlo method for Drava Basin (region 3).....	83
Figure 72. Heat content/km ² in Drava Basin (region 3).....	83

1. Introduction

The EU energy and climate objectives, established as 2020 and 2030 targets, as well as the 2050 Energy Roadmap command a significant reduction in energy consumption and moving towards the decarbonisation of the energy sector, in which renewables have a key role. The more efficient use of the already existing geothermal applications is an important contribution to these targets.

The main objective of the DARLINGe project is to enhance the sustainable and energy-efficient use of the still untapped deep geothermal energy resources in the central and south-eastern part of the Danube Region (HU, SLO, SRB, HR, BH, RO). This fully tackles the challenge of increasing the security of supply and decarbonisation of the heating sector in the Danube Region.

In order to achieve the project objectives of increasing geothermal energy in the heating sector, a holistic approach of identifying and characterizing the main geothermal reservoirs of the project area was applied.

A novel methodology of outlining and characterizing large transboundary geothermal reservoirs based on harmonized geological, geothermal and hydrogeological data, maps and models from six project partner countries has been elaborated. The reservoirs were also characterized with regard to their lithology, main porosity types, temperatures and chemistry of the stored fluids. Furthermore their geothermal resources has been estimated based on a probabilistic method. These results are presented in this report.

Much of the large geothermal aquifers of this deep sedimentary basin, determined by regional geological structures, are shared by neighbouring countries and a significant basin-scale cross-border groundwater flow occurs (Nádor et al. 2013, Rman et al. 2015, Szócs et al. 2015). Development of this harmonized methodology allows identifying transboundary geothermal reservoirs to serve as a basis for further estimations of the existing geothermal potentials and resources in a transnational scale, in order to distinguish between prosperous and non-prosperous regions and for sustainable management of geothermal resources.

2. Methods for the identification of geothermal reservoirs

The basic types of geothermal aquifers are well known in the Pannonian basin (Almási 2001, Horváth et al. 2015, Lenkey et al. 2017, Rotár-Szalkai et al. 2017, Tóth and Almási 2001, Tóth 2009, Tóth et al. 2016). There is relatively detailed information available on their regional, cross-border extension at the western part of the Pannonian basin, whereas less data are known from the south-eastern regions. Large-scale geothermal reservoirs from these south-eastern parts have not been outlined and characterized yet in a uniform way considering aspects such as potential future uses, their depths, temperatures, chemistry of stored fluids, etc.

Identifying geothermal reservoirs of the DARLINGe project region was based on available geological, hydrogeological and geothermal information. Both the content and the data format largely varied in the partner countries. In addition to these differences at national scales, the density of the available information and the level of knowledge of the geological and hydrothermal systems were significantly diverse in the different regions. Due to these large

differences, it was not possible to harmonize the source data and create unified basic geological-hydrogeological-geothermal maps from scratch. Therefore, after some simplification and generalization, a new approach was applied for reservoir delineation. The developed uniform methodology was based on the common geological, hydrogeological and geothermal features which are typical for the Pannonian Basin.

The first step was to identify the most important geothermal reservoir types, where the lithology and type of porosity was taken into consideration. Utilization aspects were also important, therefore, reservoirs related to different temperature categories were distinguished. For assigning the main thermal aquifer formations, different geological horizons as boundary surfaces of these reservoirs were constructed, and simplified geological-hydrogeological cross-sections were also edited. Characterization of the temperature distribution of the basin fill sediments was carried out by creating different isotherm surfaces, and a geothermal potential map of the basement formations was created.

Delineation of geothermal reservoirs was based on the combination of the new harmonized geological and isotherm maps and surfaces. According to the project partners' agreement, groundwater exceeding 30 °C was considered as thermal water.

3. Geographical setting of the project area

The investigated area covers the central and south-eastern part of the Danube Region, encompassing southern Hungary (south-Transdanubia and southern part of the Great Plain), north-eastern Slovenia (Pomurje and Podravje), northern Croatia (Međimurje, Hrvatsko zagorje, Podravina, Posavina, Moslavina, Slavonia), western Republika Srpska and the central and northern parts of Bosnia-Herzegovina, northern Serbia (Vojvodina) and western Romania (Crisana and Banat), altogether 99,372 km². In geological-geographical terms the project area is found at the southern part of the Pannonian Basin, bordered by the Dinarides in the west, the Apuseni Mountains and the Southern-Carpathians in the east, whilst the Mecsek Mountains and the Zala-Hills constitute the north-western boundary (Figure 1). In the north-eastern part the project area has a continuous transition into the Great Hungarian Plain. Lowlands make up the bulk of the region, but in some places lowland regions are separated by hilly territories and smaller inselbergs (island-hills) (Fruška Gora and the Vršac Mountains in Serbia, the Villány mountains in Hungary, Medvednica, Strahinjščica, Ivanščica, Kalnik, Bilogora, Požeška Gora, Psunj, Papuk, Krndija and Dilj in Croatia).



Figure 1. The DARINGe project area

4. Geological conditions

The research area was formed by the currently active global tectonic processes that evolved the Pannonian Basin inside the Alp-Carpathians and the orogenic zones of Dinarides. Therefore, dealing with a southern area of the basin, it is important to review the structure and development of the entire Pannonian Basin (Figure 2) to understand the genetics of the research area.

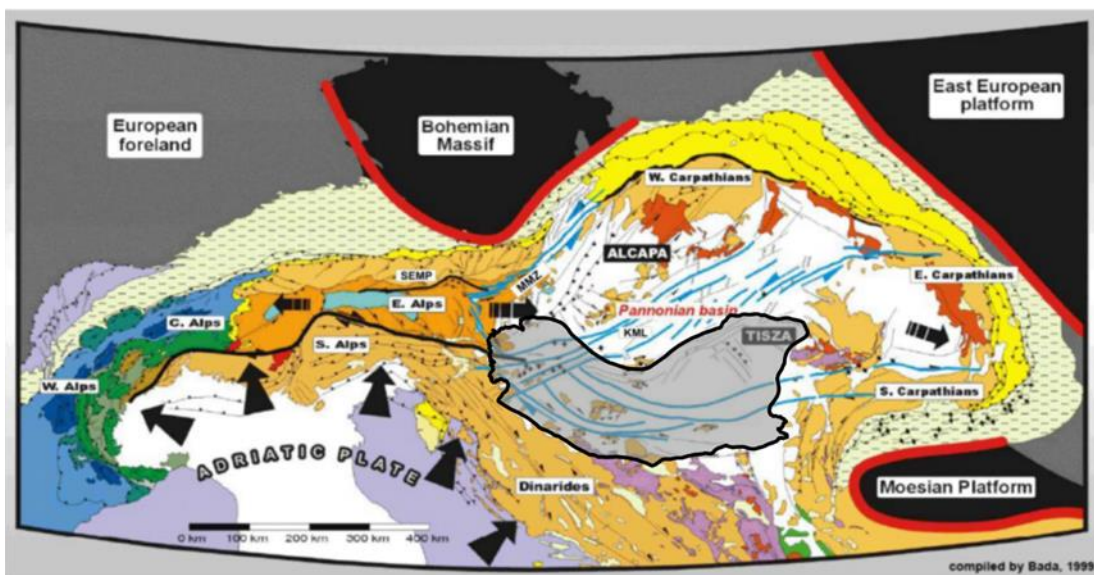


Figure 2. Plate tectonic setting of the research area based on Bada (1999)

The Pannonian Basin is a back-arc basin, its formation occurred in the northern stripe of the Alpine Tethys. The current structural aspect of the basin represents mainly extensional features and renewed elements. The basin's evolution is explained by the thermomechanical model of McKenzie (McKenzie 1978; Royden & Horváth 1988). Accordingly, development of the Pannonian Basin can be divided into two main consecutive phases: the tectonically more active syn-rift, and the following thermally controlled post-rift phase of long subsidence and sediment accumulation (Horváth 2007, Figure 3.).

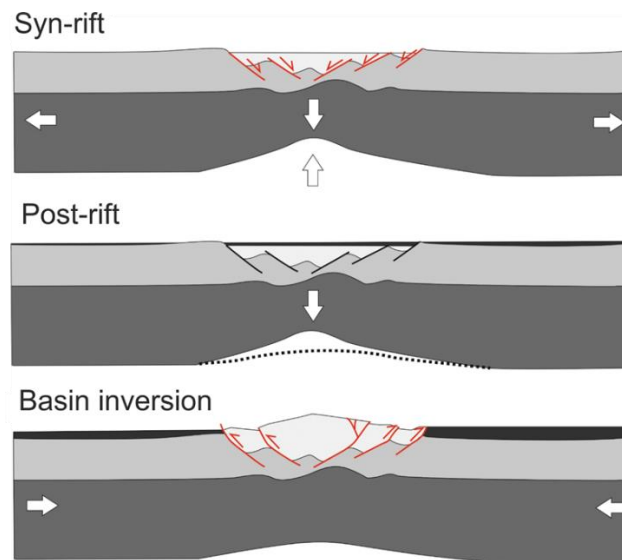


Figure 3. Sketch of the basin forming phases of the Pannonian Basin (Horváth 2007)

The formation of the basin began in the late Oligocene - early Miocene (Tari et al. 1993) and it opened in the post-genetic extension of the collision zone between African and European plates (Royden 1988). The consequence of this is the extrusion of the Pannonian basin's basement to the NE direction, and its two main tectonic components are the "pressure" of the Alpine compression tectonics and the "rollback" extension of the Magura Ocean subduction (Csontos et al. 1992; Csontos 1995). The two mega units which create the basement of the basin, the ALCAPA and the Tisa-Dacia were docked in their current position in Sarmatian, while counter-rotating each other (Balla 1984). Based on paleomagnetic measurements, the ALCAPA unit rotated counter-clockwise about 100°, while the Tisa-Dacia unit rotated clockwise about 80° (Márton & Fodor 1995, 2003; Márton et al. 2007). At the border of the two mega units the Central-Hungarian Fault Zone is located with the E-W direction normal fault and dextral strike-slip faults (Csontos et al. 1992) (Figure 4).

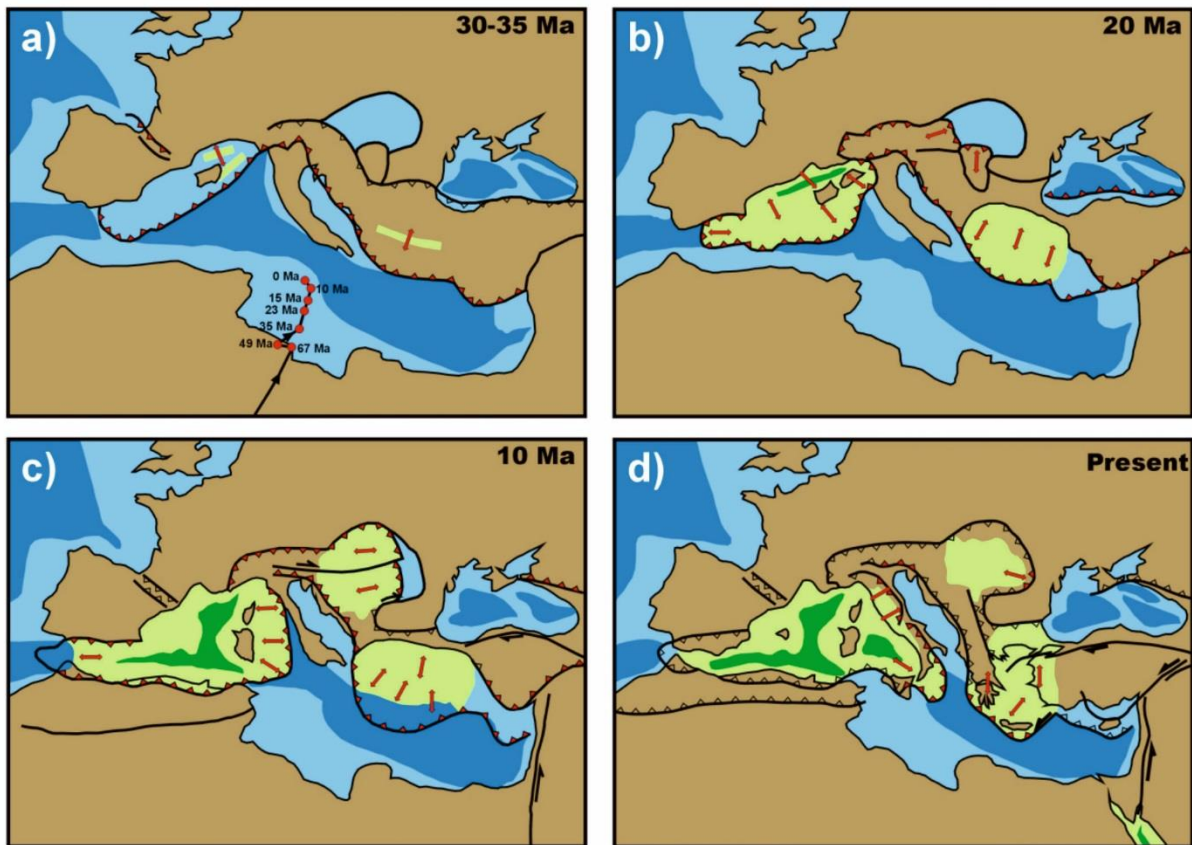


Figure 4. Geodynamic reconstructions of the Mediterranean area (Csonotos et al. 1992)

During the initial part of the basin development, the extension and thinning of the lithosphere occurred (Figure 5). Isostatic compensation due to the thinning of the crust is the reason for both simultaneous and subsequent subsidence (Royden & Keen 1980, Sclater et al. 1980). In the Pannonian Basin, the beginning of the syn-rift phase is dated to sediment formation and volcanism from the early Miocene (Eggenburgian-Ottnangian), its main phase was in the middle Miocene (Badenian) and the end of the phase is dated to the end of Sarmatian (Royden & Horváth 1988, Horváth et al., 1988), although the extension shows unclear spatial distribution differences from SW to E-NE, and according to some interpretations this continued in the Pannonian (Balázs et al. 2016). The basin-forming extension is called “wide rift” which is also associated with the development of metamorphic core complexes in the rim of the area (Horváth 2007). During the thermal subsidence large amounts of sediments accumulated and deep sub-basins evolved during Carpathian and Badenian (Fodor et al. 1999, Hámor et al. 2001). This type of area included the Drava-, the Sava-, the Zagyva Basins and the other sub-basins in the vicinity of the Mid-Hungarian Shear Zone, as well as each half graben of the Great Hungarian Plain (Horváth 2007).

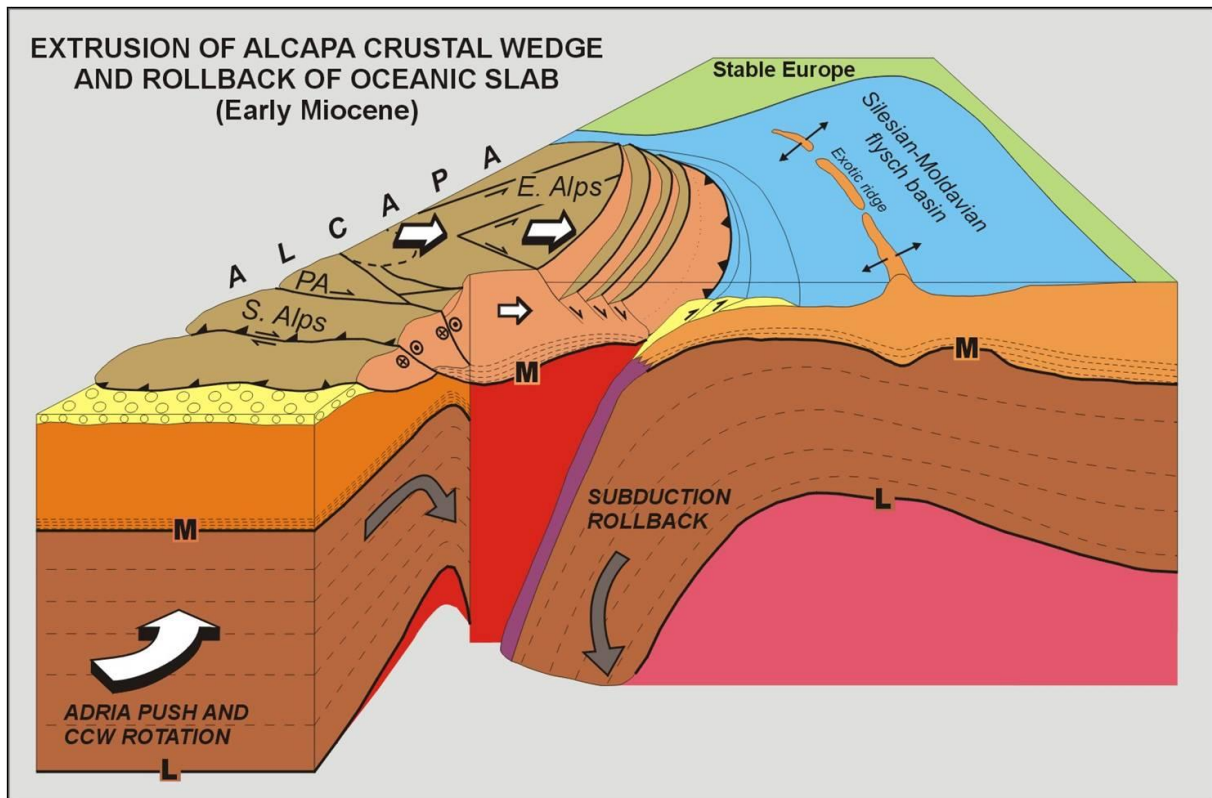


Figure 5. Geodynamic model of the Early Miocene extrusion of the ALCAPA terrane (Horváth 2007, Horváth et al. 2006)

In the early Miocene, the Tisa-Dacia unit was adjacent to the ALCAPA in the syn-rift phase, but they moved to the East Carpathians at different extent. Although there was a longer oceanic lithosphere section in front of ALCAPA, it reached faster the eastern European foreground which was incapable of subduction. This event occurred at the end of the rifting process and it led to the rapid inversion event approx. 11 to 12 million years ago. The same happened to the Tisa-Dacia unit with 1-2 million years delay. This is the post-Sarmatian tectonic inversion, and it has been observed in several areas of the pre- and syn-rift sediment uplifts and the lower Pannonian and Sarmatian disconformity, as well as it has been shown in the strike-slip faults of the Eastern Alps direction change.

The post-Sarmatian tectonic event ended 8 million years ago at the latest. Due to density increase resulting from the cooling, the lithosphere continued to sink, but not as intensively as during the syn-rift. The rate of sedimentation and the growth of accommodation space were reversed (Horváth et al. 1988) and alluvial sediments were deposited from NW and NE, causing the filling of the basin (Figure 6).

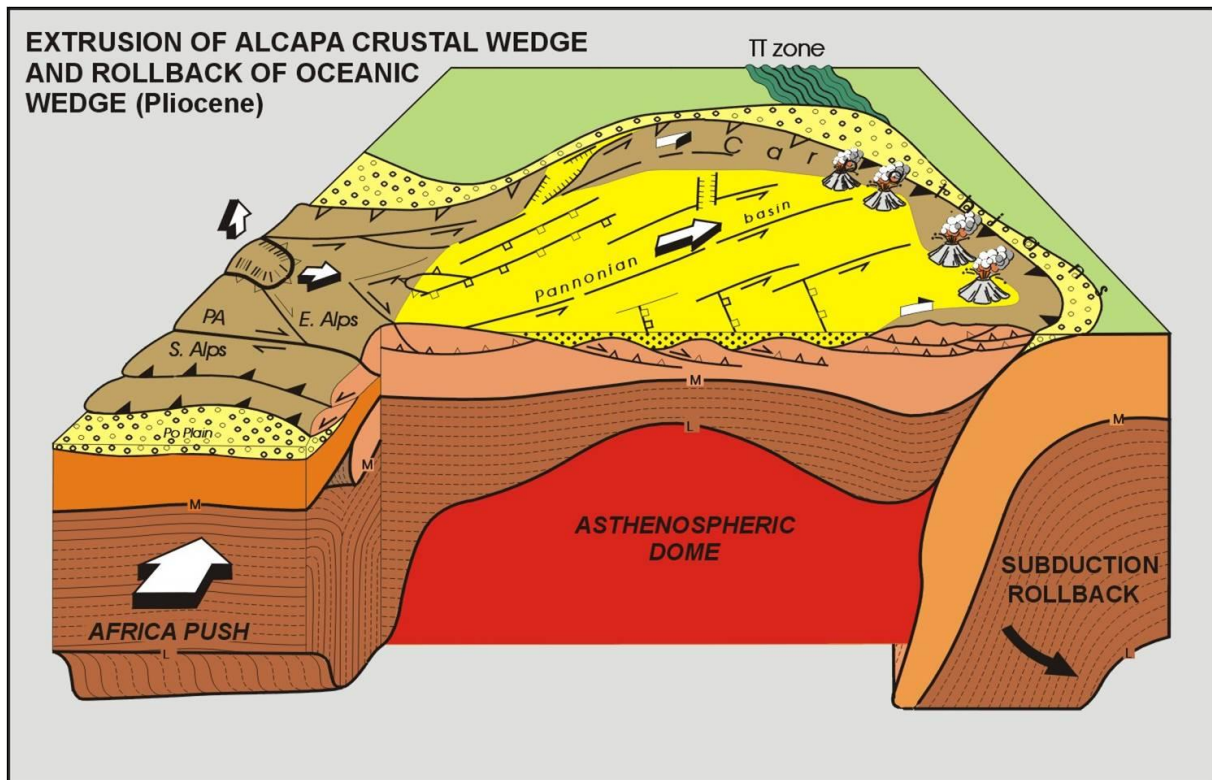


Figure 6. Geodynamic model Pliocene state of the Pannonian Basin (Horváth 2007, Horváth et al. 2006)

Though at the time of soft collision the slanted subducted plate was not able to drift considerably, it continued the deflection and its dip became nearly vertical that caused a tectonically inactive period. It happened in the beginning of Pliocene, and it was caused by a new compression phase of the Pannonian Basin.

After the continuous growing of the subduction angle, the subduction substantially stopped in the early Pliocene and the basement rocks which make up the Tisa-Dacia and the ALCAPA blocks drifted to NE with different speed. At the same time with a counter-clockwise rotation the Adria microplate made a northern pressure to the area of the basin (Handy et al. 2014).

As a result, a compression stress field occurred in the Pannonian Basin, when the late Miocene post-rift phase sinking was changed to an uplift (inversion) in the highland, while sinking of deep grabens continued (Horváth & Cloeting 1996). This stress field is still active, which is confirmed by the in situ stress field surveys (Gerner et al. 1999), and space geometrical measurements (Grenerczy et al 2005) and model calculations (Bada et al. 2007) (Figure 7 and Figure 8).

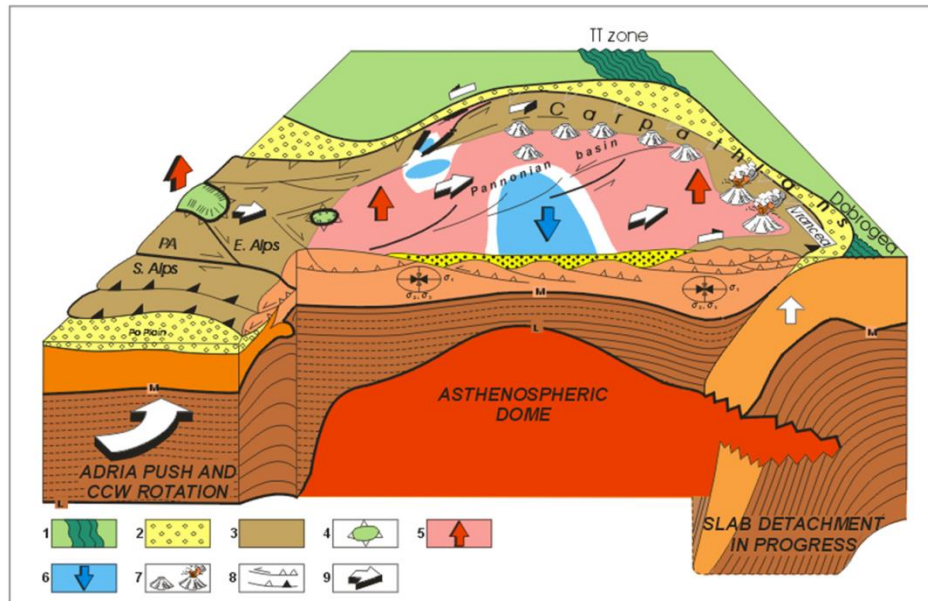


Figure 7. Geodynamic model of Quaternary to recent of the Pannonian Basin and surrounding orogens (Horváth 2007, Horváth et al. 2006)

1. European foreland with Transeuropean Suture Zone (TT); 2. Foreland molasse basin; 3. Alpean orogenic wedge on the surface; 4. Tectonic window; 5. Emerging parts of the basin; 6. Sinking parts of the basin; 7. Inactive and active volcanoes; 8. Transpressional strike slip and inactive and active thrust; 9. Movement direction.

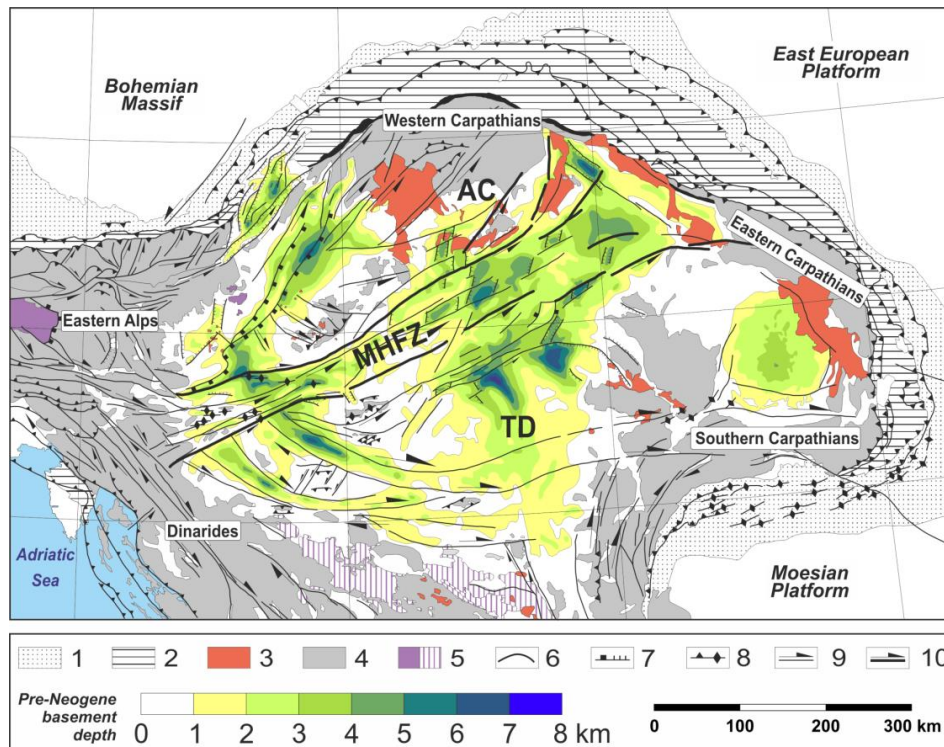


Figure 8. Map of thickness of Neogene sediments of the Pannonian basin and surrounding regions (Horváth et al. 2015)

1. Foredeeps; 2. Flysch belt; 3. Miocene volcanoes and approximate position of explosive centres erupting rhyolitic volcanoclasts; 4. Inner Alpine, Carpathian and Dinaric mountains; 5. Penninic windows; 6. West- and East-Vardar ophiolites; 7. Detachment and normal faults; 8. Thrusts and folded anticlines; 9. Strike-slip faults; 10. First order strike-slip faults; AC = Alcapa terrane; MHFZ = Mid-Hungarian Fault Zone; TD = Tisza-Dacia terrane.

4.1. Pre-Cenozoic basement

In the following we add a short description of the pre-Cenozoic basement units grouped by its plate tectonic origin (Figure 9). These units built up the basement (BM) reservoir beneath its top horizon (BM top horizon).

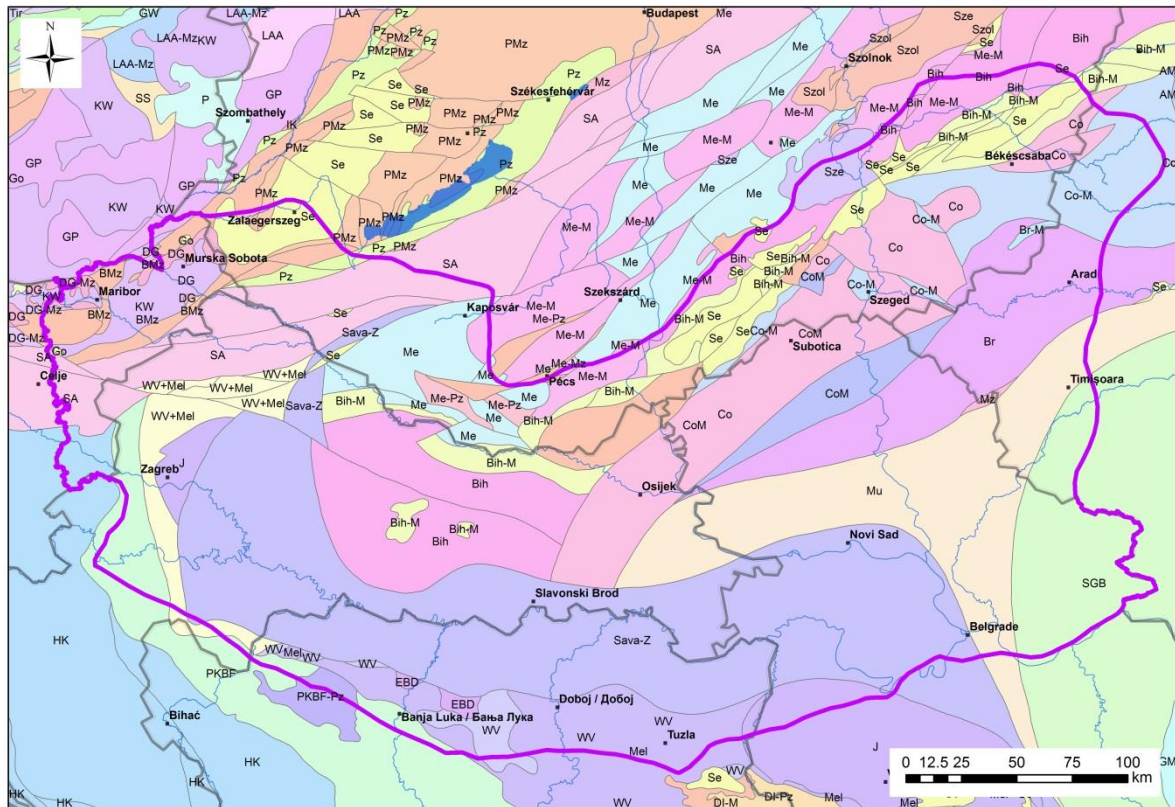


Figure 9. Pre-Cenozoic basement units in the DARDINGE territory (based on Haas et al. in press) (The abbreviations of geological units see further in the 4.1.1. chapter)

4.1.1. ALCAPA

Description of the Austroalpine basement nappes and cover:

GP – Graz Paleozoic: The Graz Paleozoic is an exposed basement unit of the Upper Austroalpine system. It crops out north and west of Graz and then sinks below the Neogene sediments of the Styrian basin. It forms a complex pile of nappes with different lithostratigraphic and metamorphic styles. Three major nappes can be recognised. All nappes contain thick Devonian sequences which evolved from the Silurian and more condensed Carboniferous layers of two facies groups. They are unconformably overlain by Gosau sediments.

DG – Drauzug, Gurktal: The Upper Austroalpine Unit has a weakly metamorphosed Variscan basement that is overlain by a nonmetamorphic Permo-Mesozoic cover. It can be correlated to the Transdanubian Range which escaped to the east along the Periadriatic-Balaton line. It comprises the block units bordered by steeply dipping faults. There are blocks of crystalline basement, Paleozoic metasediments and Permo-Mesozoic strata. On top of the Gurktal nappe there are Gosau sediments along an unconformity.

KW– Koralpe, Wölztz: It is a basement crystalline series of different metamorphic grade. No Permo-Mesozoic cover sediments are found. It crops out in the Koralpe and Pohorje Mts. The

southern part of this unit contains eclogites of Cretaceous age. The metasedimentary formations show Permo-Triassic amphibolite-, possibly Cretaceous eclogite- and subsequent amphibolite-facies overprints. This unit has a Cenozoic tectonic contact to the NE with the Transdanubian Range unit, and near the Hungarian border it forms a tectonic window. The formations of this unit show similarities to the Lower and Upper Austroalpine system. The greenschist grade metamorphic formations can be correlated with the Upper Austroalpine, and the eclogite- and amphibolite-facies metamorphic formations with the Lower Austroalpine nappes. The formations of this unit are affected by mylonitisation as well.

BMz-Ötztal-Bundschuh cover: The Upper Austroalpine Unit overlies the Koralpe-Wölztal nappes. The Prealpine basement is composed of gneiss, mica schists, amphibolites. Migmatites and eclogites also occur. Transgressive Permo-Triassic sediments are present on top of the crystalline rocks.

Transdanubian Range: Thick, Paleozoic-Mesozoic mainly sedimentary sequence represents the Southern margin of the Meliata-Maliac Ocean. Its northwestern border is a Neogene strike slip and normal fault system, which is partly a Cretaceous nappe sheet. It is the highest positioned Austroalpine nappe.

As a consequence of denudation of younger Mesozoic rock sequences, the Upper Triassic platform carbonates were exposed and karstified. By Santonian, a large sedimentary basin developed in the western side of the synform. In the northern part of depressions fluvial and lacustrine sediments were deposited. Coevally, in some sub-basins in the southeast lakes and freshwater swamps developed. As a result of the ongoing transgression, brackish-water and subsequently marine basins evolved, while the elevated ridges were colonized by rudist reefs. These platforms drowned in the middle Campanian and a pelagic basin formed.

The units' southern border is the Periadriatic-Balaton line system, acting as a strike slip zone in the Paleogene. Its recent position evolved by a complex Paleogene extrusion and Neogene extensional collapse due to the subduction related roll-back extension forces and rotations. The Periadriatic-Balaton line can be correlated in Slovenia with the Ljutomer belt consisting of Triassic formations. In the south-western part of the unit, there are metamorphites under the Paleozoic-Mesozoic system: greenschist facies Kobansko and Koralpe-Wölztal nappe system which crops out in Pohorje.

4.1.2. Europe derived units

SGB – Supra-Getic basement: It is the continental crustal thick skinned material (Dacia) that was separated from the European foreland along the Ceahlau-Severin oceanic rift, and it consists of low- to medium-grade metamorphic rocks of Late Precambrian to Cambrian, separated from each other, either by pre-Alpine thrusts, or by Triassic to Lower Cretaceous sedimentary series. The uppermost Alpine tectonic unit is the Bucovinian nappe whose Mesozoic cover series grade upward into Early Cretaceous wildflysch.

To the south, in Serbia and western Bulgaria, it also includes the structurally highest unit, referred to as Serbo-Macedonian "Massif". The Getic-Supragetic nappe sequence involves a medium- to high-grade metamorphic Neo-Proterozoic to Early Paleozoic gneissic basement and sub-greenschist to epidote-amphibolite grade Paleozoic successions. These are unconformably overlain by Late Carboniferous to Permian continental clastics and Mesozoic strata. The Mesozoic rocks contain Middle Triassic carbonate platform deposits followed by detrital Early Jurassic strata (Gresten facies). Local sedimentation ended with Middle Jurassic radiolarites, but

elsewhere it was followed by Late Jurassic to Early Cretaceous pelagic series. Post-tectonic strata begin with Albian to Cenomanian Molasse-type deposits.

BR - Biharia pre-Alpine basement. Previously it was considered as part of the Tisza Unit, however according to Schmid et al. (2008), it is part of the Dacia Unit. The rocks suffered poly-metamorphism in the Jurassic (186–156 Ma) and in Early to middle Cretaceous (124–111 Ma). Gosau-type sedimentary cover occurs in the eastern parts of the Biharia nappe system.

4.1.3. Adria derived units

SA - Southern Alps: It means South Alpine and related to South Alpine units as well. It has weakly metamorphosed Variscan basement that is overlain by a non-metamorphic Permo-Mesozoic cover. It is situated in two main territories connecting each other by tectonics, mainly strike slips. 1. SW Slovenia, South Alpine units and 2. Sheared, deformed strike slip duplexes along Mid-Hungarian Deformation Belt.

1. Located south of the Periadriatic fault. It has no Alpine metamorphism. Nappe stacking faces to the south. Variscan part is composed of Late Ordovician to Early Carboniferous sediments (Auernig strata), Permian marine shelf limestones and then Gröden redbeds, dolomites, evaporites in the Late Permian. Deposition of Lower Triassic Werfen strata are followed by strong rifting of the Meliata Ocean. A stable carbonate platform initiated after a Ladinian volcanic event. Limestones deposited in Jurassic and marls in Cretaceous.

2. It's tectonical position is between the Periadriatic-Balaton line and the Mid-Hungarian Line (former Zagreb–Zemplén Line). This Southern Alps - Karavanke related unit has a very complex build-up and represents strongly sheared and deformed strike slip duplexes of various origins. This is mirrored in the various synonyms used for this unit [Mid-Hungarian unit (Haas et al. 2000), Zagorje–Mid-Transdanubian unit (Pamić and Tomljenović 1998), Sava Composite unit (Haas et al. 2000)]. The relation to the Southern Alps is derived from correlation to the Carnic Alps, Southern Karavanke, Sava folds. This tectonic mega-melange is thought to be a junction complex of the Southern Alps, the Dinarides and the Tisa unit which incorporates Cretaceous nappes, Paleogene thrusts and strike slips, Neogene transpression and extension structures, half-grabens and pop-ups.

HK - High Karst: It is composed of Paleozoic basement, Triassic to Paleogene mainly platform carbonates.

PKBF - Pre-Karst and Bosnian Flysch: The Bosnian Flysch was deposited on the slope (margin) of the Adriatic-Dinaridic carbonate platform and on its foot. In the present structure of the Dinarides, the Bosnian Flysch is thrust by the Dinaridic Ophiolite Zone. To the southeast, the zone of passive continental formations are thrust onto the HK-External Dinarides (carbonate platform), including the Mid-Bosnian Schist Mts.

Formations of the Bosnian Flysch form a continuous zone from Slovenia, where they build up tectonic windows beneath the Sava nappe composed of Paleozoic-Triassic formations, this is called the "Slovenian trough". Bosnian Flysch occurs at Topusko, south of Zagreb, between Banja Luka and Sarajevo, and in the area of the Igman and Bjelašnica Mts. (near Sarajevo). Further south-eastward, from Bjelašnica to Gacko and northern Montenegro, they again form a continuous zone, i.e., the Durmitor flysch.

In the Bosnian Flysch, which attains a total thickness of about 3000 m, two subgroups can be distinguished which display differences in stratigraphy and lithology:

a) The older Vranduk subgroup is represented by sandy-clayish carbonate sediments, whereas the younger Ugar subgroup is largely of carbonate-marly composition. The older subgroup is Tithonian-Berriasian in age (calpionelles, tintinopsels) and it grades into mainly arenitic unit of Cenomanian-Turonian age (orbitolines, kuneolines, globigerines).

b) The «Ugar Subgroup» is a typical carbonate flysch series from the carbonate shelf margin. It ranges in age from Albian to Senonian and rarely contains Early Paleogene microfossils.

EDB – East Bosnian-Durmitor: It is a composite tectonic unit; it consists of Paleozoic and Mesozoic formations detached from the Adriatic passive margin in Cenozoic times in its basal part, and of the Western Vardar Ocean ophiolites that were obducted during the Late Jurassic to earliest Cretaceous in its upper part. An out-of-sequence thrust that post-dates the Late Jurassic obduction of the Western Vardar Ophiolitic Unit over the East-Bosnian-Durmitor Unit is also found in the hanging wall of the East Bosnian-Durmitor composite thrust nappe.

J – Jadar-Kopaonik-Bükk: this innermost thrust sheet passively carries previously obducted ophiolites of the Western Vardar Ocean. The Jadar-Kopaonik thrust sheet represents the third and innermost thrust sheet that was activated after the Late Jurassic obduction of the Western Vardar Ophiolitic Unit. The Jadar “block” consists of non-metamorphic Paleozoic basement schists that is covered by Permian Bellerophon limestones, which are followed by a Triassic succession of Lower Triassic Werfen beds, Middle-Upper Triassic carbonates (marbles), Jurassic shallow water carbonates to deep water radiolites, and finally Senonian flysch.

4.1.4. Europe-Adria derived units

Me – Mecsek: The pre-Triassic basement of the Tisa Mega-Unit consists of various Variscan high-grade metamorphic series and lower grade granites. The Permian sequence consists of terrestrial, fluvial, lacustrine sediments, while the Triassic from a Germanic Muschelkalk-type facies then coastal shallow marine siliciclastic ramp formations, pelagic marls in Lower and Middle Jurassic. A dramatic change occurred during the Bathonian, as documented in the Mecsek Unit by an increase in depositional water depths that can be related to the separation of the Tisa from the European continent, presumably in connection with the opening of the Alpine Tethys. Oxfordian marls, radiolarites, followed by Ammonitico Rosso and Calpionella Limestone, combined with the faunal characteristics indicate that the Tisa unit had now become part of the Adriatic paleogeographic realm. Valanginian to Barremian basaltic volcanic activity is present.

Bih – Villány-Bihor Massive Mid-Triassic carbonate build-ups that are overlain by a Late Triassic Keuper facies cropping out in the Villány Mountains, as well as in the North Apuseni Mountains of Romania. Units that crop out in the Papuk inselberg are also included. In the Jurassic discontinuous shallow marine carbonate deposition happened, afterwards up to the middle Cretaceous carbonate platform development took place. Coeval with the nappe formation siliciclastic marls, Senonian flysch-like sediments were deposited.

Co – Codru: The Triassic Schreyeralm-Hallstatt-type facies corresponds to the Békés-Lower Codru nappe system, but it includes also the Upper Codru nappes that are considered as part of the Biharia nappe system. The Codru nappe system mostly consists of a succession of exclusively sedimentary nappes, mostly preserved in the western parts of the North Apuseni Mountains (Codru Mountains). In the basement of the Pannonian Basin Jurassic and Lower Cretaceous marls, limestones of deeper, more distal paleoenvironment were originated.

4.1.5. Neotethys Ocean

Mel – Tectonic and sedimentary melange of Western Vardar.

WV Western Vardar ophiolite: It is a tectonical composite unit. At the lowest tectonic position there is an ophiolitic mélange. On that a high-grade metamorphic sole is found, followed by the obducted ultramafic massifs. On the top the post-obduction series, the overlapping younger strata are incorporated into this tectonic unit.

Three types of rock formations are present: metamorphic rocks, ophiolitic sequences and ophiolite melange. The metamorphites are in olistolites derived from the metamorphic sole. The ophiolites are s. str. fertile mantle rocks (lherzolites), though the harzburgites of Jurassic age occur locally as well including their overlying Jurassic radiolarites. The ophiolite melange consists of a mixture of Triassic Meliata ophiolites and Triassic radiolites. Triassic strata consist of platform carbonates, slope to basinal facies such as Hallstatt limestone, cherty limestone, thin-bedded radiolarite – pelagic limestone successions or radiolarites that are of Late Anisian to Norian age.

The ophiolitic mélange is interpreted as an accretionary prism that formed during the late emplacement stages of the obducted upper plate ophiolites.

After a period of erosion, when parts of the obducted ophiolites were removed, sedimentation locally resumed with platform carbonates and reef environment build-ups of Late Jurassic, fluvial conglomerates and sandstones in Tithonian to Berriasian. These deposits were involved in Early to mid-Cretaceous folding and thrusting, subjected to erosion and subsequently unconformably covered by the Senonian series. These series grade upward into latest Cretaceous flysch.

Mu – Mures, Eastern Vardar ophiolite: The Eastern Vardar Ophiolitic Unit in Serbia (“Central Vardar Subzone, Main Vardar Zone”) represents a piece of oceanic lithosphere, ophiolites and island arc volcanics. Following their emplacement on the Serbo-Macedonian Massif, these ophiolites were overstepped by Late Jurassic reef limestones that are succeeded by a Cretaceous flysch (“Paraflysch”).

4.1.6. Suture

Sava-Z – The suture zone between the Tisza and Dacia units and the Inner Dinarides is a belt of ophiolitic, magmatic and metamorphic rocks. The structurally lowermost unit of the Sava Zone consists of the Late Cretaceous ophiolites. Northward these Late Cretaceous ophiolites are covered by Maastrichtian to Eocene siliciclastic flysch. Still further to the north, this flysch becomes progressively metamorphic and is followed during the Late Oligocene by the intrusion of S-type granites.

Based on recent data, the Sava Zone consists of the formations as follows: 1) Cretaceous-Early Paleogene paraflysch; 2) Ophiolite mélange; 3) Late Paleogene regionally metamorphic sequences originated from the surrounding Late Cretaceous flysch; 4) Synkinematic granitoids and 5) Post-orogenic volcanics. The Sava-Zone, particularly its northern parts, are covered by Neogene sediments of the South Pannonian Basin.

a) The «Cretaceous-Early Paleogene Flysch Sequence» is composed of Early Cretaceous to Albian-Cenomanian formations, which are disconformably overlain by the Turonian-Maastrichtian-Early Paleogene turbidite. In some areas, the lower parts of the flysch are

interlayered with coeval subduction-related basalts and rhyolites intruded by comagmatic A-type granites.

b) The «Progressive Metamorphic Sequence» is composed of slate and phyllites, containing a Cretaceous/Paleogene microflora, as well as of greenschist, quartz-muscovite schist, gneisses (48-38 Ma), amphibolites and marbles, which originated under P-T conditions of very low-, low- and medium-grade metamorphism from the surrounding Cretaceous-Early Paleogene flysch formations.

c) The «Tectonized Ophiolite Mélange» which differs from the Jurassic olistostrome mélange by a higher degree of tectonization of its matrix by ophiolite fragments of Cretaceous/Early Paleogene age, and coeval limestone exotics.

d) Granitoid rocks which are represented by collisional S-type, I-type and A-type granites (55-48 Ma), which intrude into Cretaceous/Paleogene flysch. More common are Oligocene post-syn collisional I-type granites (32-28 Ma), correlative to Periadriatic tonalites, which are accompanied by contemporaneous and more abundant shoshonites and calc-alkaline volcanics.

4.1.7. Senon cover

Go – Gosau sediments and Se – Senonian sediments: Postorogenic cover of orogenic extensional collapse mentioned in case of occurrences of each unit.

4.2. Cenozoic

Subsequently to the closure of the Neotethys Ocean, tectonic uplift of the Alps started. During the Eocene, an epicontinental sea, i.e. the Paratethys evolved; it was separated from the Tethys Ocean. Its clastic and carbonate sediments can be traced from the Oligocene up to the end of the Miocene. In the course of the Miocene the uplift of the Carpathians commenced, and the continuous denudation led to an increasing sediment influx into the basin, in which initial sedimentation took place in an archipelago environment. In the late Miocene the Pannonian Basin was separated from the oceanic realm, and sedimentation took place in the Lake Pannon characterised by decreasing salinity and the gradual filling up by fine-grained sediments derived from the Alps and the Carpathians. Since at that time the basin evolution was determined by lithospheric thinning associated with thermal subsidence, thus, several kilometer-thick clastic successions accumulated in the deep basins.

The filling up of the Lake Pannon was initially the most intense from the NW: Later, deltaic environment started to develop basinwards from the NE, too (Figure 10). The rate of sediment influx into the basin from the South, i.e. from the Dinarides (made up predominantly of limestone) was much smaller. Deltaic systems prograding from the Alps and the East Carpathians reached the study area approximately 6.5–7 million years ago. The so-called Lake Paludina of freshwater facies – representing the last phase of the evolution of the Lake Pannon – became filled up about 4 million years ago.

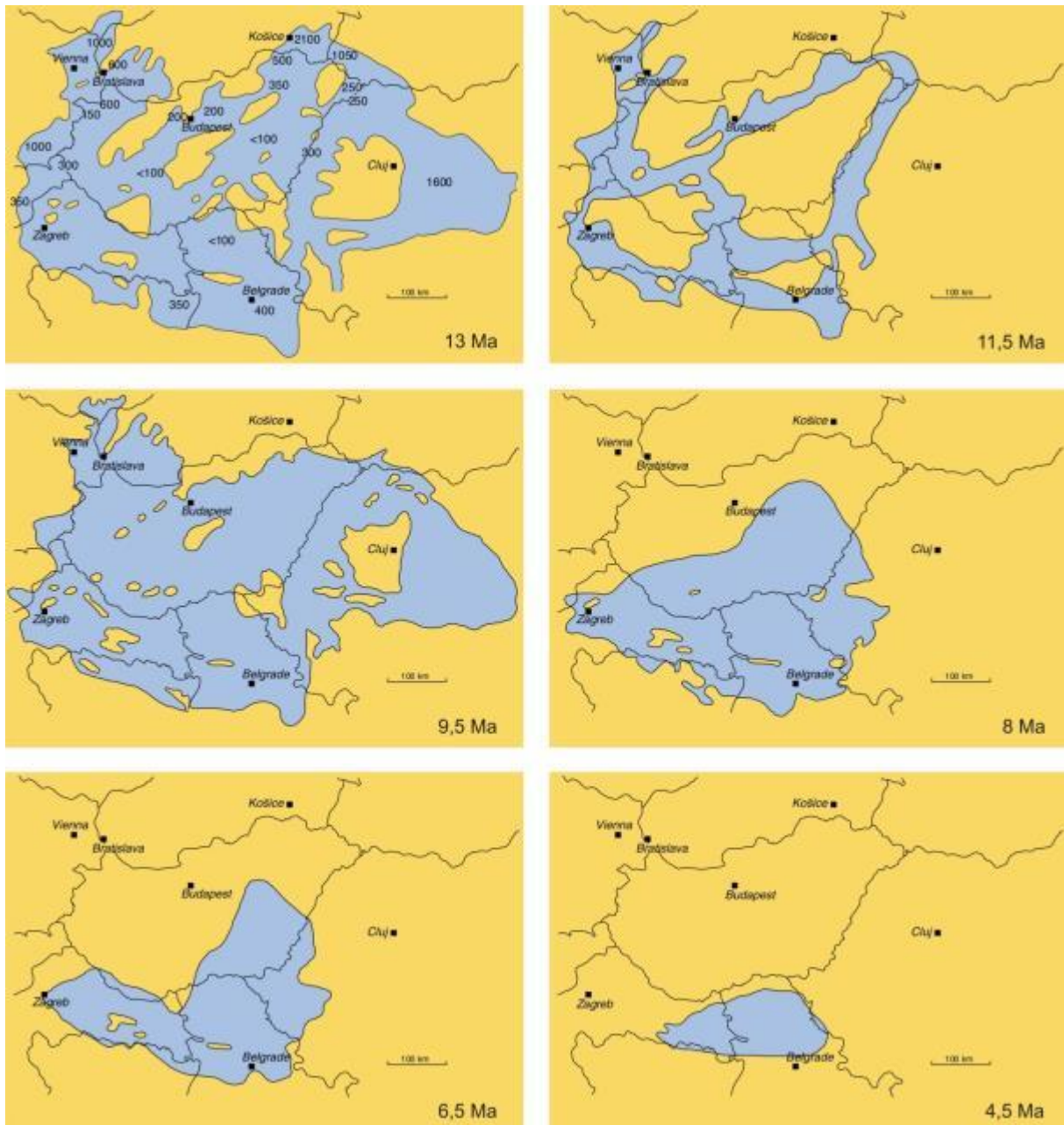


Figure 10: Change of the shorelines of the Pannonian Lake from the Late Sarmatian to the Early Pliocene. On the first map the thickness of the Sarmatian is given in metres; blue – covered by water; yellow – land) (after Magyar et al. 1999)

The nearshore environments of the Lake Pannon and the surroundings of islands were characterised by the deposition of the transgressive basal conglomerate and basal sandstone (Figure 11). Far from the sedimentary influx areas, in the innermost part of the basin the condensed succession of the so-called „basal marls” deposited; they are rich in organic matter and from a lithostratigraphic point of view they can be classified into different members. In the deep troughs these successions are much thicker. Locally, in patches, „basal conglomerate” can be found under the marls; it comprises interbeddings of varying grain size. Pebbles – derived from the islands – may reach a diameter size of even 10 cm. These interbeddings were deposited from debris flows near the foot of the slope. Upwards, the interbeddings – derived from low-density turbidity currents – are thin and comprise only silt- and sand-sized grains.

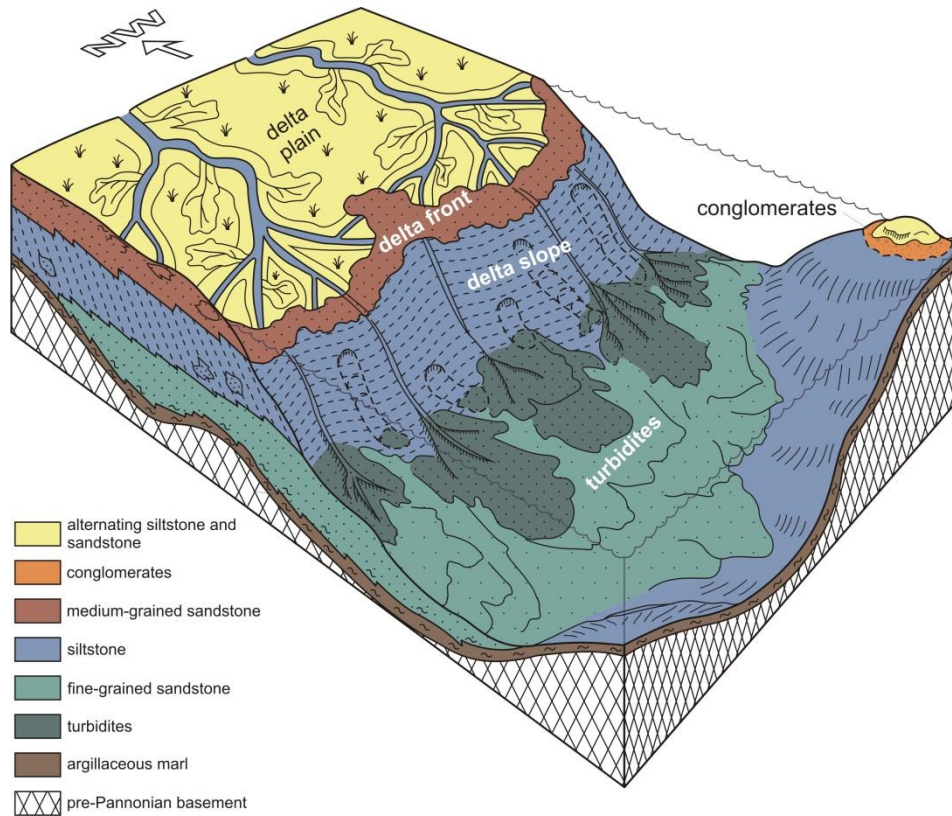


Figure 11: Block model of a prograding shelf-system in the Pannonian Basin (after Juhász 1992)

The deep-water marls are overlain by turbidite sequences made up of the alternation of fine-grained sandstone and clay marl, accumulated in the deep parts of the basin. On the elevated highs/ridges their thicknesses are not significant; however, in the area of the troughs their thicknesses are considerable, exceeding even 1000 m. They comprise upward-thickening/coarsening and then upward-thinning/fining sedimentary cycles of thicknesses of 10 to 15 m. They are arranged into larger, 150–200 m thick units, dissected by 5–10 m thick clay and laminated silt lithofacies. The 10 to 15 m thick sedimentary cycles form sand lobes and sheet-like sand bodies (of an aerial extension of some km) were fed by sediments transported in shallow-flat or wide channels, as long as the sediment supply was provided from the marginal slope. If there was a break in the sediment influx, hemipelagic clayey sediments were deposited both in the channels and in the area of the meander lobes.

The turbidites are overlain by a pelitic succession deposited on a basin slope of a considerable angle ranging from 5° to 20° (Figure 12). Since gravitational mass movements started on the slope, the deposition here was dominated by clay with small sedimentation rate. Pelitic sediments are dissected by the sand derived from slides; sandy deposits could also accumulate on the slope. On the foot of the slope a significant amount of sediments accumulated, because – besides the lobes of the considerable slides – sediments were deposited even by the dense mass movements as well. During the transportation of coarse sediments along the slope, erosion took place in smaller or larger areas. If the sand (arriving from the shelf) was not transported into the deep zones, elongated, apron-like sand accumulations came into being on the upper part of the slope.

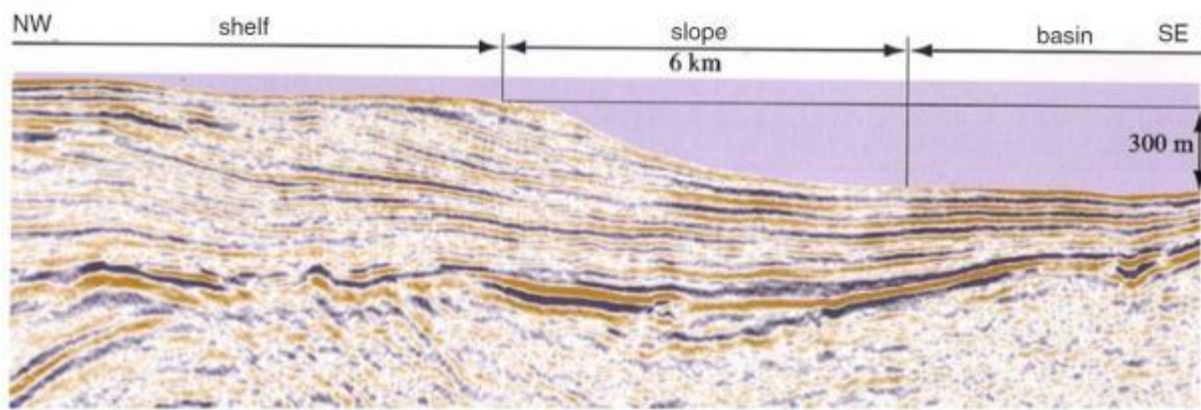


Figure 12. 3D seismic section in the Algyó-region (SE Hungary), showing typical transition of the relief from the shelf toward the basin (Magyar 2010)

The lower boundary of the main thermal water aquifer is marked by the boundary between the pelitic succession (deposited on the basin slope) and the sandy succession of nearshore environment; this boundary can be well traced throughout the basin.

Along the basin margins, sedimentation took place in nearshore environment producing predominantly shelf deposits. Sediments trapped at the mouths of rivers, or deposited in shelf-front, shelf plain and coastal plain environments are made up prevalingly of fine- and medium-grained sandstone comprising clay marl, silt – and in the upper section – paleosol and lignite interbeddings. The sandstone bodies are of channel-mouth bar, distributary channel and channel fill origin, or they are derived from lobes related to crevasse splay. The intercalating fine-grained sediments are remnants of interdistributary bays, abandoned channels and swamp–alluvial plain environments. The area of the shelf plain was characterised by an anastomosing channel system of slightly meandering channels, in which, infrequently, point bars developed along the larger channels.

In the hinterland of the prograding shelves an alluvial (i.e. fluvial - flood plain, lacustrine and paludal) sedimentation took place; a succession made up of the frequent alternation of siltstone, clay marl and sandstone was deposited. The area of the alluvial plain is characterised by meandering riverbed geometry with abandoned channels (bends), point bars and sediments' lobes.

The upper boundary of the main basin fill aquifer layer is marked by the boundary between the sandy sediments (deposited on the delta plain and alluvial plain in the end-phase of the filling up of the Lake Pannon) and the Quaternary deposits.

During the Quaternary, the SW–NE compression triggered uplift and erosion in the area of the submarine ridges, whereas intensive subsidence took place in the troughs. In the latter the thickness of the Quaternary sediments may reach even 600 to 800 m.

5. Hydrogeological settings

While the DARLINGe study area is characterised by a wide range of geological formations, two major regional hydrogeological settings can be differentiated. One is characteristic for the porous intergranular basin fill sediment sequence, while the other is for the basement rocks. Although connections between the two systems occur locally, the two regional flow systems are

mostly separated by thick, at some places even a few thousand meters, low permeable Miocene (Carpathian – Upper Miocene delta slope sequence) sediments, which act as aquitards.

The study area that is found in the Pannonian Basin is characterised by several sub-basins (eg. the Great Hungarian Plain, Mura-Zala, Drava, etc.), where the general hydrogeological features are similar to those in the basin fill sequence. Two characteristic (transboundary) cross-sections in the western part of the Pannonian Basin (Tóth et al. 2016) are shown in Figure 13.

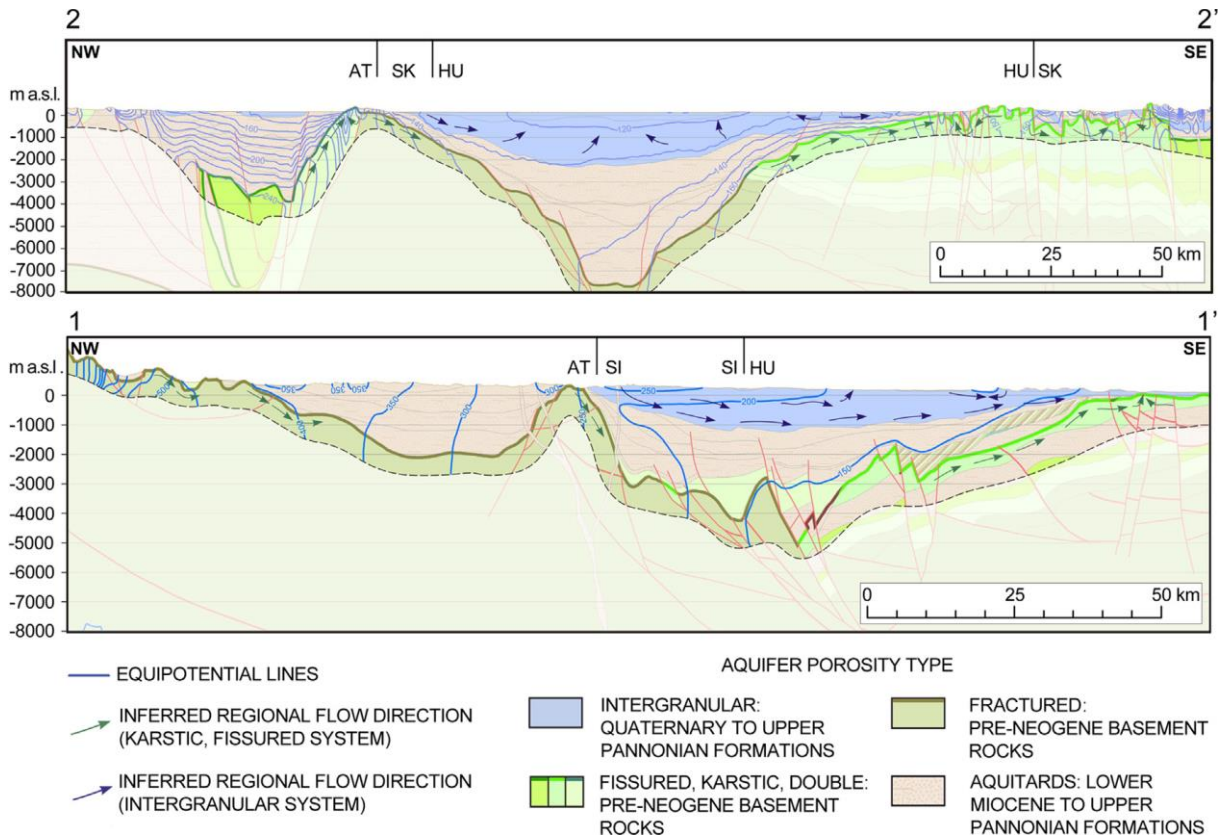


Figure 13. Cross-sections with groundwater flow paths characteristic of the regional groundwater flow systems in the western part of the Pannonian Basin (Tóth et al. 2016)

The upper part of the porous intergranular basin fill sediment sequence is characterised by local and intermediate flow systems. Local flow systems occur either at the margins of the basins or between the intermediate flow systems, often found in hilly areas. These unconfined aquifers can be found typically in the Quaternary alluvial and fluvial sediments. The intermediate flow systems are characteristic for the Quaternary formations and for the shelf plain part of the Pannonian sediments. These flow paths can reach to several hundred meters below surface, in some cases even around 1000 meters. These waters comprise the main drinking water aquifers and in general these aquifers are the source of the main freshwater production. They are mainly of Ca-Mg-HCO₃ water type, with an increasing Na content with depth and along the flow paths. In the deeper sub-basins their water type can evolve to Na-HCO₃ type. The groundwater residence times vary from a few thousand years to a few tens of thousands years, and it is very common to have fresh water abstraction deriving from Pleistocene infiltration.

The deeper part of the porous intergranular basin fill sediment sequence is characterised mainly by regional flow systems. These flow systems can be found in the lower part of the shelf front sediments. Their average depth is between 500 and 2500 meters. This sediment sequence hosts

the main geothermal aquifers which are the main source for thermal water abstraction in the whole study area. There are currently more than 700 operating thermal water wells in the DARLINGe study area, most of them can be found in the porous intergranular basin fill sediment sequence (Rman et al. 2018). Their water type is typically of Na-HCO₃, which can evolve along the flow path to Na-Cl type, especially at greater depths where the gravitational flow interferes with density and heat-driven flow components. In these areas the outflowing water temperatures can reach over 90 °C.

Groundwater flow in the basement is connected to the Palaeozoic and Mesozoic crystalline and carbonate rocks. These flows are mainly connected to the upper few hundred meters thick weathered rocks or to fractures, and to karstified zones in the carbonates. The tectonic zones and fractures can play an important role in the groundwater abstraction, however not all faults are hydrogeologically active. Some of the faults act as pathways for free convection. The fractured crystalline rocks in the basement mostly store stagnant water. Cold and thermal karst systems play an important role in the supply of drinking and thermal water respectively as they store large amounts of extractable water. Their water type is Ca-Mg-HCO₃ with relatively low TDS. Those carbonate rocks which are partly or completely isolated from the regional flow systems have a groundwater composition with even few ten thousand mg/l TDS and their Na and Cl content can increase significantly reaching even Na-Ca-HCO₃, Na-Cl-HCO₃ or Na-Cl water types. The outcrops in mountainous or hilly areas can serve as recharge areas for the different flow systems.

Local aquifers can be found in the Miocene sediments, which sometimes form a hydraulic unit with the basement rocks. Minor – thermal – aquifers with low connectivity are also developed in Miocene turbiditic sand bodies.

The groundwater compositions of the gravitational flow systems were defined by the infiltration processes, which were further modified along the flow paths due to the water-rock interaction, mixing, organic matter evolution and degradation and geothermal effects. The proximity of oil fields to some aquifers suggests the possibility of mixing with oil field waters. Previous noble gas studies indicate the presence of an active connection between the mantle and the aquifers in the Upper Miocene and Quaternary sediments in the Pannonian Basin (Bräuer et al., 2016; Palcsu et al., 2014; Szócs et al., 2017).

Cross-border flow has already been demonstrated in several parts of the Pannonian Basin (Szanyi and Kovács 2010; Szócs et al. 2013; Tóth et al. 2016). This will be further surveyed within the DARLINGe project, including the existing and potential effects of current and new thermal water abstractions.

6. Geothermal conditions

The Pannonian Basin extending across eight countries in Central and Eastern Europe is well-known of its good geothermal potential (Dövényi and Horváth 1988; Lenkey et al. 2002; Szanyi et al. 2009; Horváth et al., 2015) due to its favourable geological conditions, being rich in thermal waters. The Pannonian Basin is characterized by a positive geothermal anomaly, with heat flow density ranging from 50 to 130 mW/m² with a mean value of 90-100 mW/m² (Hurtel and Hanel 2002; Lenkey et al. 2002; Horváth et al. 2015) (Figure 14) and geothermal gradient of about 45 °C/km (Dövényi and Horváth 1988). The wide range of the HFD values is explained by the presence of recharge areas and the cooling effect of the infiltrating meteoric waters. The

overall positive geothermal character of the Pannonian Basin is related to the Early-Middle Miocene crustal extension when deep basins originated.

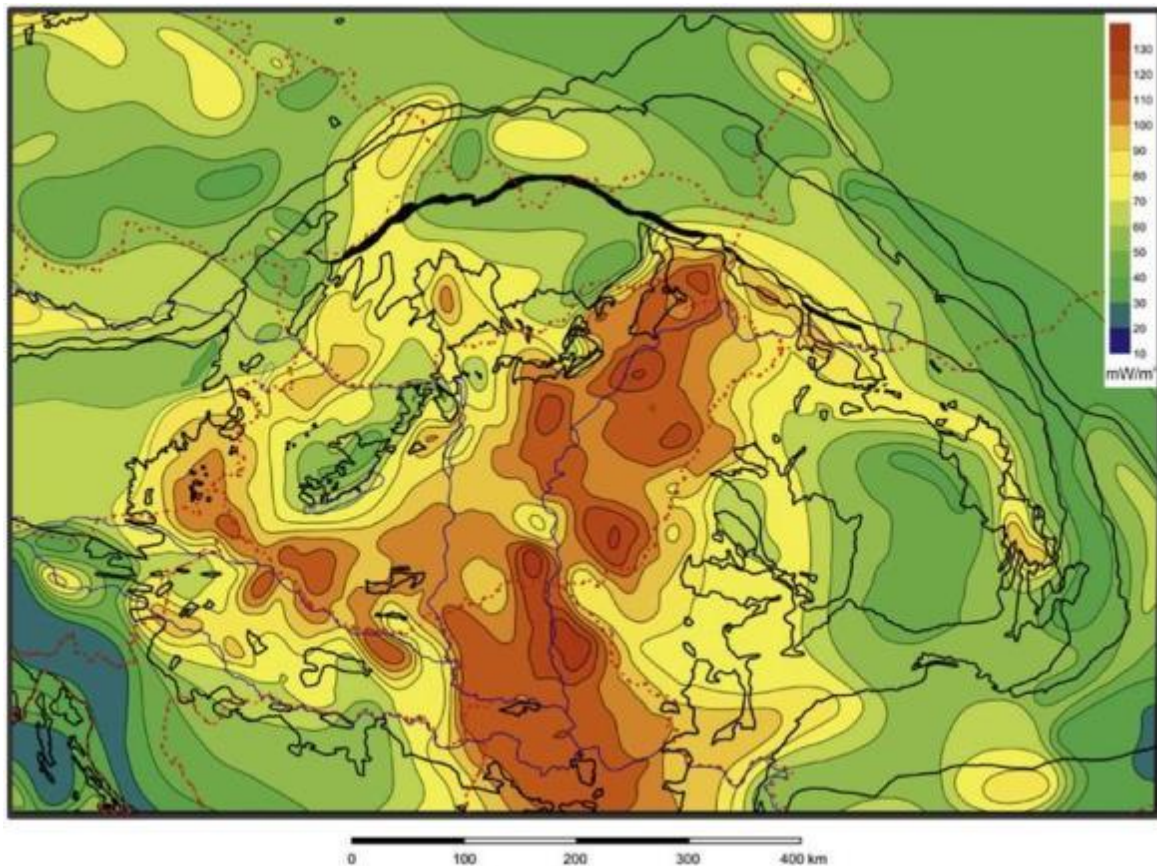


Figure 14. Heat flow map of the Pannonian Basin (Lenkey et al. 2002)

In the following we provide a brief introduction on the geothermal conditions of each partner country largely based on the “country update reports” prepared for the European Geothermal Congress 2016.

Bosnia and Herzegovina (Samardžić, Hrvatović 2016) is rich in thermal springs and geothermal potential of various origins, which is characterized by irregular distribution. The Central and northern parts – Inner Dinarides (60% of the whole territory) - have significant hydrogeothermal resources, while in the southern part - External Dinarides - there is not any indication of geothermal potential (Figure 15). From the SW to the NE the following geotectonic zones can be separated (Figure 15):

The Dinaric carbonate platform (External Dinarides) is made up of Mesozoic limestones and dolomites where there are no conditions for the formation of the geothermal systems, and the typical karstic area is rich in fresh cold waters.

The Bosnian Flysch comprises latest Jurassic to Cenozoic flysch-type deposits that vary in depositional age, where some lukewarm thermal and thermomineral waters (17 to 36 °C) are found in the Triassic limestones and dolomites. The values of the geothermal gradient and heat flow in this zone are 20-35 °C/km and 40-80 mW/m² (these values, as well as others relating to the geothermal gradient and heat flow density for Bosnia and Herzegovina are given according to Miošić and Čičić (1986)).

The Dinaride Ophiolite Zone has a complex structure, where the Triassic carbonate aquifers are sealed by intrusive, effusive and metamorphic rocks. The whole massif is tectonically dissected and it has separate occurrences of mineral, thermal, thermomineral carbon acid and hyperalkaline waters with temperatures ranging from 16 to 44 °C. The values of the geothermal gradient in this zone are 35-45 °C/km, and the heat flow of 50-100 mW/m².

The Sava-Vardar Zone also has a very complex inner structure composed of various flysch, metamorphic, ophiolite and sedimentary units, where thermal and thermomineral waters are found in Triassic limestones and dolomites, Cretaceous and Tertiary limestones and clastics covered by Tertiary seals. Aquifers with greatest yields and highest temperature are located in Semberija (Middle and Upper Triassic limestones with temperature up to 75 °C), and in Posavina (outflow temperature 96 °C) while lower potentials characterize the Tertiary sediments in the Tuzla Basin, where springs and wells are associated with fault zones in the area of Gradačac. The Sava-Vardar Zone is characterized by the highest values of geothermal gradient of 45-55 °C/km and heat flow which varies from 90 to 110 mW/m².

Allochthonous Paleozoic-Triassic formations occur in the areas Sana-Una, Ključ-Raduša Mt., Mid-Bosnian Schist Mts., Southeastern Bosnia and East Bosnia. Within that unit there are several occurrences of thermal and thermomineral waters in Paleozoic and Mesozoic carbonates. The biggest occurrences of thermomineral waters are at Ilidža (Q=260 l/s, t=57-58 °C) and Kakanj (Q=35 l/s, t=56 °C) in the Mid-Bosnian Mesozoic Basin, which is one of the most promising zones in Bosnia and Herzegovina for exploration and utilization of geothermal resources. The values of the geothermal gradient and heat flow in this basin are 30-50 °C/km and 70-90 mW/m².

There are 87 active deposits of thermal and thermomineral waters with 175 springs and 130 artesian and pumping drillholes with total yield of 2,900 l/s (Miošić, 2010). The total capacity of these 87 occurrences is 251 MWth. Currently geothermal direct heat use is about 23 MWth that shows a very low level of utilization of geothermal energy compared to its available capacities. Traditionally, the country's geothermal energy production was used for direct heat supply (21 localities), with most of the thermal and thermomineral waters used in spas and recreation centres (18 localities).

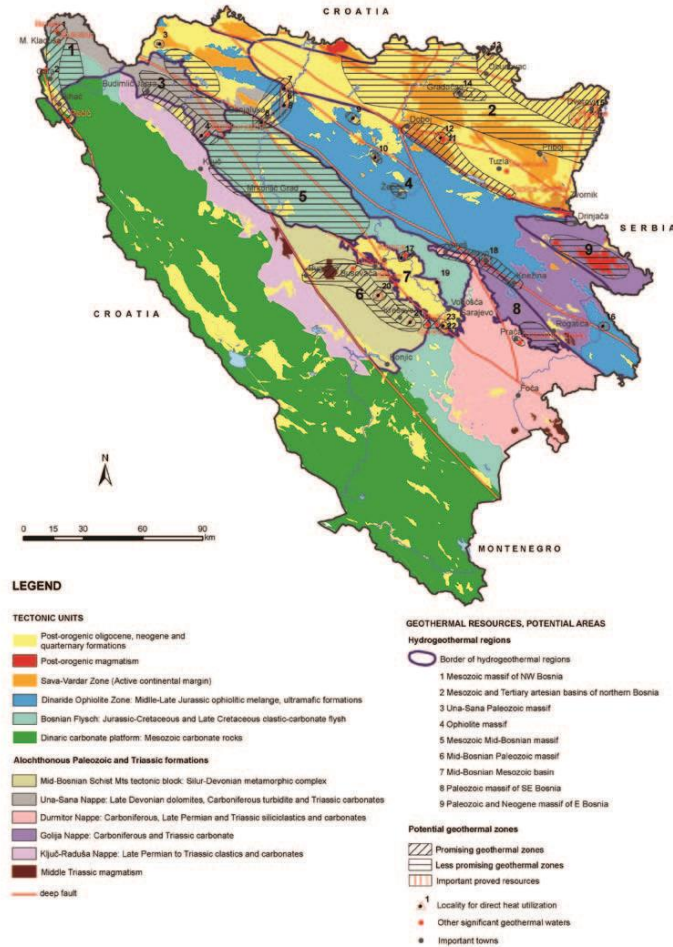


Figure 15. Geothermal areas in Bosnia and Hezegovina (Miošić et al. 2013)

With regard to geological and geothermal features, **Croatia** can be divided into two different regions: the Pannonian Basin area to the north and Dinarides to the south (Figure 16). The area of Pannonian Basin is characterized by an average geothermal gradient of 0.049 °C/m and in places reaches values of more than 0.07 °C/m, and the terrestrial heat-flow density ranges between 60 and 100 mW/m². High geothermal potential of this area is indicated by numerous spas with water temperatures up to 85 °C (Figure 17). At these locations geothermal energy is used for bathing, and only in few localities also for individual heating of associated buildings. On the other hand, in the area of Dinaridic mountains geothermal gradient ranges between 0.01 and 0.03 °C/m with average value of 0.018 °C/m.

Thermal water is today produced in 18 spas mostly for bathing and space heating. The temperature extraction level of geothermal wells varies from 25 to 85 °C. The total capacity of this production amounts to 54.45 MWt. Of this 22.15 MW is the capacity of bathing and swimming, the rest is for individual space heating. In two locations (Zagreb-University hospital and Zagreb Lučko) geothermal energy is used for individual space heating with the capacity of 13.77 MW (Živković et al., 2016). In another three locations (Bošnjaci, Krapinske Toplice and Sveta Nedjelja) greenhouses are heated by geothermal energy with capacity of 3.56 MW making geothermal use capacity total 75.74 MW.

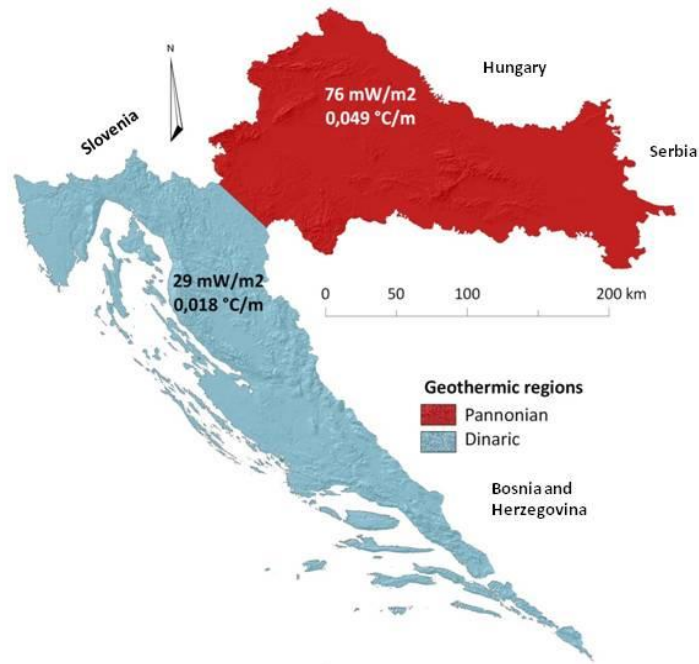


Figure 16. Geothermal potential of Croatia (modified after EIHP, 1998)

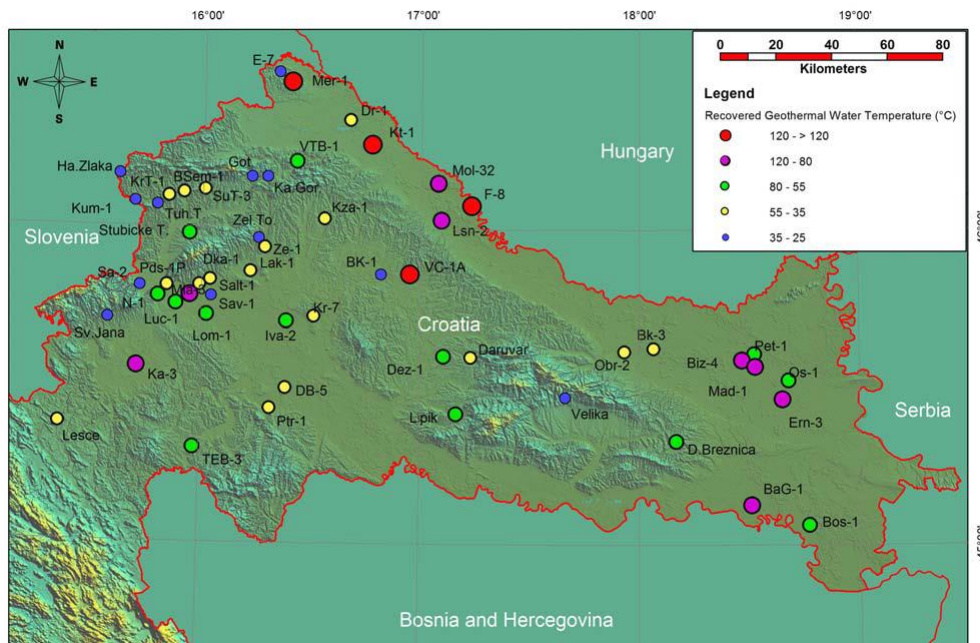


Figure 17. Known geothermal resources of Croatia (Živković et al., 2016)

There are 2 major types of geothermal reservoirs in **Hungary** (Nádor et al. 2016) which feed nearly 1000 thermal water wells (Figure 18). The several thousand meter thick multi-layered porous sediments (Upper Miocene-Pliocene “Pannonian” basin fill sequence) have low thermal conductivity and are composed of successively clayey and sandy deposits. Within this thick basin-fill sequence the main thermal-water bearing aquifers are found in a depth interval of ca. 800-2000 m where the temperature ranges from 60 to 90 °C. The other major reservoir type is

associated with the uppermost karstified zones of the deeply buried Palaeozoic-Mesozoic basement carbonates, as well as the fractured-weathered zones of the crystalline rocks, characterized by high secondary porosity. At this depth (on average 2000 m or more) temperature can exceed 100–120 °C and may provide favourable conditions even for the development of combined heat and power generation projects

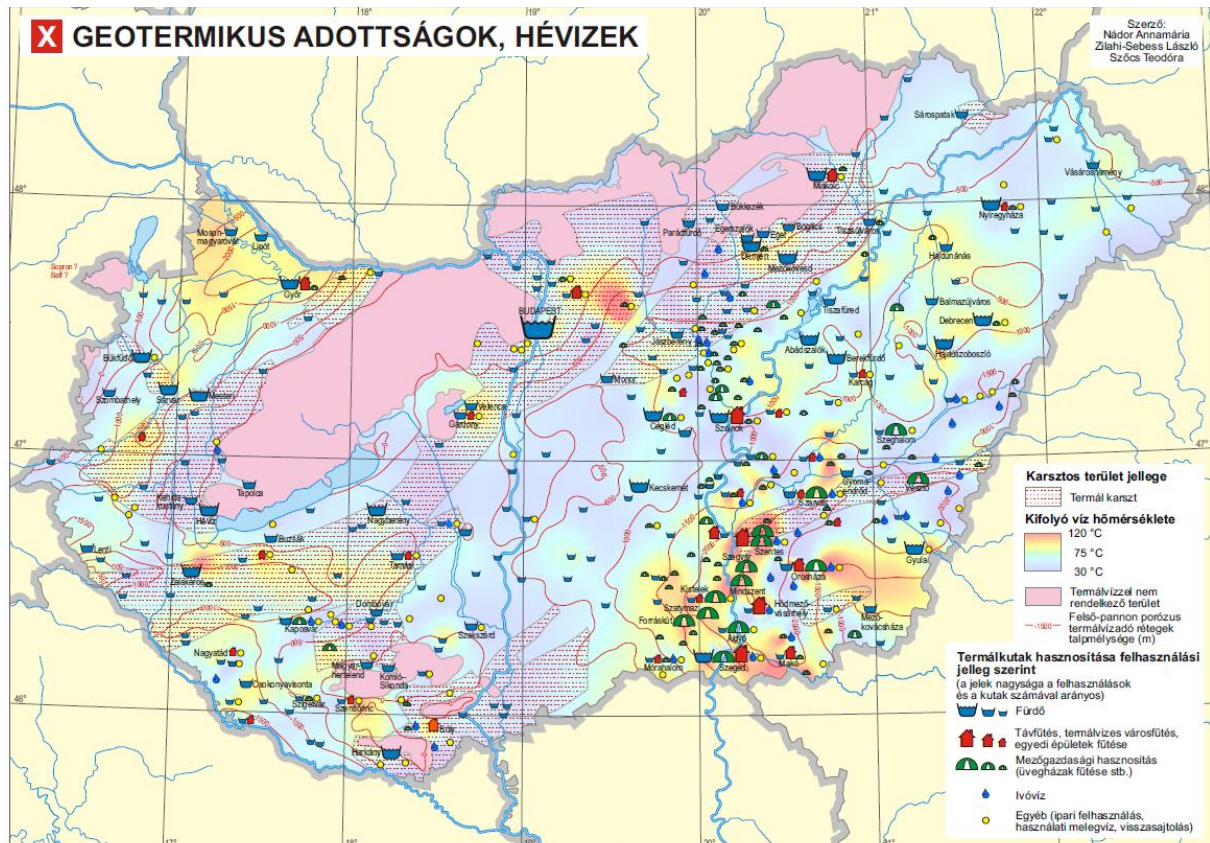


Figure 18. Thermal water utilization in Hungary (Nádor et al. in press)

The direct use of geothermal energy is well-advanced in Hungary, geothermal district-heating and thermal-water heating cascade systems are available in 21 towns representing about 210 MW installed capacity and 350 GWhth/y annual production. Individual space heating (mostly associated with spas) is available at 35 locations representing an estimated installed capacity of about 28 MW and 63 GWhth/y annual production. The agriculture sector is still a key player in direct use, especially in the S-ern part of the Hungary, where heating of greenhouses and plastic tents have long traditions. These account for about 292 MWth installed capacity and another 15.6 MWth is for “other” agriculture purposes (e.g. irrigation, soil heating, e.t.c.). Balneology has historical traditions in Hungary, more than 250 wells yield thermal water, and sometimes medicinal waters which represent a total installed capacity of 225 MWth.

The geothermal systems of **Romania** (Gavriliuc et al., 2016) are located in porous permeable formations such as Pannonian sandstone, interbedded with clays and shales specific for the Western Plain, and Senonian specific for the Olt Valley. Some geothermal systems are located in fractured carbonate formations of Triassic age in the basement of the Pannonian Basin (Oradea, Bors,), and of Malm-Aptian age in the Moesian Platform (North Bucharest) (Figure 19).

The Pannonian geothermal aquifer – the one relevant for the DARLINGe project - is multilayered, confined one and is located in the Upper Pannonian sandstones (late Neocene age), on an approximate area of 2,500 km² along the Western border of Romania, from Satu Mare in the North to Timisoara and Jimbolia in the South. The aquifer is situated at the depth of 800 to 2,400 m. It was investigated by more than 100 geothermal wells, all possible producers, out of which 37 are currently exploited. The thermal gradient is 45-55 °C/km. The wellhead temperatures range between 50 and 85 °C. The mineralisation (TDS) of the geothermal waters is 4-5 g/l (sodium-bicarbonate-chloride type) and most of the waters show carbonates scaling, prevented by downhole chemical inhibition. The combustible gases, mainly methane, are separated from the geothermal water and not used (yet). The wells are mainly artesian and very few of them operate with downhole pumps.

The total capacity of the existing geothermal wells in Romania is about 480 MWth (for a reference temperature of 25 °C). Of these total, currently only 96 wells are used (of which 40 are used only for balneology and bathing), that are producing hot water in the temperature range of 40-115 °C, equivalent of 200 MWth. For 2015, the annual energy utilisation from these wells was about 400 GWh. There are 6 reinjection wells. The main direct uses of the geothermal energy are: space and district heating; bathing; greenhouse heating; industrial process heat; and fish farming.

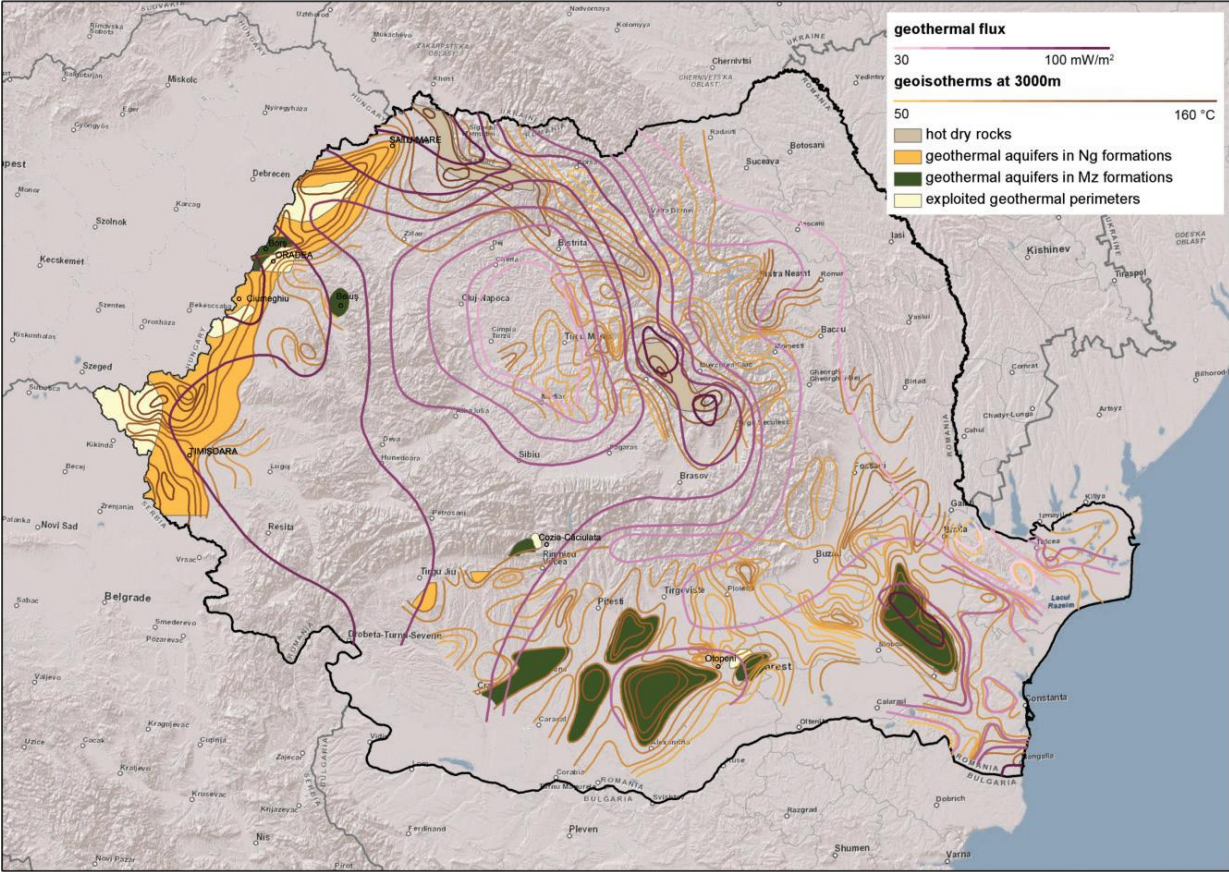


Figure 19. Geothermal map of Romania (adapted after Veliciu et al., 1985)

There are four main geothermal provinces in **Serbia** (Oudech et al., 2016): the Pannonian basin, the Dinarides, the Serbian-Macedonian massif and the Carpatho-Balkanides (Figure 20).

The most promising geothermal areas are the Pannonian and Neogene magmatic provinces located at the southern edge of the Pannonian Basin, which is part of the DARLINGe project area. In this region there are 4 hydrogeothermal systems arranged in a vertical succession.

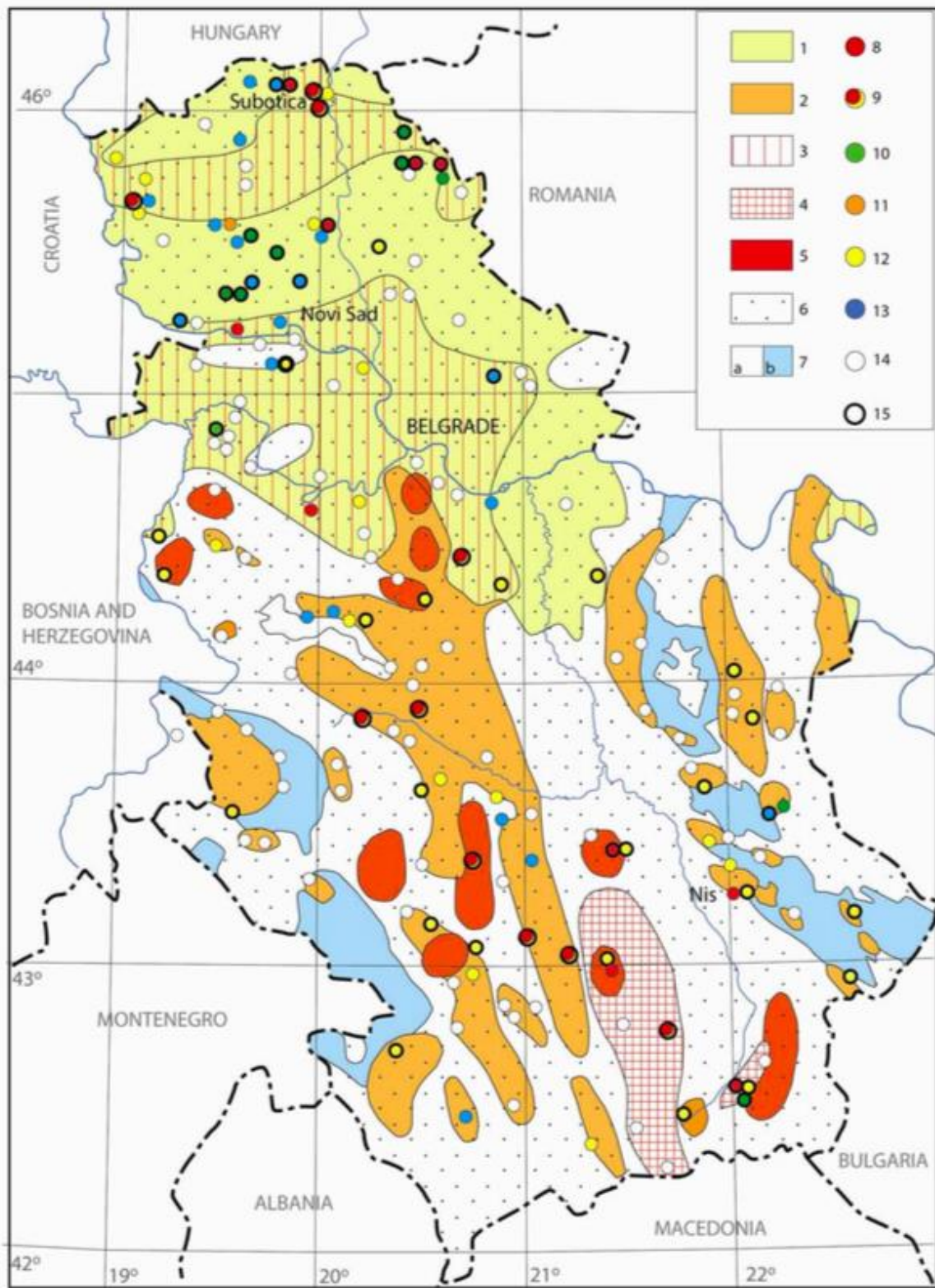
The first hydrogeological system encompasses sediments from the surface to the basement of the upper Pontian with maximal thickness of 2000 m in central part of the basin and reaches several dozen meters in the bordering zones of the Pannonian Basin. The aquifers are composed of sands and gravel. Maximal strata temperature is 120 °C. The average flow rates are 1-13 l/s, with water temperature at well-heads from 40 to 55 °C, maximum 82 °C. Chemical composition displays water of Na-HCO₃ type and mineralization 1-9 g/kg.

The second hydrogeological system is located immediately under the first one and is consisted of the lower Pontian and Pannonian rocks. The aquifers in this system are sandstones. Maximal strata temperature in this system is 160 °C. The average flow rates are 2.5-5 l/s, with water temperature at well-heads from 50 to 65 °C. Chemical composition displays water of HCO₃-Cl-Na type and mineralization 4-20 g/kg.

The third hydrogeological system is formed at the base of Neogene or Palaeogene sediments, where aquifers are made of Miocene limestones, sandstones, basal conglomerates, and basal breccias. The average flowing rates are 5-10 l/s. Water temperature at well-heads ranges from 40 to 50 °C and according to the chemical composition thermal waters are of Na-HCO₃ type and mineralization up to 50 g/kg.

The fourth hydrogeological system encompasses magmatic, metamorphic and sedimentary rocks of the Triassic and Palaeozoic age underlying the Palaeogene and Neogene sediments. The most significant aquifers are fractured and karstified Triassic limestones and dolomites. In the central parts of the basin these rocks are at the depth of about 1500 m, while in the basin margins the depth is about 1000 m. The average well yield is 12 l/s in central parts and up to 40 l/s in the marginal zones. Water temperature at well-heads is 40-60 °C. In the marginal zones due to the active water-exchange, thermal waters are of Na-HCO₃ type and mineralization up to 1 g/kg, while in central part thermal water belongs to the Na-Cl type.

The greatest number of wells are used in balneology (thermal spas), less is utilized for greenhouses heating or in industrial and agriculture processes.



Legend: 1-Hydrogeothermal aquifer in Cenozoic rocks; 2-Hydrogeothermal aquifer in Mesozoic rocks; 3-Hydrogeothermal aquifer in Mesozoic rocks below Cenozoic rocks; 4-Hydrogeothermal aquifer in Paleozoic rocks; 5-Petrogeothermal resources in Tertiary granitoid rocks; 6-Hydro-petrogeothermal resources to 200 m deep for exploitation of geothermal energy with heat pumps; 7-Areas without significant geothermal resources: a) terrains with rocks of Paleozoic and Proterozoic age, b) karstic terrains; UTILIZATION OF RESOURCES: 8-heating; 9-heating, balneotherapy and recreation, 10-Food production; 11-Industry; 12-Balneotherapy; 13-Recreation and sport; 14-Occurrences not used, 15-In operation in 2015.

Figure 20. Map of geothermal resources of Serbia (Milivojevic, 2001)

Slovenia (Rajver et al. 2016) lies in the convergent area of the African and Eurasian tectonic plates, consequently its geological and tectonic setting is quite complicated. It is subdivided into several tectonic units with different hydrogeological properties and geothermal conditions (Figure 21). In the northeast, the Mura-Zala basin (the southwestern part of the Pannonian Basin) and the Eastern Alps (incl. magmatic rock complex) are parts of the European plate. Predominately carbonate Southern Alps, the External and the Internal Dinarides and the Adriatic foreland represent parts of the Adriatic microplate.

The best geothermal conditions are found in the Mura-Zala Basin, which is the south-western part of the Pannonian Basin. The area has an elevated surface heat flow density (HFD), above 100 mW/m², with expected temperatures above 80 °C at 2 km depth east of the Maribor and Ptuj line. All production wells exploit thermal water from Neogene aquifers with exception of those in Maribor and Benedikt. About 19 inactive and potential wells in the area exhibit wellhead temperatures of 28 to 62 °C, and have a total yield of 68 kg/s, resulting in the ideal thermal power of 9.4 MWth. The geothermally most utilized north-eastern area that belongs to the Mura-Zala basin is filled by Neogene marine and fresh water sediments. Clays and marls predominate, with intercalations of porous sands and sandstones, where mineral, thermal and thermo-mineral waters are found. The most extensive Upper Pannonian-Pontian geothermal sandy aquifers are widely utilized by Hungary and Slovenia. Hydraulically connected sandy lenses of the Upper Pannonian-Pontian Mura Fm. represent the best yielding low temperature geothermal aquifer in the sedimentary basin in Slovenia.

Geothermal utilization of thermal water heat is based on direct use from 57 production wells plus 3 thermal springs, implemented at 34 localities (Figure 21).

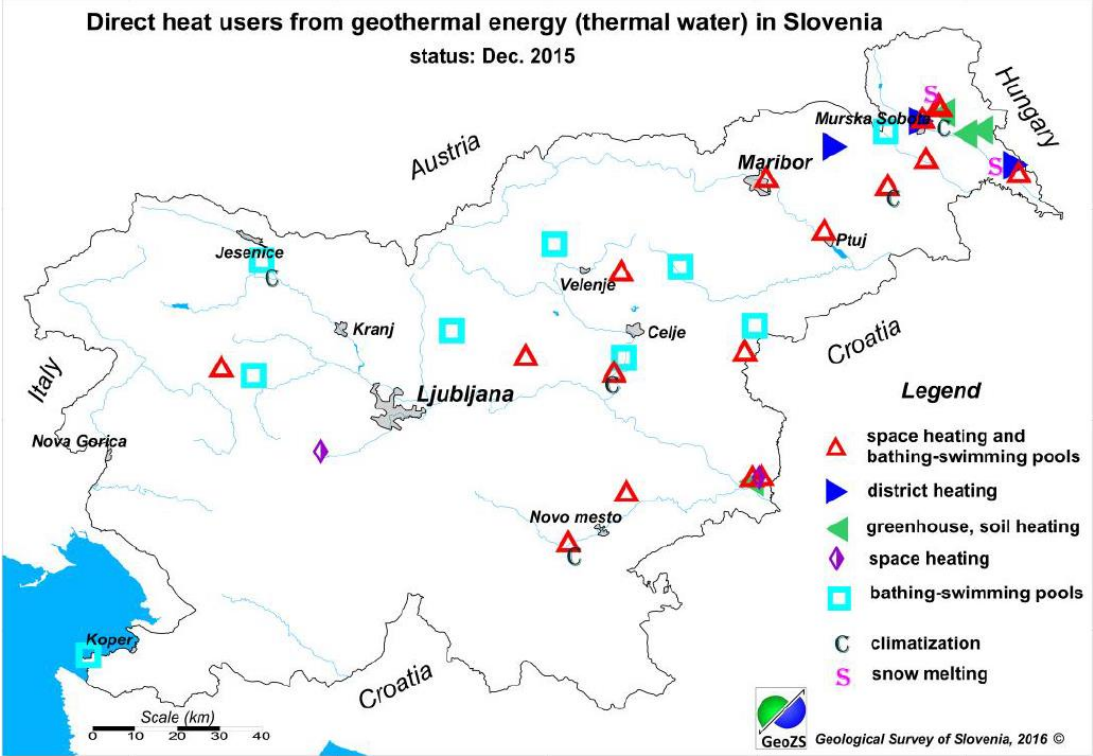


Figure 21. Main types of utilization for direct use in Slovenia (Rajver et al., 2016)

7. Outlining geothermal reservoirs

As it was mentioned in Chapter 2 (Methods for the identification of geothermal reservoirs) outlining of geothermal reservoirs was based on the combination of geological and geothermal data. The steps of this task were the separation of different reservoir types according to their hydrogeological and geothermal behaviour, construction of common geological and isotherm surfaces. Finally, based on these results and matching different surfaces the spatial location of different types of geothermal reservoirs was determined.

7.1. Reservoir types

Due to the above presented very complex geological build-up of the project area and scattered, inhomogeneous data distribution, it was not possible to make a detailed harmonization of the geological formations. In the absence of a common geological model, the most important hydrostratigraphical units (rock assemblages having the same hydrogeological behaviour) were identified as potential geothermal reservoirs applying some simplification. These units contain the most often exploited thermal water aquifers.

Two main types of geothermal reservoirs were determined. The thermal aquifer layers of the Pannonian shelf front and shelf plain formations was called “basin fill reservoir (BF)” in this work, while potential thermal aquifers of the basement formations were called “basement reservoirs” (BM). The two main reservoir types represent different types of porosity.

BF reservoirs consist of porous formations of shelf front and shelf plain formations deposited in the Pannonian Lake. The sediment succession is built up of alternating sand and sandy clay layers characterized by a strong anisotropy in hydraulic conductivity (K_h/K_v) often higher than 5000 (Tóth et al. 2016). Despite of the lower permeability of the clayey-marly strata, hydraulic connection exists between the sand layers, which make the entire Upper Pannonian sedimentary series one hydrostratigraphic unit, characterized by an almost uniform hydrostatic pressure. The reservoir is built up from 30 to 100 m thick sand-prone units which can be tracked regionally. The sandy aquifer layers have got intergranular porosity of 20-30% and hydraulic conductivity of 4×10^{-6} – 5×10^{-5} m/s (Rotár-Szalkai et al. 2017).

Some potential geothermal reservoirs occur in the Quaternary formations as well, but they are out of the scope of our study, because of their relatively lower temperature (usually slightly exceeds 30°C in the central parts of the basin) and principal importance of these aquifer layers in drinking water supply despite their slightly elevated temperature.

BM reservoirs may contain different types of fractured and fissured formations consisting of crystalline metamorphic rocks, or carbonate complexes of different age. The fractured crystalline rocks may exhibit an enhanced permeability in the main tectonic zones, as well as in their upper weathered zones. The fractured, partially karstified carbonate rocks are characterized with enhanced porosity in their intensively karstified zones, most commonly in the upper part of the carbonate sequences. Some tectonic zones in the basement rocks, especially in the neotectonically active regions have got individual importance with high hydraulic conductivity and active hydraulic connections to other large aquifer systems.

Considering utilization schemes, different temperature categories were distinguished within the main types of reservoirs (BF and BM). The subcategory of 30-50 °C can be important mainly for balneology. Reservoirs having temperature between 50 and 100 °C are primarily suitable for direct heat utilization. Within that the 75-100 °C subcategory represents the temperature range

where thermal water can be applied for district heating systems. Reservoirs having temperature between 100 and 125 °C, 125-150 °C, or temperature exceeding 150 °C have the potential for combined heat and power generation (CHP) projects using binary technologies.

To provide the opportunity of resource estimation, reservoirs were identified as closed 3D bodies. As a consequence sometimes geological different formations belong to one reservoir. For similar reason the surface projection of the top and the basement of a reservoir can be composed of different formations as well. The theoretical section of the identified geothermal reservoirs is shown on Figure 22, where the top surface and the bottom surface of the reservoirs were illustrated with separate lines.

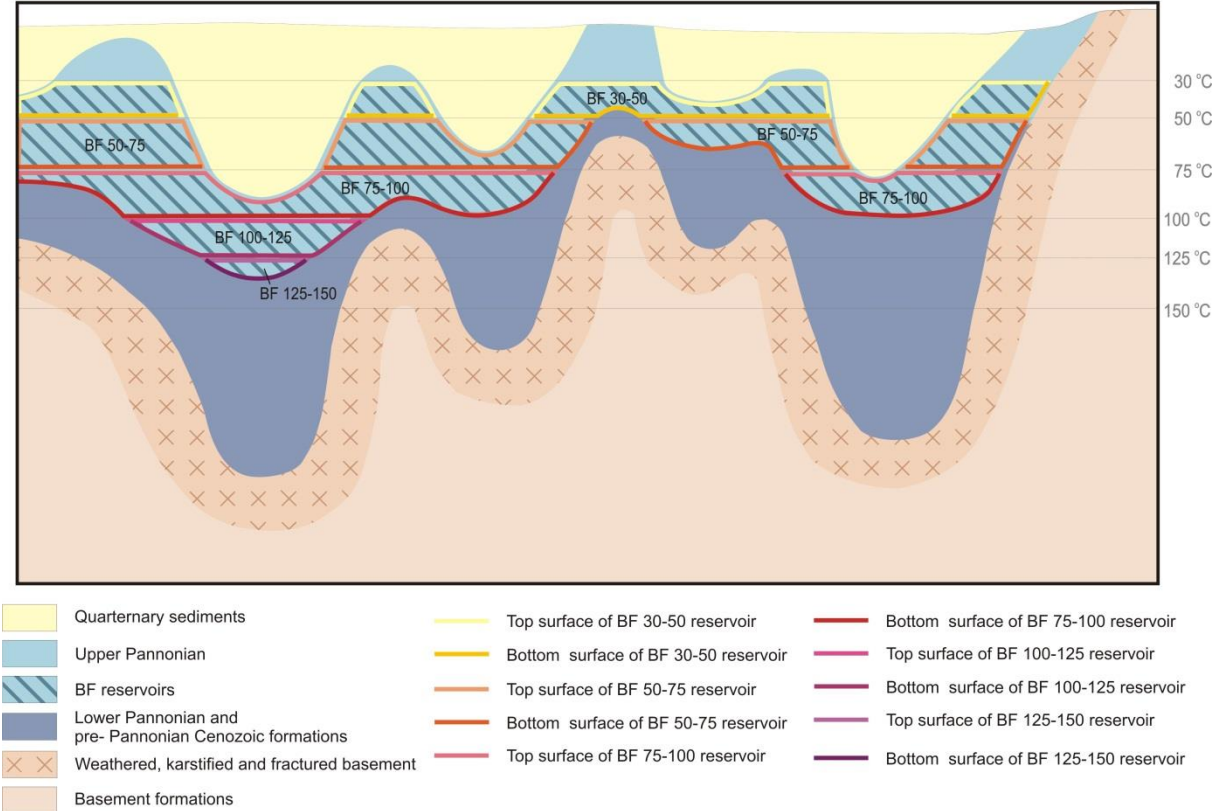


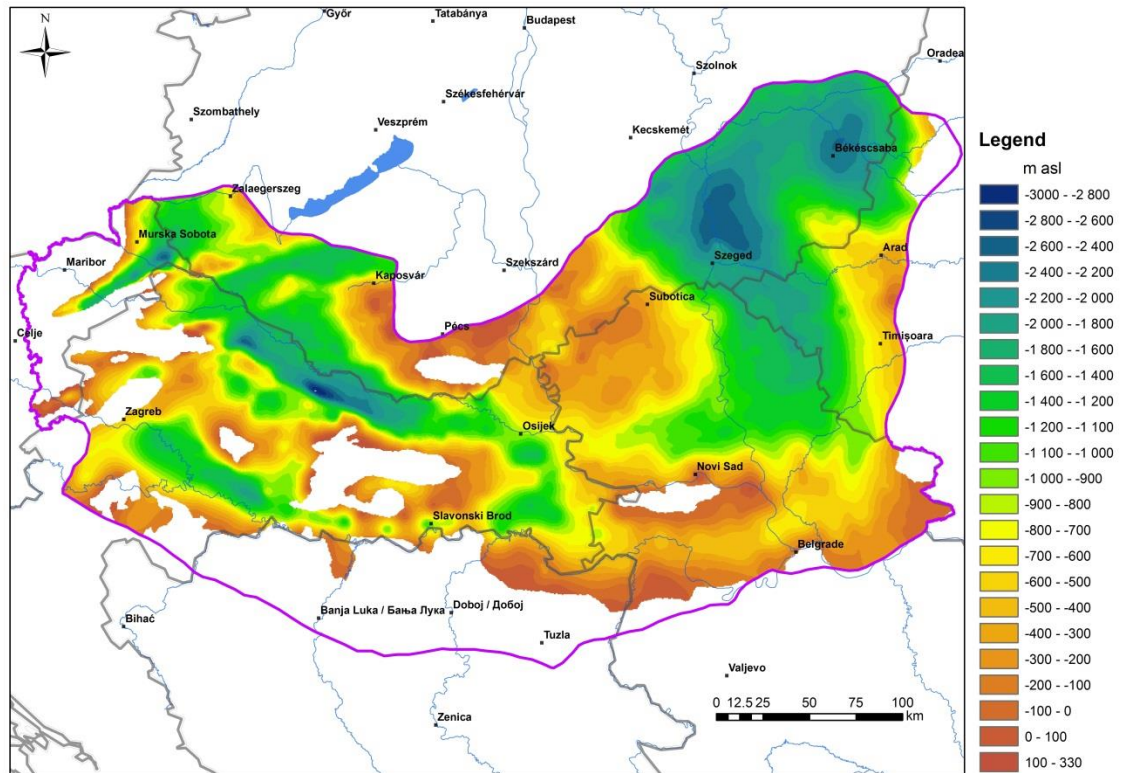
Figure 22. Schematic view of reservoir types

7.2. Geological surfaces delineating potential reservoirs

Several depth surfaces of various geological units were created for the subsequent modelling and calculations. These surfaces were the following:

- top surface of the basement formations (the Pre-Cenozoic basement), which can represents the BM-top without the Senonian sediments. Latter was not isolated from the Pre-Cenozoic formations (Figure 23.).

- the shelf-edge of the Pannonian Lake, representing a shale-sand lithological boundary, forming the BF-bottom (



- Figure 24),
- the top surface of the shelf sediments forming the top of the basin fill reservoir (Figure 25).

The geological descriptions of the reservoir rock bodies are summarized in Chapter 3.

For the preparation of the above identified geological model horizons, relatively large datasets were available, mainly borehole data (412 boreholes), although they were not sufficient for the desired resolution of 500x500 meters due to the uneven data distribution. Therefore, the surfaces were edited on the basis of results of previous modelling and publications (grids, iso-maps). The used data for producing the top of the basement (BM_top) were:

- grid from the Slovenian partners,
- the geothermal project of the Drava Basin and iso-map of Horváth et al. (2012) in the Croatian area,
- iso-maps based on borehole data and other relevant elements from Serbia,
- constructed iso-map based on borehole data from Romania,
- a published basement map for the Hungarian area (Haas et al., 2010).

Data for the bottom of basin fill reservoir were:

- grid from the Slovenian partners,
- the geothermal project of Drava Basin in Croatian area,
- iso-map based on borehole data and other relevant elements from the Serbia,
- constructed iso-map based on borehole data from Romanian area,
- deep geological model of Hungary (related to the Hungarian part of the project area).

Data for top of the basin fill reservoir were based on:

- grid from the Slovenian partners,
- the outcrop levels in Croatian and Serbian areas,
- the bottom of the Quaternary surface (Magyari et al., 2010) for the Hungarian area.

The different surfaces were prepared with simple kriging methods at 500x500 meters resolution, during which the contour lines of iso-maps were sampled every 100 meters, than completed with the data from the project and interpolated. In the data-poor areas and areas with controversies (mainly near the outcrops) manual corrections were implemented.

For the overall characterisation of the project area, geological cross-sections were compiled (Figure 26). On the sections (Figure 27, Figure 28, Figure 29, Figure 30, Figure 31) the basement top, the bottom of the basin fill reservoirs, top of the basin fill reservoirs and the topographic surface horizons were visualized, as well as the basement units, the tectonic lines with indications on movements along them, the used boreholes and occasionally the names of the relevant sub-basins. The rejuvenation of some fault planes is indicated with different colours. The exaggeration of the sections is generally 10×, with exception of the section-5 (5×). The visualised depth spans from 0 to 6-8 km.

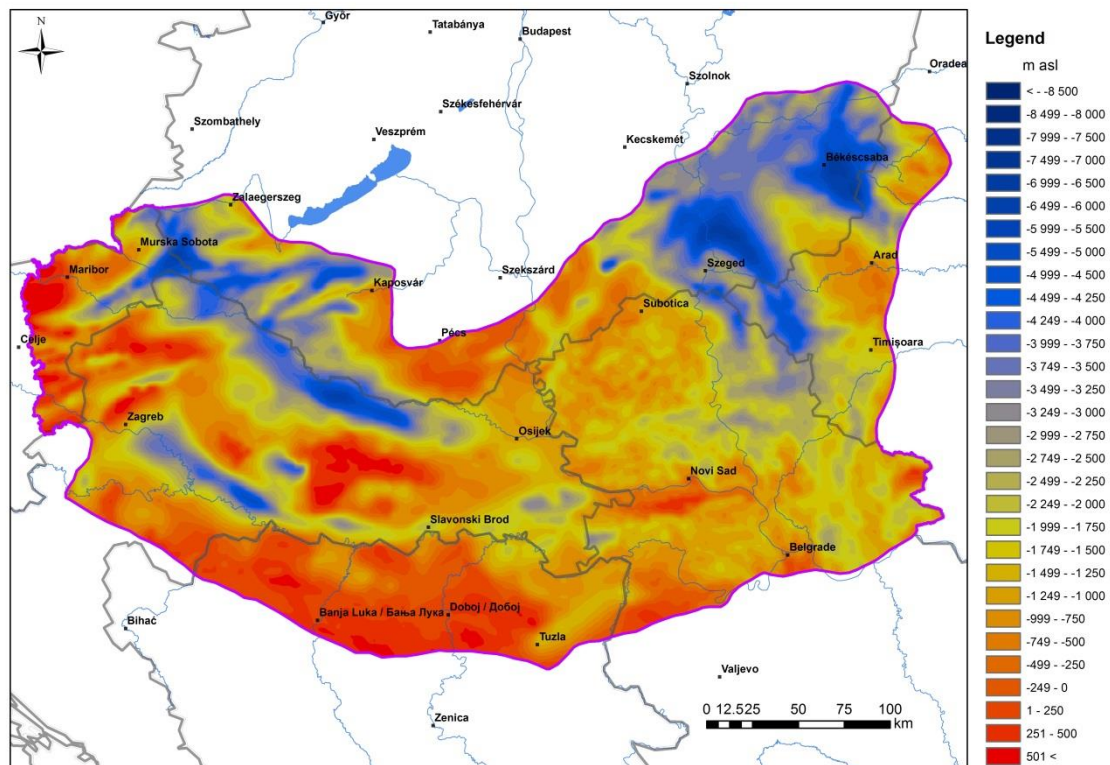


Figure 23. The depth horizon of the pre-Cenozoic basement formations (BM top)

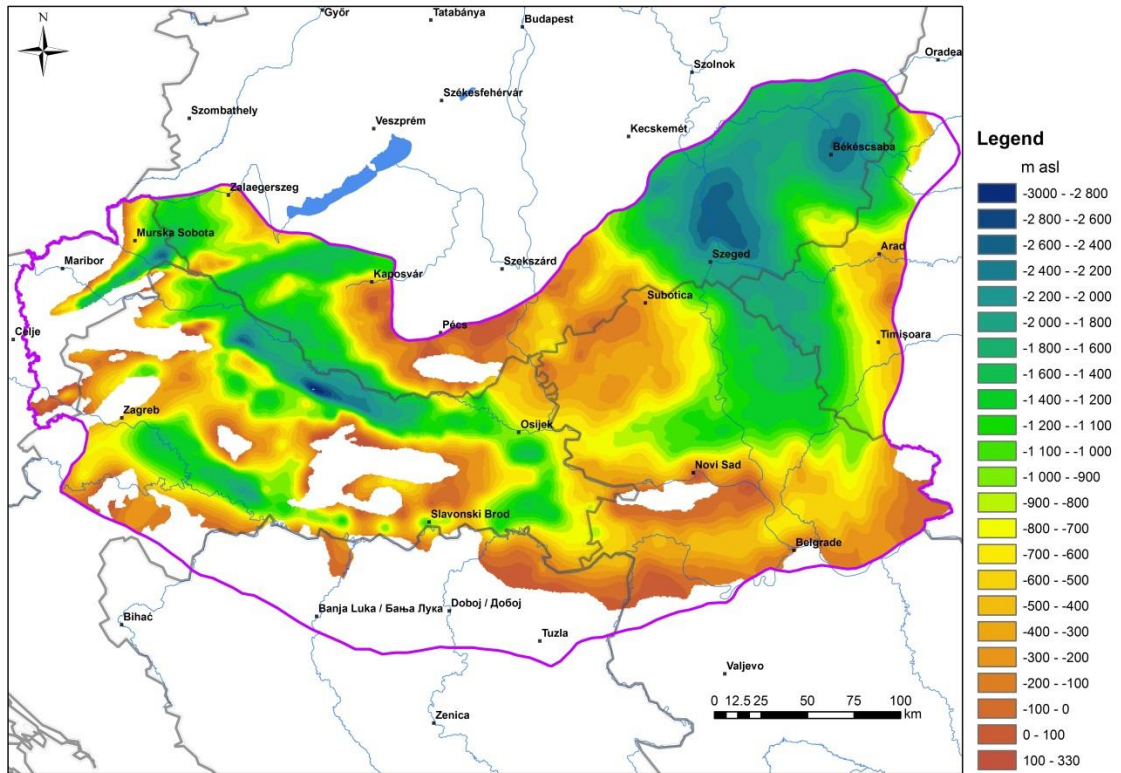


Figure 24. The depth horizon of the bottom of the nearshore sandy succession deposited in the Pannonian Lake (BF bottom)

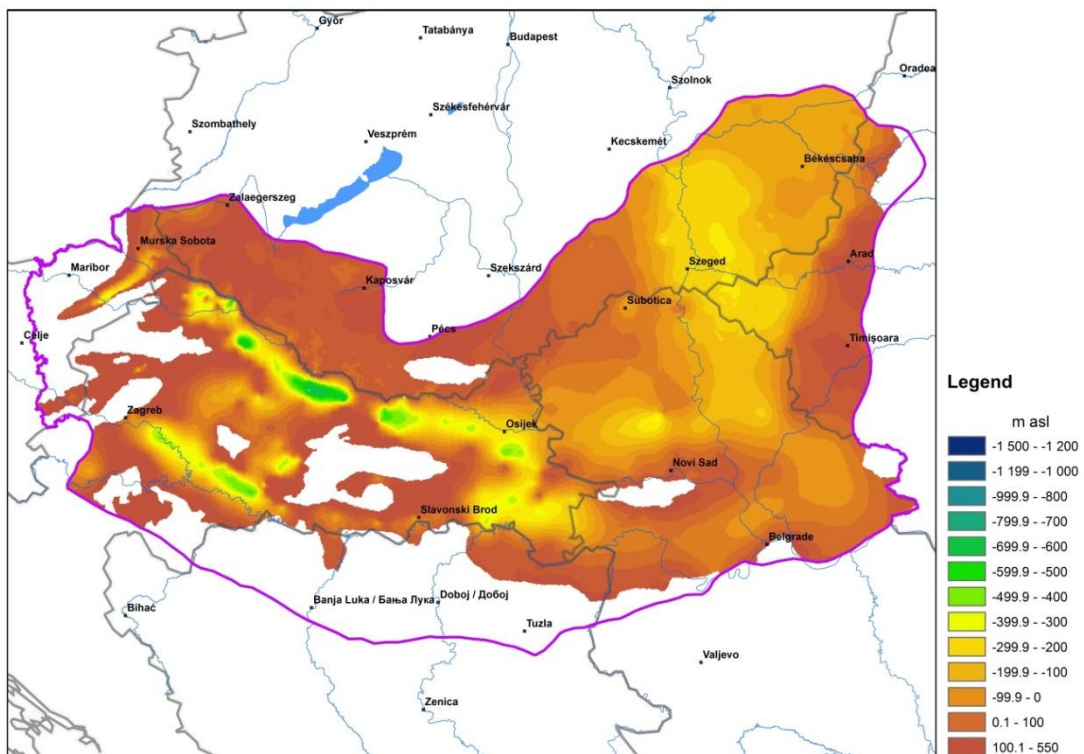


Figure 25. The depth horizon between the Pannonian Lake deposits and Quaternary terrestrial sequences (BF top)

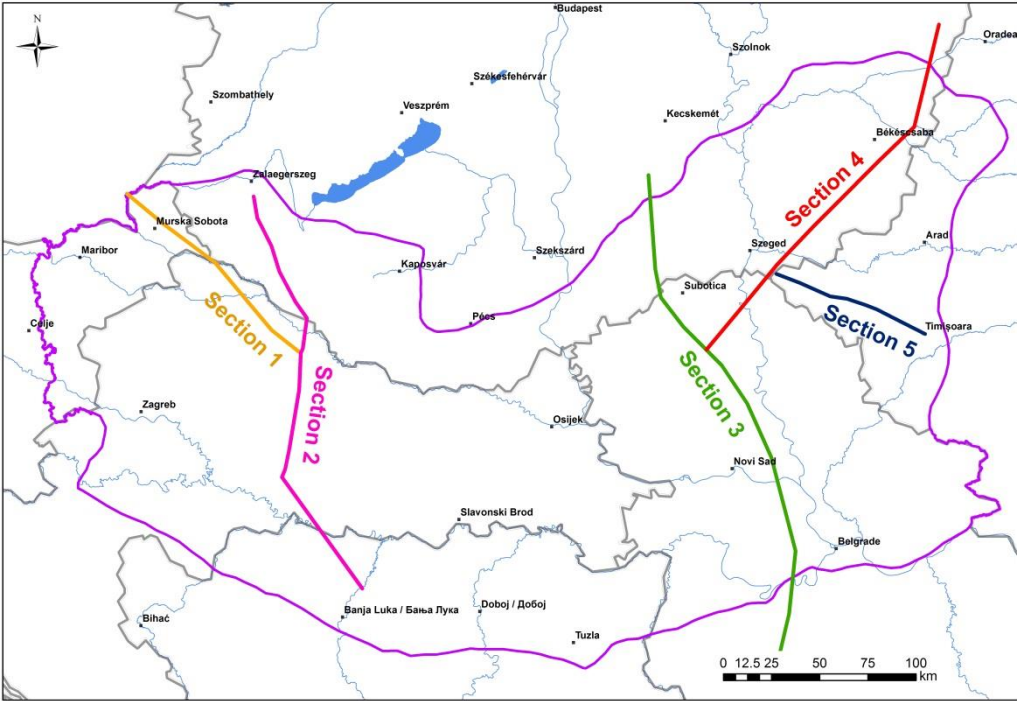
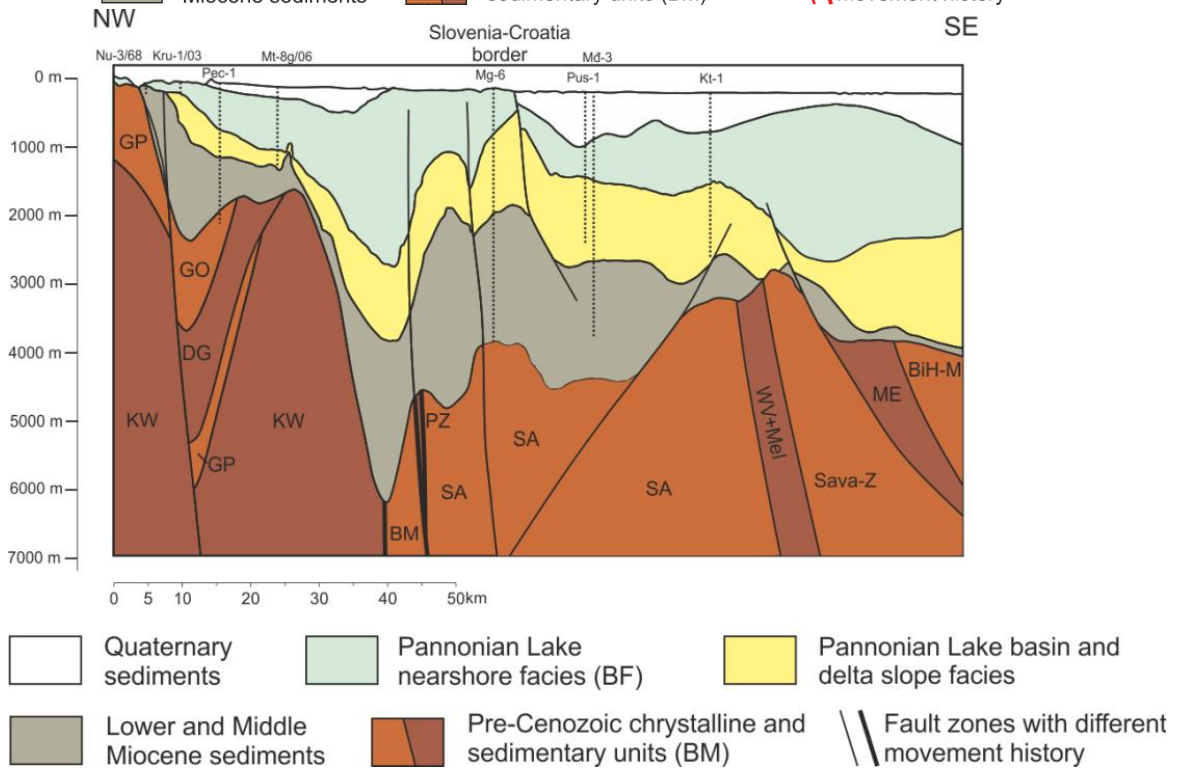
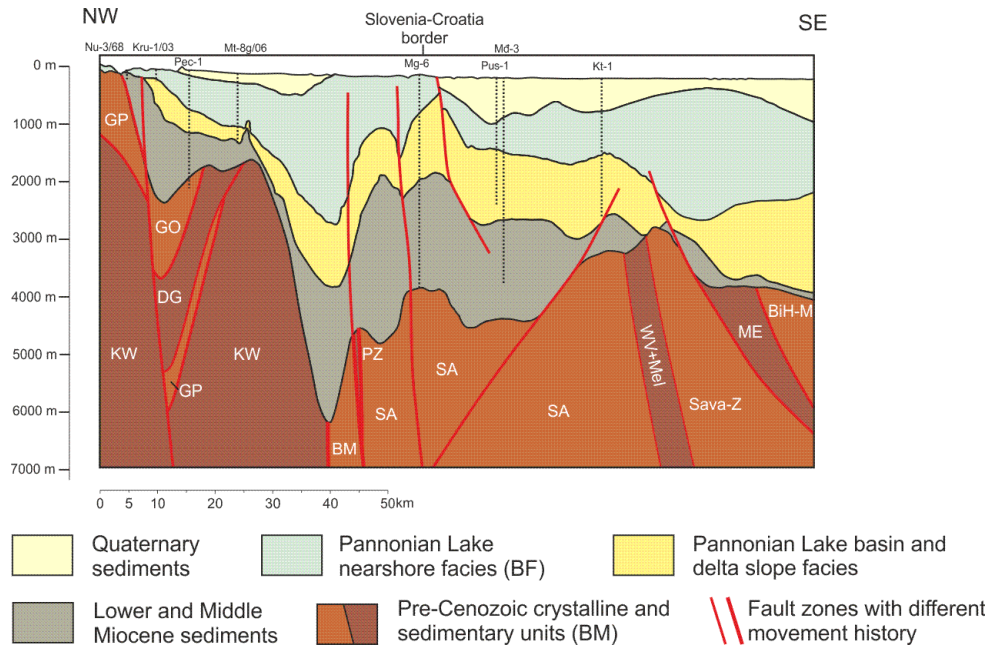


Figure 26. Index map of the geological cross-sections in the project area



**Figure 27. Section 1 in Slovenia–Croatia
(For the abbreviations of the basement units see chapter 4.1.1)**

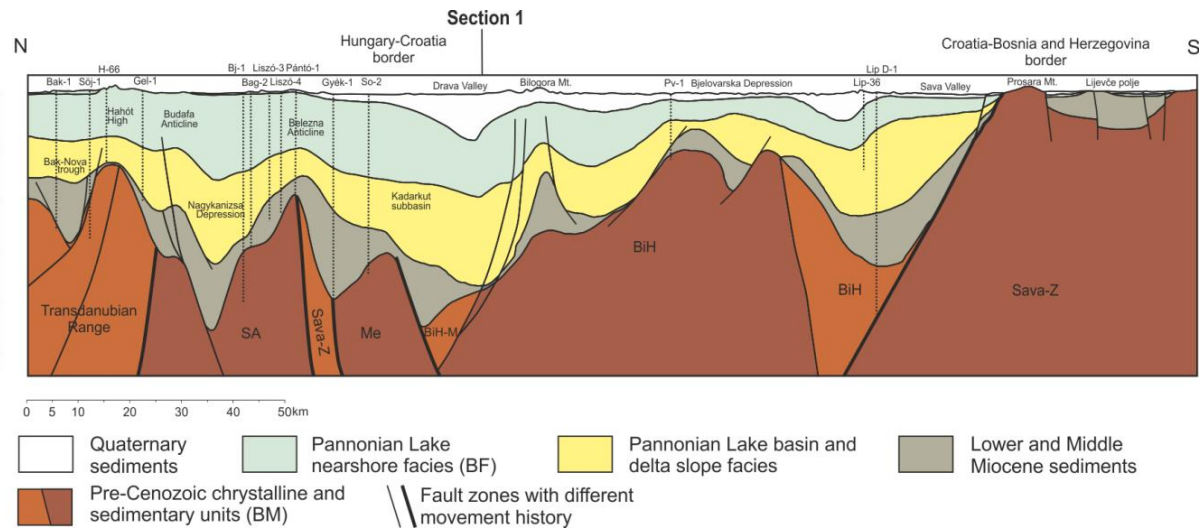
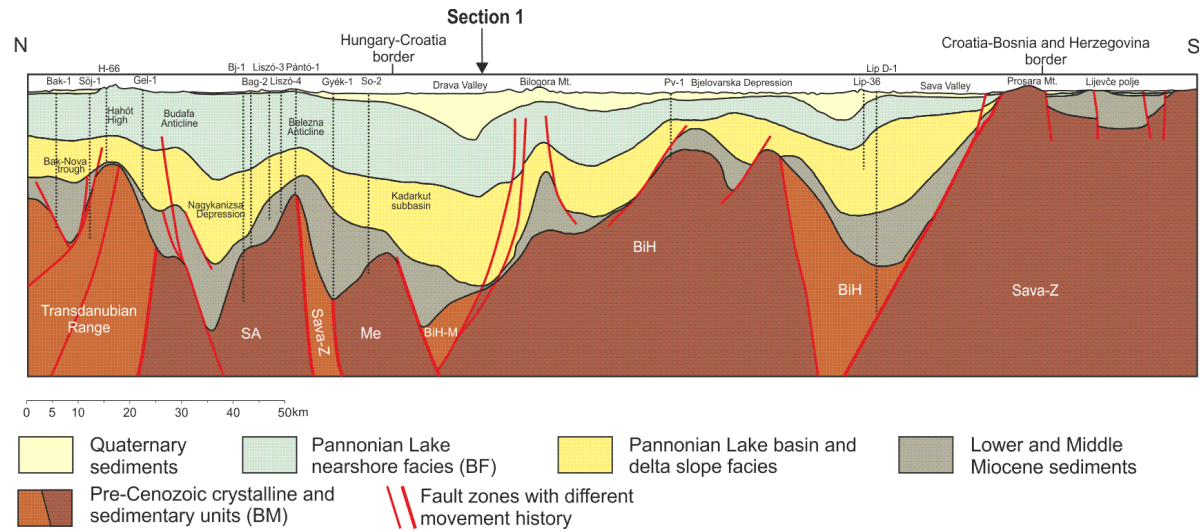


Figure 28. Section 2 in Hungary-Croatia-Bosnia-Herzegovina

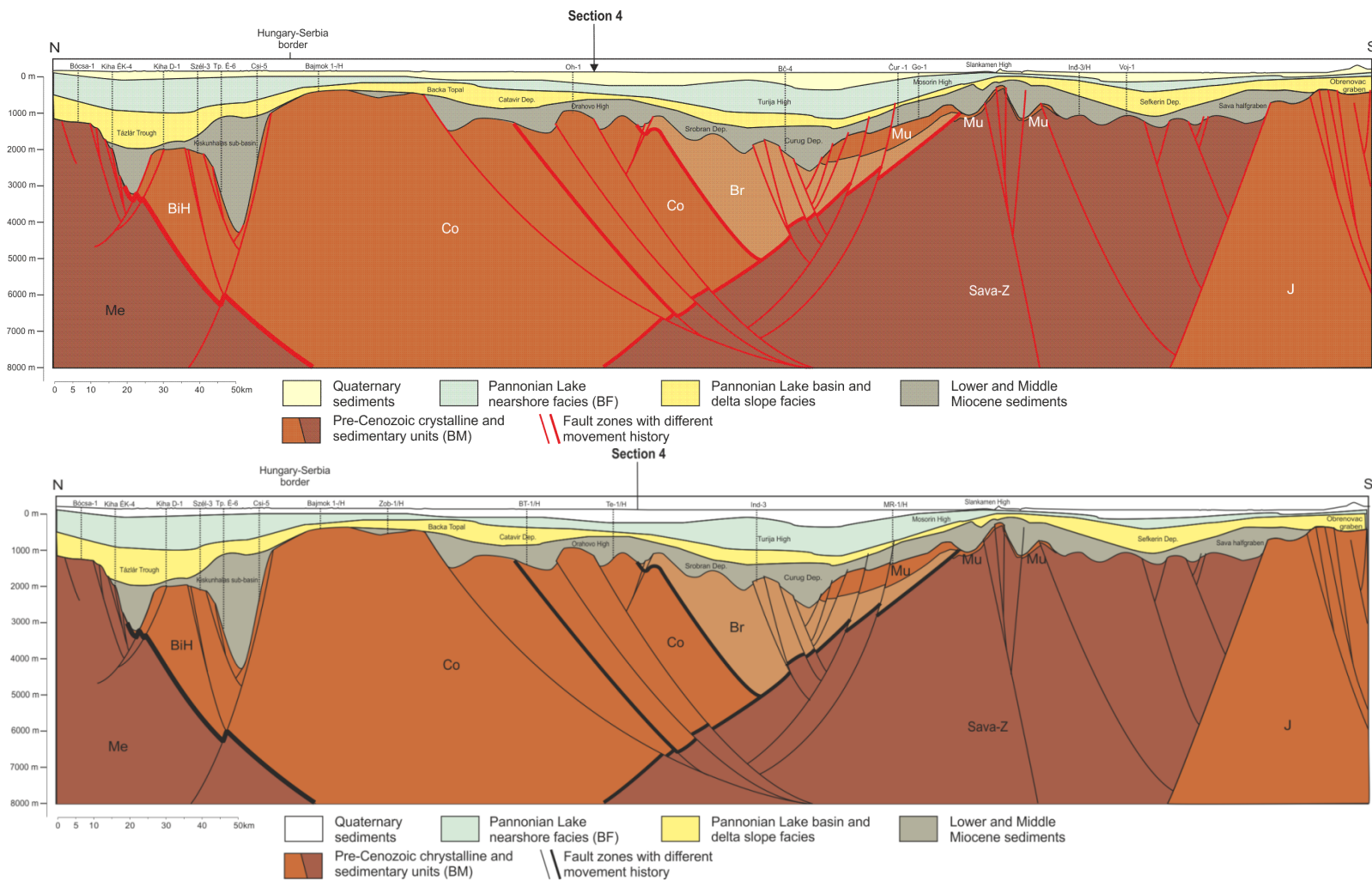


Figure 29. Section 3 in Hungary-Serbia
(modified after Matenco and Radivojevic, 2012.)

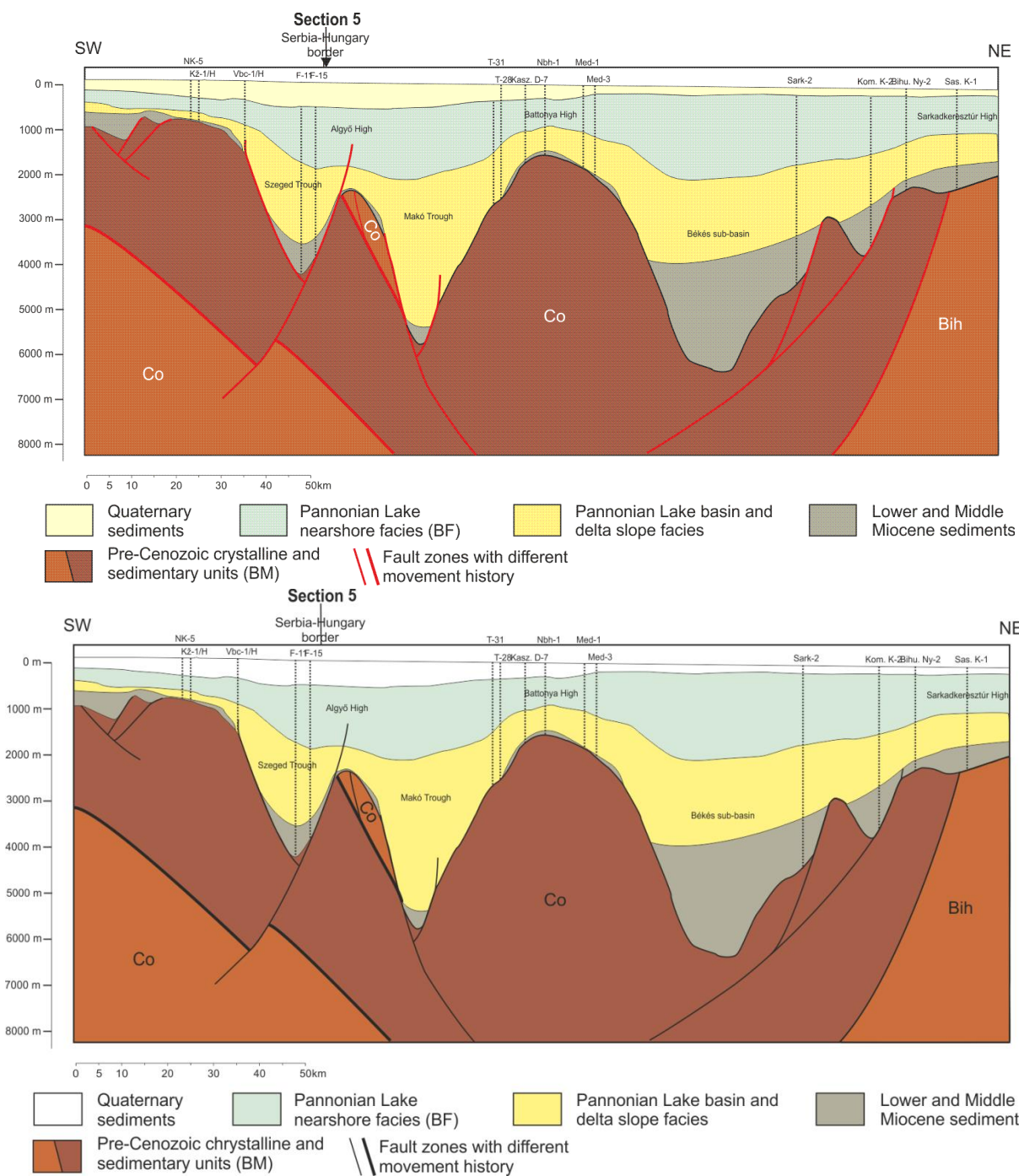


Figure 30. Section 4 in Serbia-Hungary

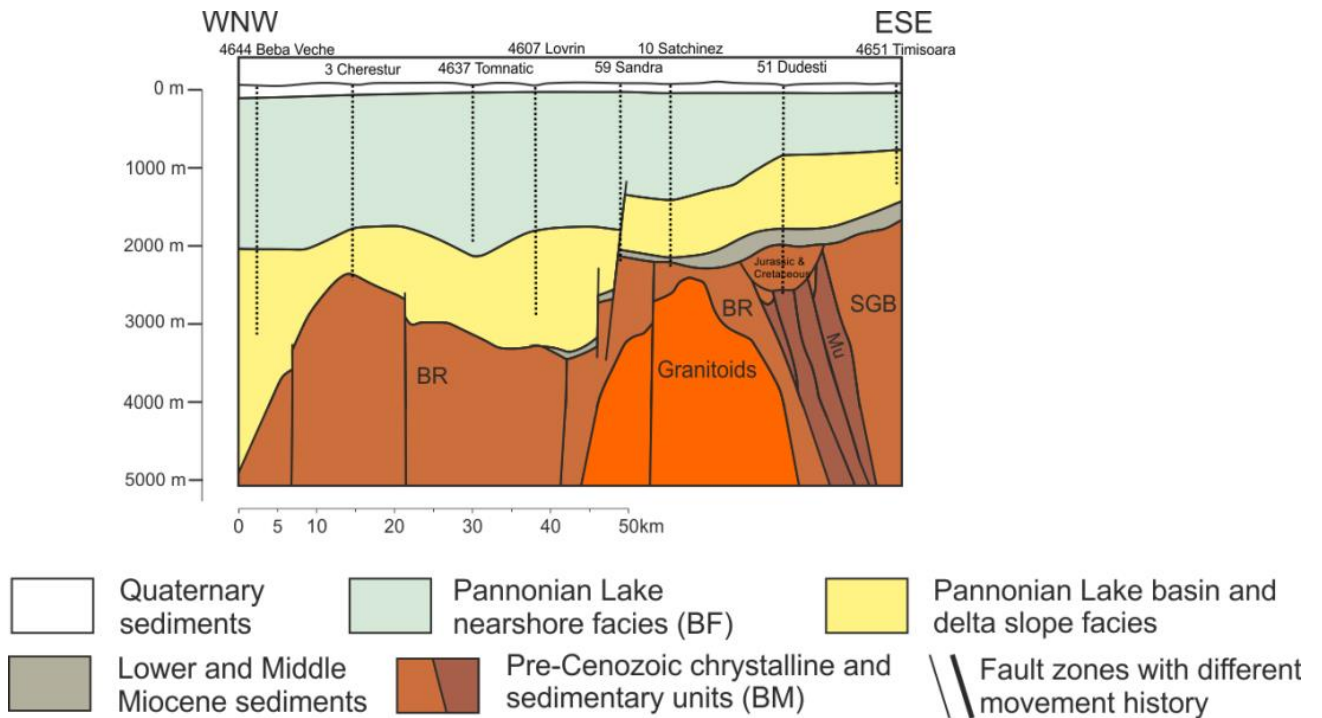
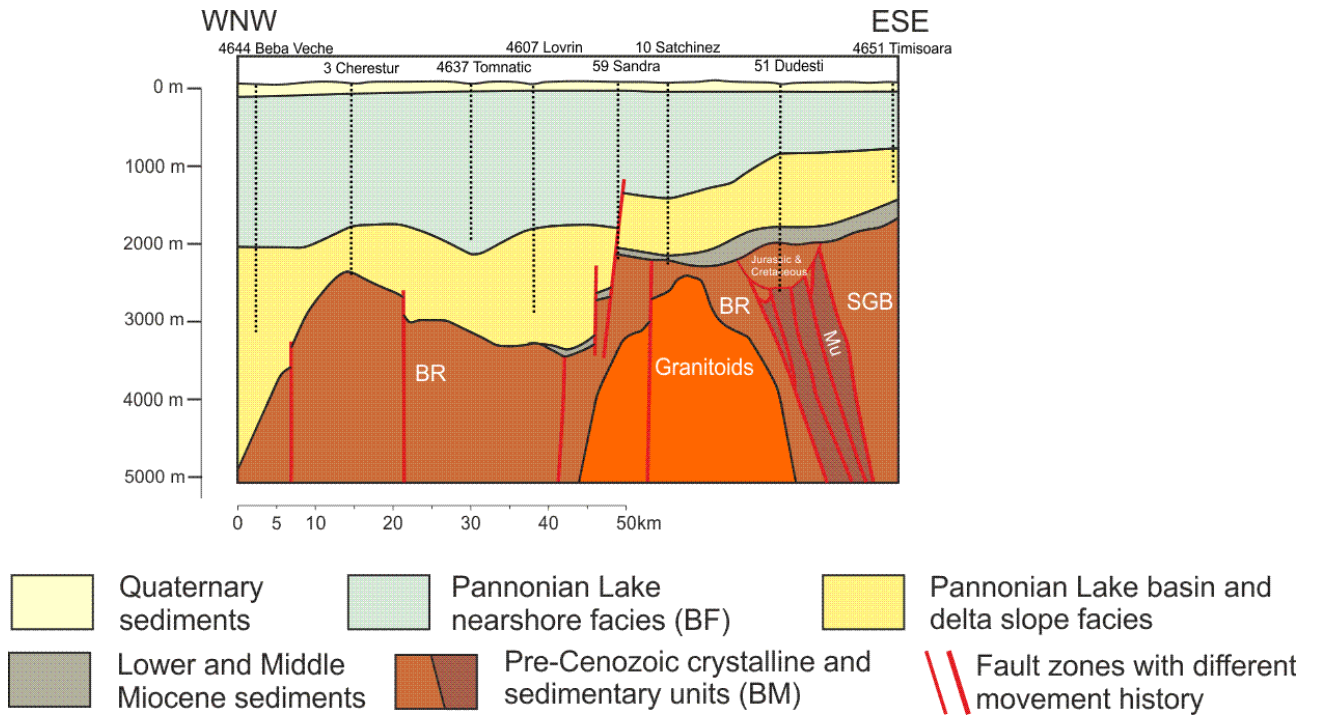


Figure 31. Section 5 in Romania

7.3. Construction of the isotherm surfaces

In the following chapters (Chapter 7.3.1 and 7.3.2) the principles of calculation and constructions of isotherm surfaces are summarized.

Information about geothermal conditions derived from temperature measurements performed in thermal water wells, or in hydrocarbon boreholes. Since these measurements usually have a great uncertainty, thermal data (temperature, geothermal gradient, etc.) may show a big standard deviation even within a small region. To increase the reliability, average values can be used. Another possibility to eliminate measurement errors and the problem of unfavourable spatial distribution of temperature data is the application of a geothermal model (Lenkey et al. 2017). We applied the latter method, with a simplified analytical conductive model which is briefly introduced below.

For the characterization of the BF reservoirs, temperature values in the sedimentary basins were estimated for the entire sedimentary succession that deposited in Lake Pannon, i.e. from the depth of the pre-Pannonian “basement” surface (that is not equal with the pre-Cenozoic basement that is relevant for the BM reservoirs). For the basement formations a further simplified estimation was done based on conductive heat-flow. The results for basin and basement formations were combined in each created temperature iso-surface maps.

7.3.1. Estimated temperature values in the sedimentary basins

The applied model for the calculation of temperature data in basin fill sediments was developed and validated with Hungarian data, where the highest density of measured temperature values existed. Then the calculation model was extended to the entire project area. The basic hypotheses of the calculation method was that the higher heat-flow (higher values than world average) in the Pannonian Basin is caused by the thinning of the lithosphere (Ádám et al. 1982) that resulted from lithosphere stretching coeval with the formation of the basin (Horváth et al. 2015). Considering that the recent relief of the pre-Pannonian basement evolved parallel with the intensive inflow of sediments, we can suppose that the depth of the basin is proportional to the degree of thinning of the crust (**Hiba! A hivatkozási forrás nem található.** and Figure 33).

In the case of sinking of large sedimentary basins at regional levels, isostasy acts similar to mountain regions, but in the case of the development of deep troughs, another kind of sinking mechanism has to be taken into consideration. We suppose that the less flexible upper crust became fragmented because of the extension of the more ductile lower crust (Kovács et al. 2012). So the main factor in thinning of the lithosphere is the extension of the lower crust (also called lithospheric mantle), while the thickness of the upper crust generally remained quasi constant (**Hiba! A hivatkozási forrás nem található.** and Figure 33). In the case of deep troughs the subsidence by isostasy is not a sufficient explanation, because the calculated missing thickness from the crust would be larger than the world average (40 km) crust thickness. Therefore we cannot calculate the crust thickness under deep troughs, as in the case of isostasy. Deep troughs are considered extension rifts and shear zones caused by horizontal movements in the mantle. These forces cause the thinning of the ductile lower crust and the tear of the rigid upper crust (Figure 33). So we chose a limited non-linear function for the calculation of the crust thickness. The limit of regional sinking by isostasy is approximately 2 km, the troughs originated from the fragmentation of rigid upper crust.

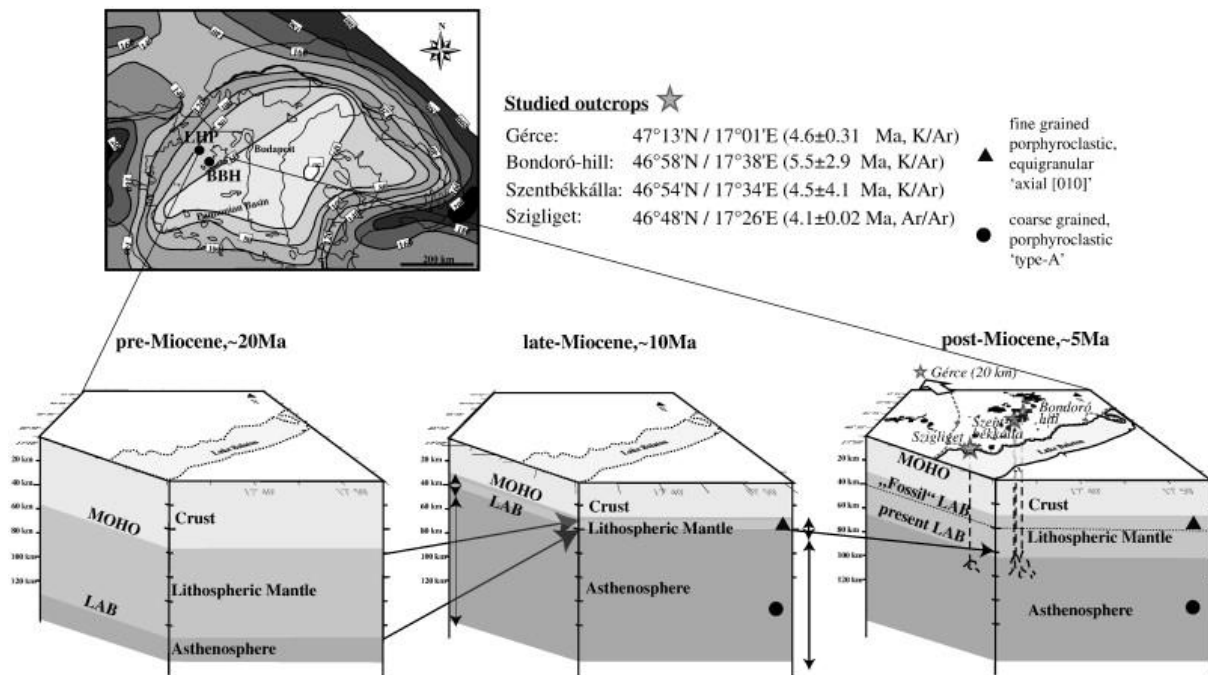


Figure 32. Lithospheric cross-section of the central CPR before the Miocene extension (~20 Ma), immediately after the extension in the Late Miocene (~10 Ma) and in the post extensional (thermal relaxation) stage in the Pliocene (~5 Ma) (Kovács et al 2012).

Abbreviations: BBH — Bakony-Balaton Highland; LHP — Little Hungarian Plain; MOHO — crust-mantle boundary, LAB — lithosphere-asthenosphere boundary, 'fossil LAB' refers to the depth of the LAB immediately after the extension, but note, however, that the present LAB (also probably the one during the alkaline basaltic volcanism) is in a deeper position due to the thermal cooling following the extension, which lead to lithospherization of the extruded asthenosphere

In the model we estimated the heat-flow density in two different ways. The first type of calculation of heat flow is based on the estimated thickness of the pre-Pannonian crust (as upper crust) and from the sediment side considering the followings:

- In the conductive model the temperature of the top of the mantle at the MOHO (the surface between the upper and lower crust (Figure 32) can be considered uniform everywhere (Lenkey et al 2017), it is 1000 °C in our model. Therefore from the scale of the lithosphere thinning, in other words from the crust thickness below the pre-Pannonian basement, we can determine the heat-flow and the basement temperature. The value of the constant thermal (heat) conductivity is supposed to be $\lambda=2.5 \text{ W}/(\text{m}^*\text{K})$ in the pre-Pannonian basement.
- The average bulk heat conductivity of the basin fill sediments depends on the average porosity, while porosity is the function of basin depth. In equilibrium state the primary heat-flow has the constant value (it can be considered as boundary condition of the conductive model) independent from time and depth, only horizontal changes are supposed which only can derive from changing of crust thickness. It means that the heat-flow depends only on the crust thickness, while radioactive decay is neglected (Zilahi 2013).

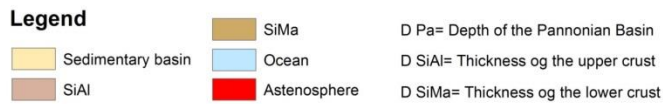
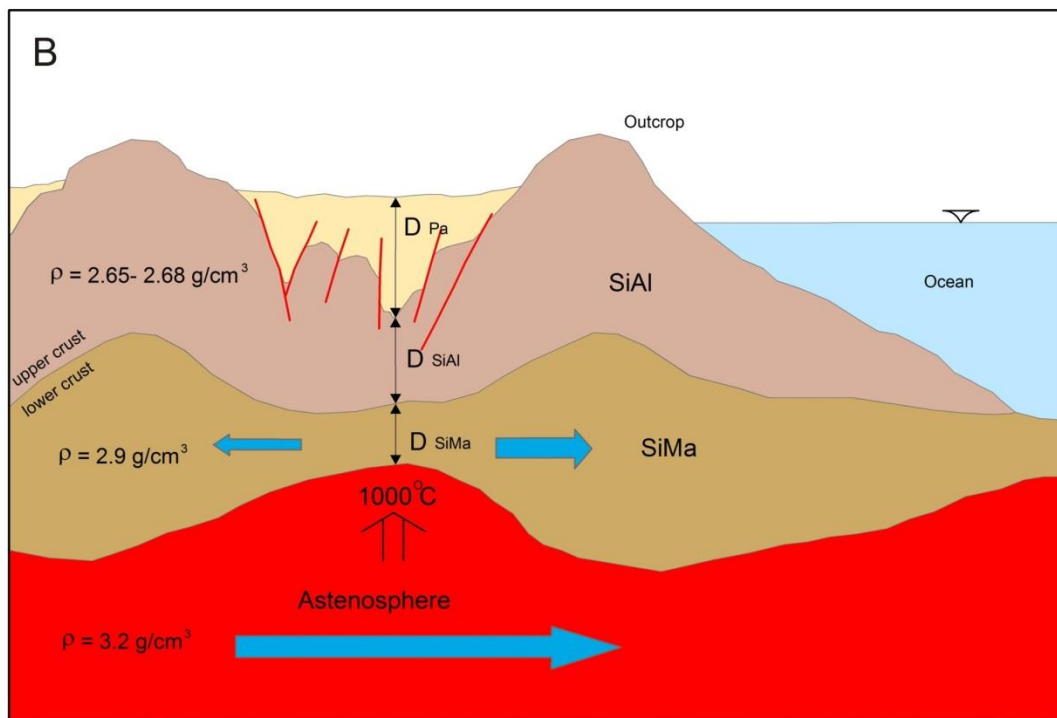
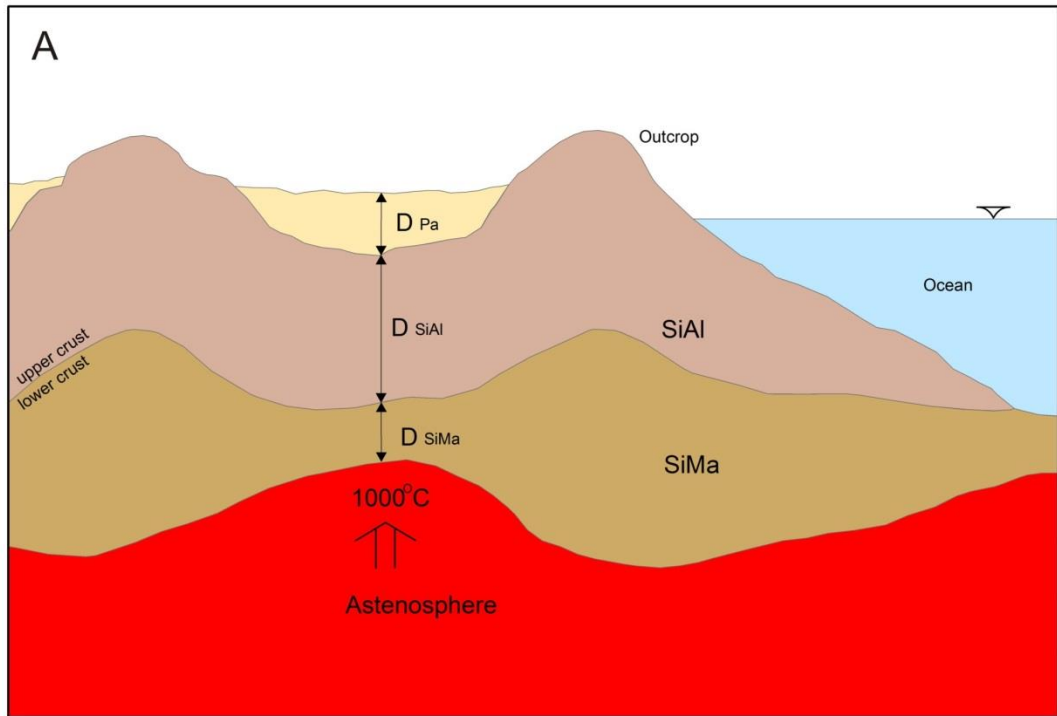


Figure 33. Theoretical scheme of isostatic sinking (A) and the crust fragmentation due to asthenosphere movement (B)

The two different calculation methods have to result the same value. Applying these estimations we can express the depth of the pre-Pannonian Basin.

The calculations of the isotherm surfaces in the basin fill sediments are performed as multiplying the depth with the average geothermal gradient. It means that horizontal variation of the temperature is considered as a function of the actual depth of the pre-Pannonian basement (Figure 34).

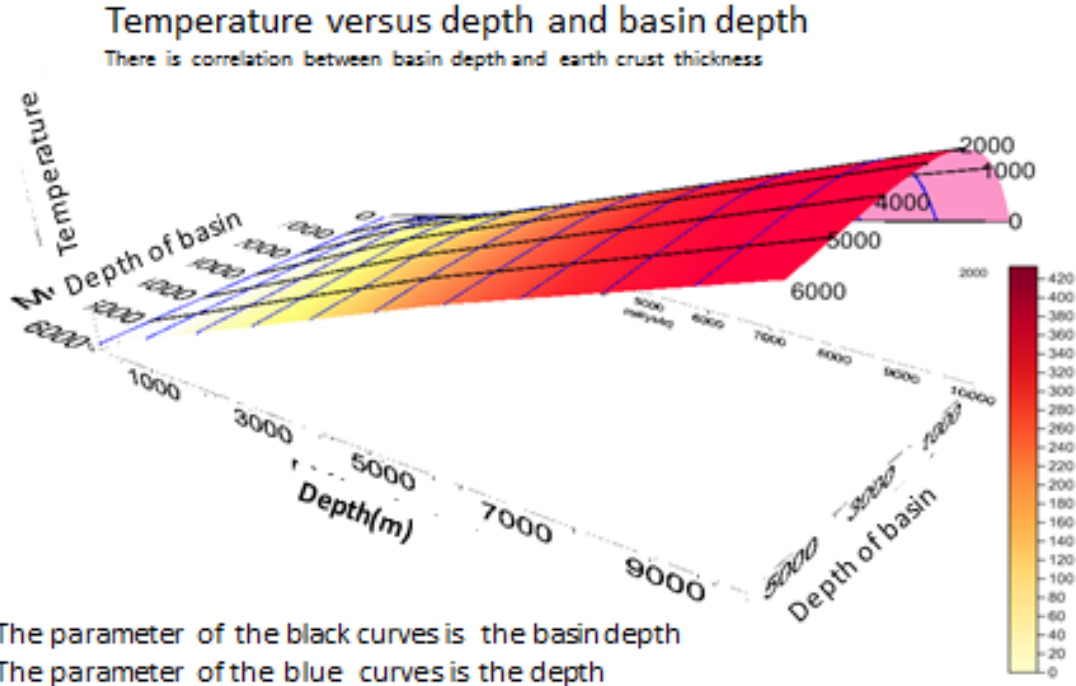


Figure 34. Temperature vs. depth and basin depth

So the actual temperature in the basin fill sediments can be calculated with a function where the parameter of this function is the spatial variation of heat-flow density, which represents the changes of the basin depth (depth of the pre-Pannonian basement). The latter reflects the changes of the crust thickness.

The contour maps of the resulted isotherm surfaces are illustrated in Figure 35 -Figure 40.

For the validation of the modelled temperature distribution, we compared the real temperature measurement data with the same location of the grid map. The comparison statistically shows very close connection, but locally some differences occur. It has to be noted the isotherm surfaces are based on a conductive model, therefore don't contain the effect of advection. So, bigger differences are expected in the regions where convection (modifying effect of groundwater flow) has important role in spatial subsurface distribution of temperature (Figure 41).

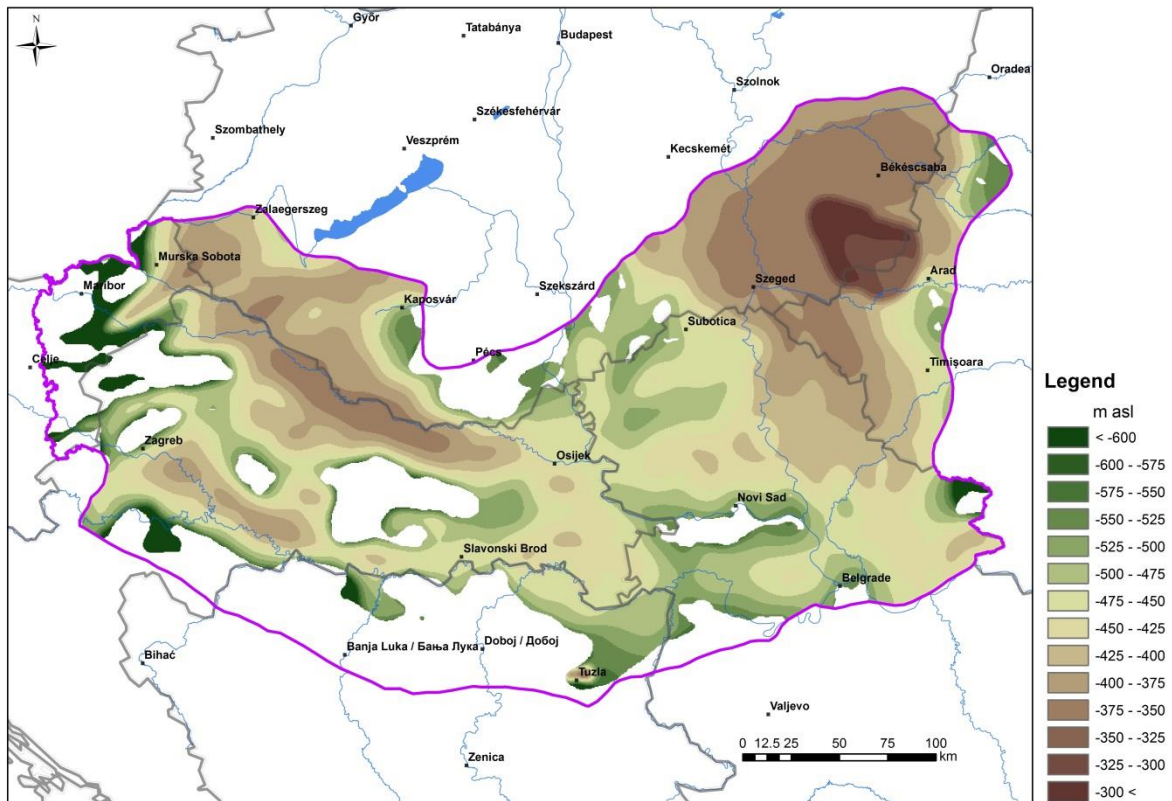


Figure 35. Calculated 30 °C isotherm surface in the Neogene sediments

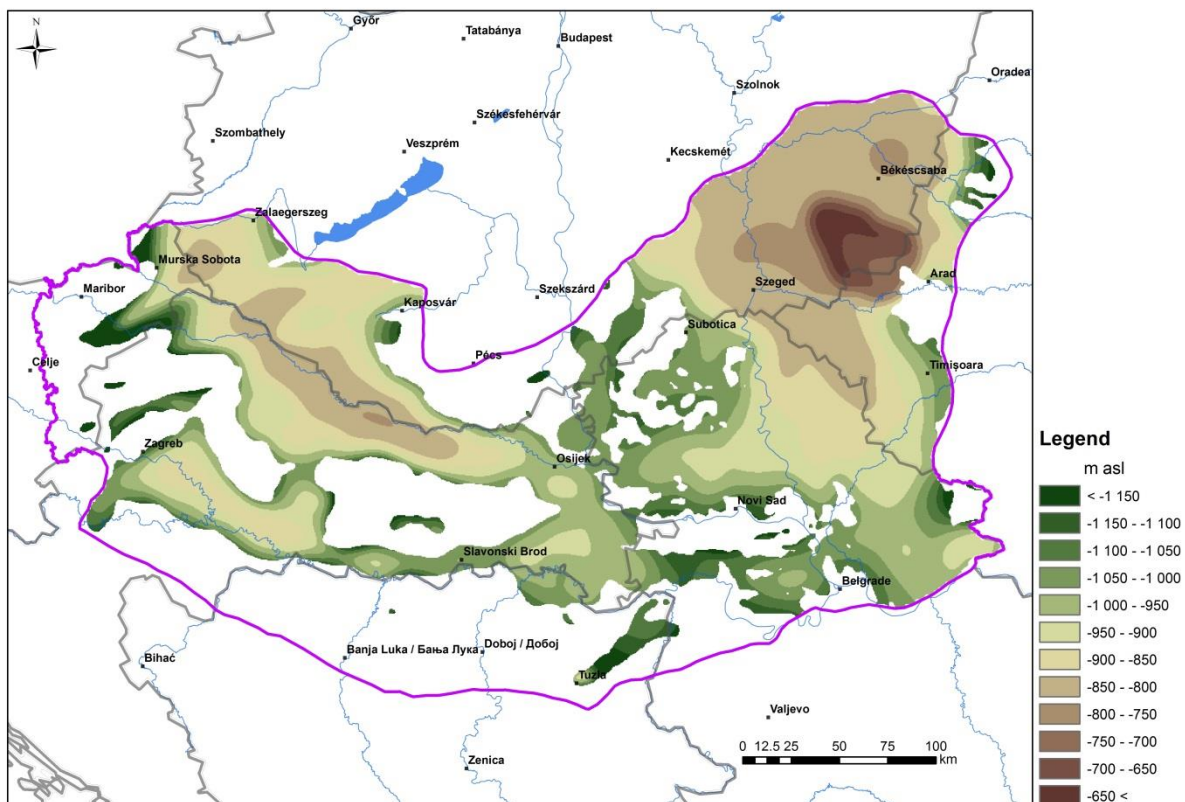


Figure 36. Calculated 50 °C isotherm surface in the Neogene sediments

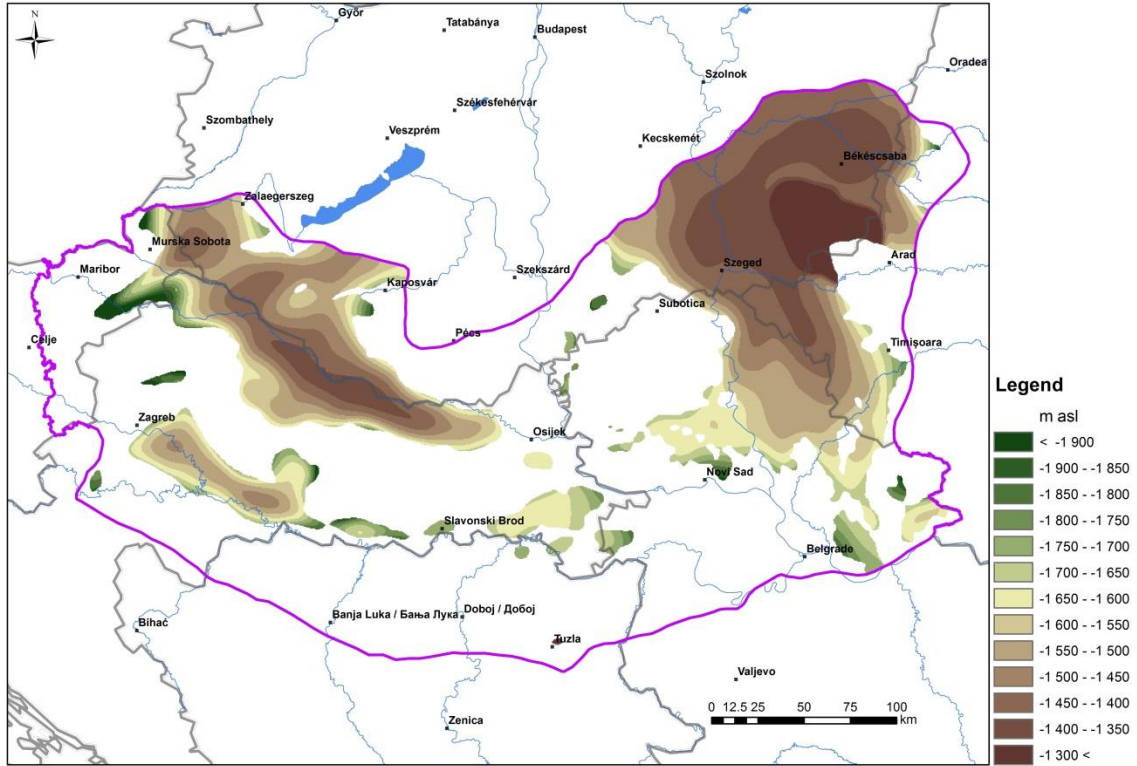


Figure 37. Calculated 75 °C isotherm surface in the Neogene sediments

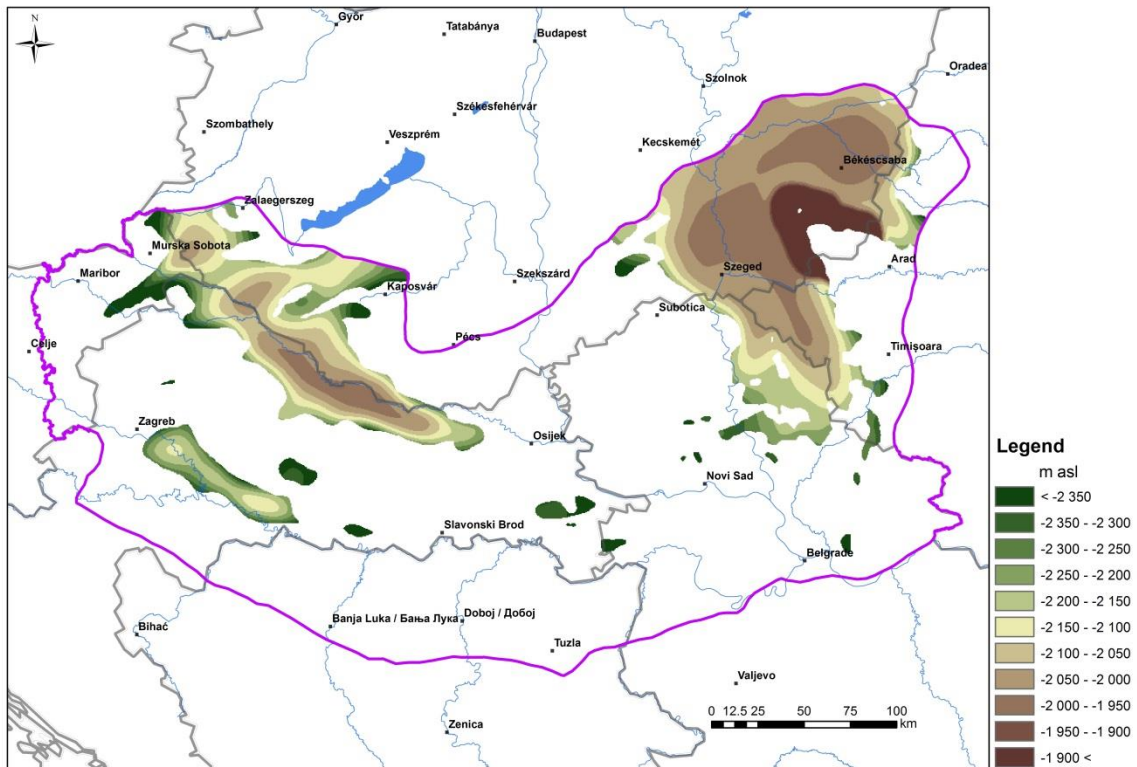


Figure 38. Calculated 100 °C isotherm surface in the Neogene sediments

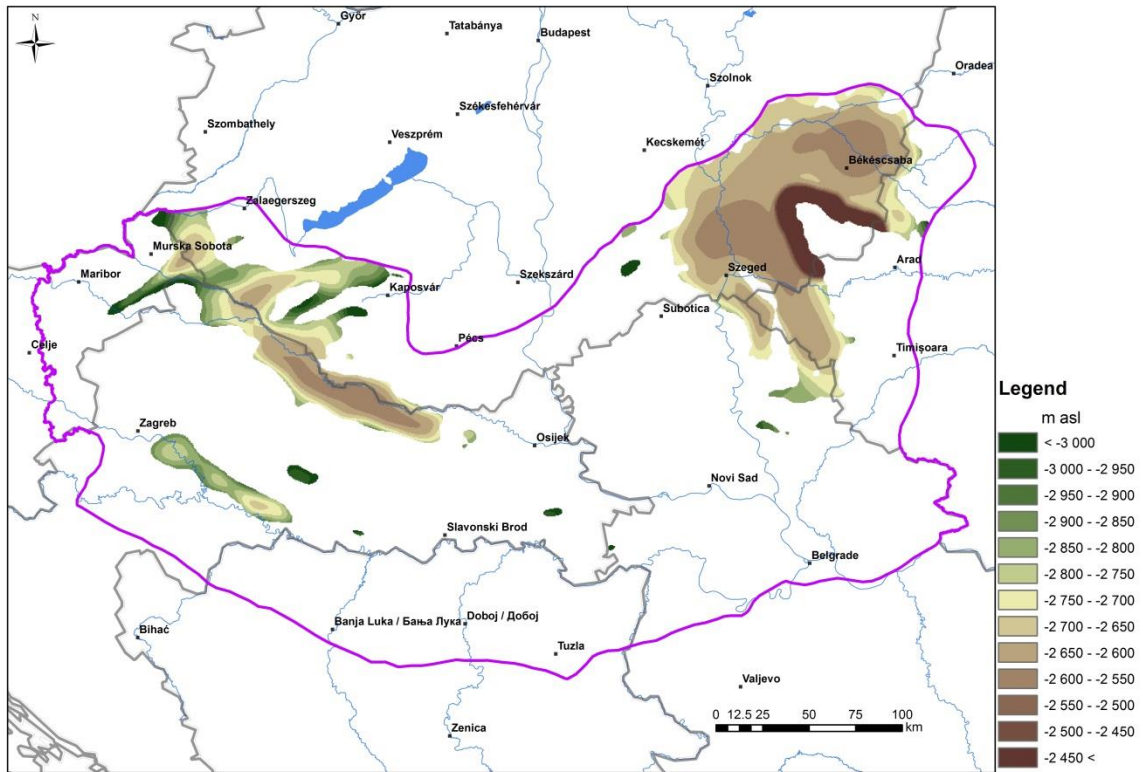


Figure 39. Calculated 125 °C isotherm surface in the Neogene sediments

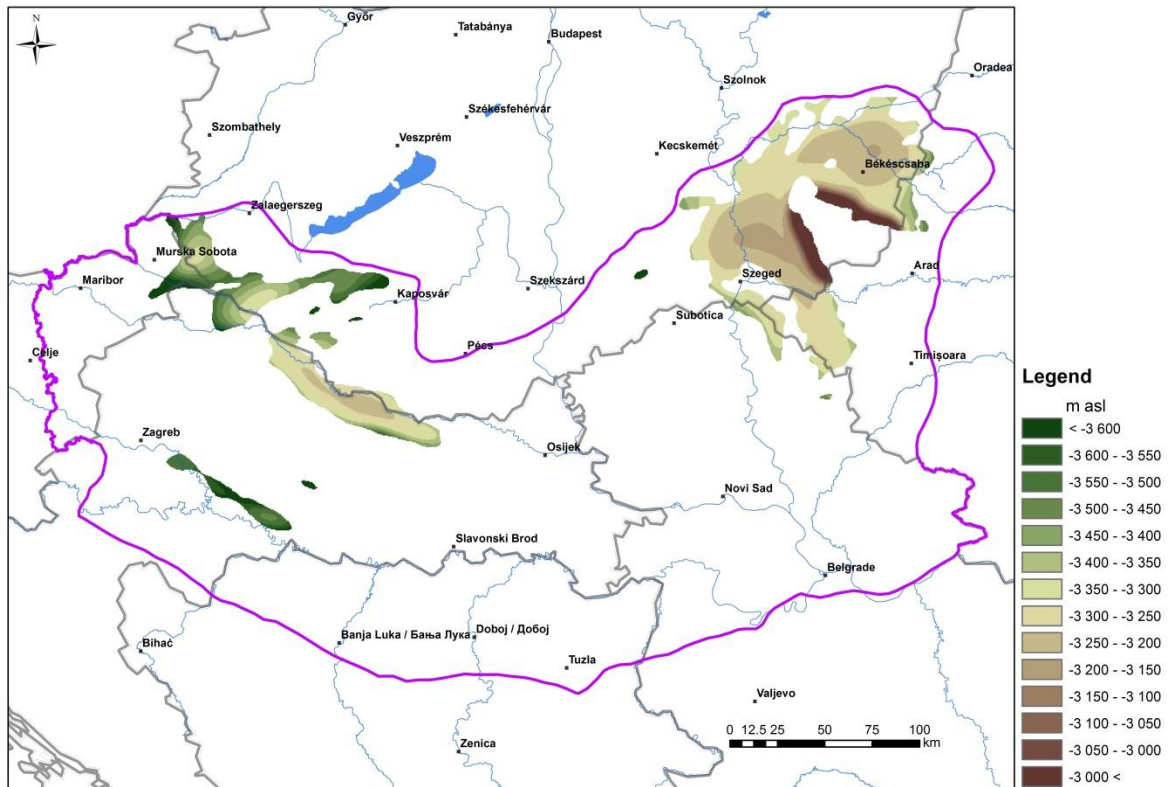


Figure 40. Calculated 150 °C isotherm surface in the Neogene sediments

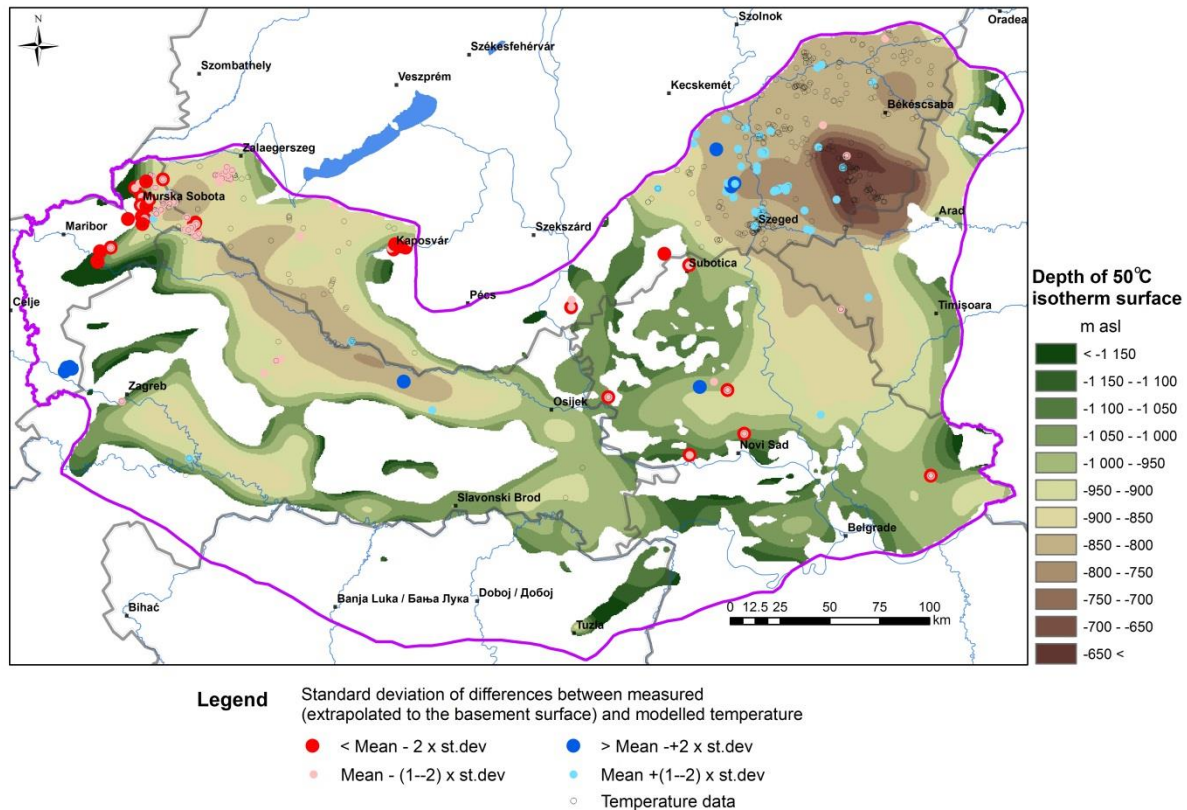
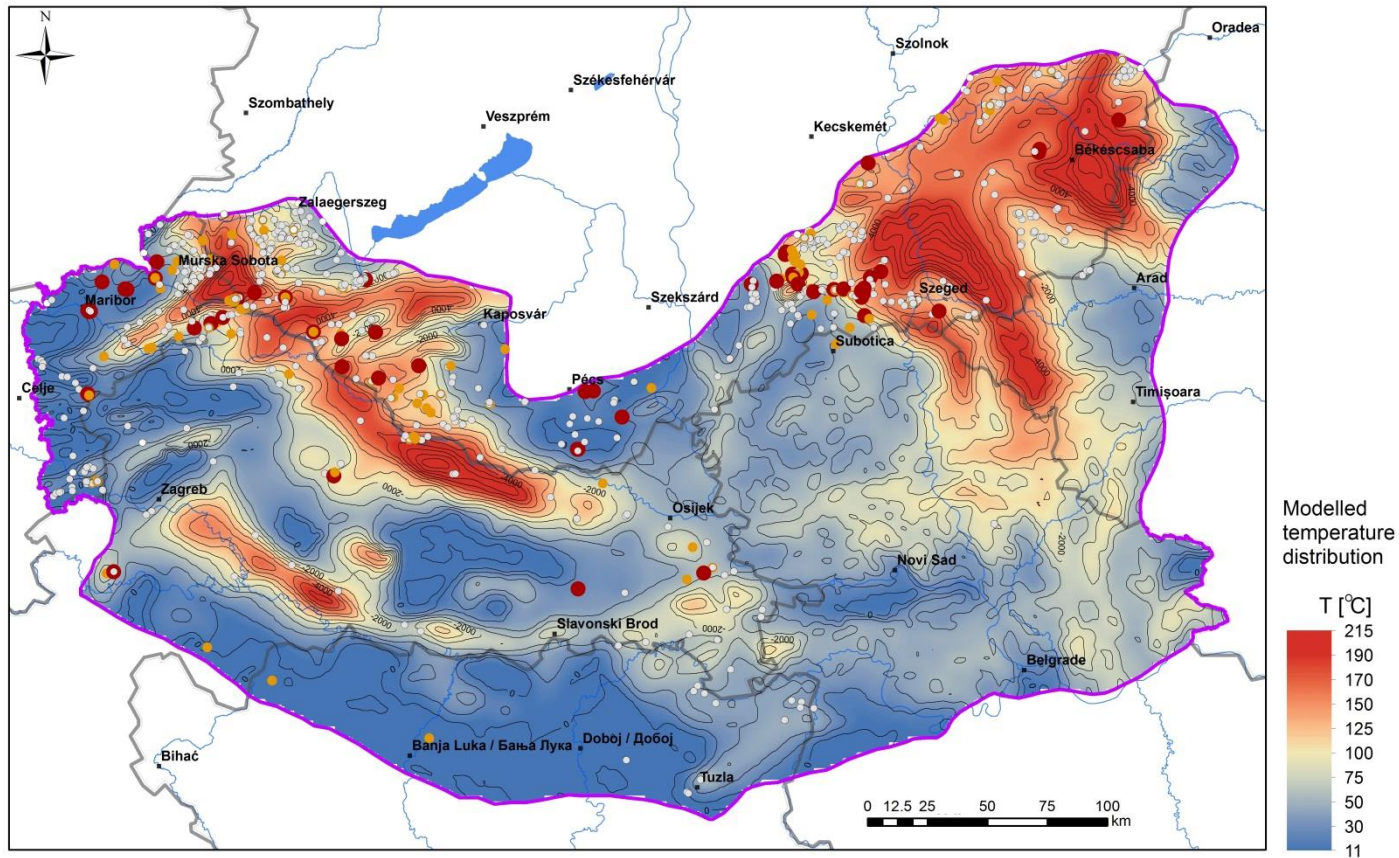


Figure 41. Comparison of 50 °C isotherm surface to calculated depth of 50 °C value from measured temperature values in wells

7.3.2. Temperature calculation in the pre-Cenozoic basement

The temperature value of the pre-Cenozoic basement surface was also determined by conductive modelling. A more simple formula was used, which is also based on the estimated thickness of the Pannonian basin. Further modification (simplification) was applied in the regions where the pre-Cenozoic basement outcrops.

It is important to mention, that the estimated temperature is the result of a conductive geothermal model applied, but in most of the cases convection is the prior process in basement formations (especially in karst formations) and in the case of convection, calculated data can differ from the real values significantly. Nevertheless, the comparison of the calculated values of the conductive model to the measured temperature values in the basement formation is very important from geothermal potential point of view, because anomalies indicate the regions of intensive thermal convections. These regions are the most prosperous regions with high thermal potential (Figure 42). Regions with high differences can be interpreted as areas with high geothermal potential, but low reliability of temperature measurements must be considered in case of individual measured temperature data.



Legend Standard deviation of positive differences between measured (extrapolated to the basement surface) and modelled temperature

- < Mean + 1.5 x standard deviation
- Mean - (1--1.5) x standard deviation

— Depth of Pre-Cenozoic basement m a.s.l.
 ○ Temperature data

Figure 42. Geothermal potential map of the basement reservoirs
 Comparison of the temperature estimated (by the conductive model) at the top of the basement to the measured temperature values which was extrapolated to the top of the basement

7.4. Reservoir delineation

Delineation of the two main types of geothermal reservoirs (BF and BM) was carried out by different ways.

7.4.1. Basin fill (BF) reservoirs

Delineation of BF reservoirs was based on the combination of their bounding geological surfaces and the respective isotherm surfaces. Technically the outlining of reservoirs was carried out by applying SURFER and ArcGIS softwares. The combination of selected geological and isotherm surfaces needed several detailed considerations. The grid structure of the geological and isotherm surfaces has to be totally identical with the grid size of 100x100 m. Outcropping regions were considered as grid points without values (blank nodes). Reservoirs are identified as 3D bodies; therefore both the grids of the top and bottom surfaces of the reservoir bodies were constructed.

BF reservoirs with all temperature categories (up to 150 °C) are located in the deep sub-basins of the Pannonian Basin (Makó Trough, Békés Basin, Drava Basin, Sava Basin). A significant decreasing in the reservoirs' extension can be observed parallel with increasing depth and temperature.

For example, the combination of the top of the BF reservoir geological surface and 30 °C isotherm surface designates the minimum depth of available thermal water (temperature higher than 30 °C) in the Pannonian sedimentary succession. In most of the places the BF top horizon coincides with the bottom of Quaternary sediments, however in some deep sub-basins it cuts into the deepest layers of the Quaternary deposits. These deep parts of Quaternary sediments are also considered as potential geothermal reservoirs, but due to their shallow depth usually their temperature is just slightly above 30 °C. There are only some exceptions for this, for example in the deepest part of the Drava sub-basin and the Makó Trough where temperature can exceed 50 °C in the Quaternary formations. However, it is worth to mention that the separation of Quaternary and the very similar Pliocene fluvial sediments sometimes is rather uncertain in these areas (Figure 43 and 44).

Similarly to the above mentioned methodology, the combination of the geological horizon showing the top of the BF reservoir and 50 °C isotherm surfaces designates the minimum depth of available thermal water with temperature higher than 50 °C in the Pannonian sedimentary succession, and so on. The deepest reservoir is the BF125-150, which is restricted for a very small area within the Drava basin where temperatures are slightly above 125 °C.

The locations of the different reservoirs are illustrated in Figure 45-Figure 52.

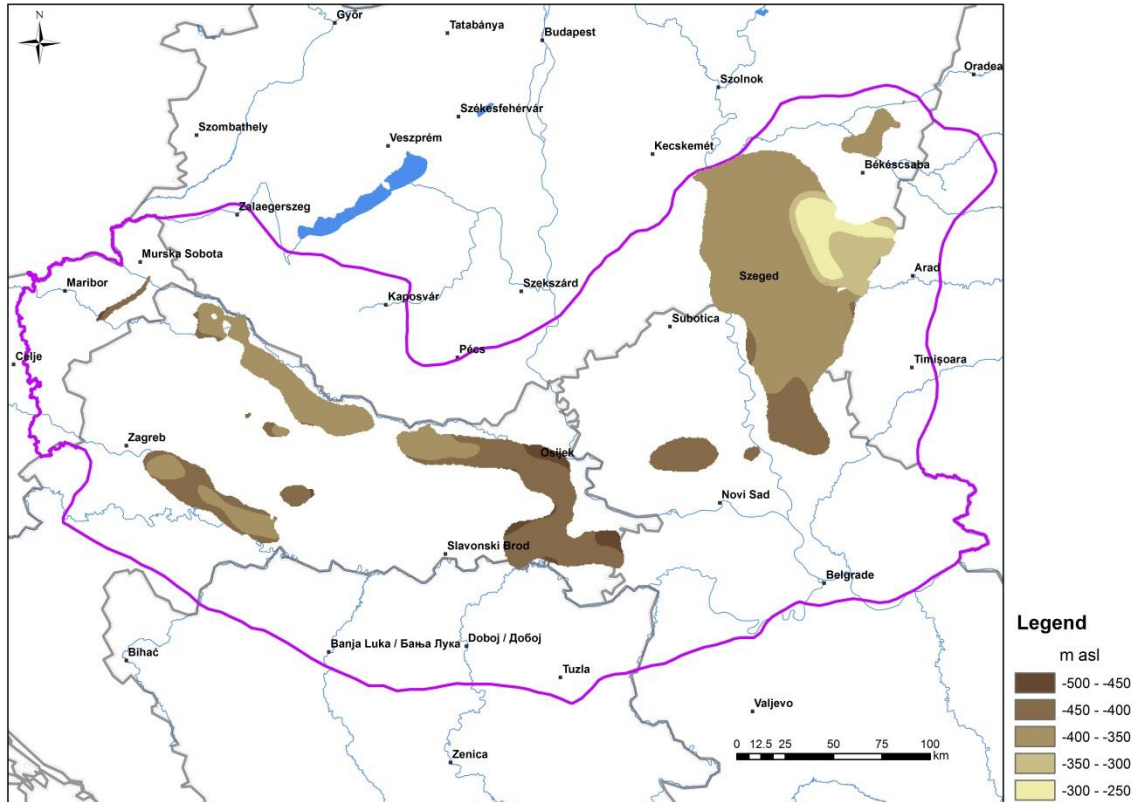


Figure 43. Top surface of the low temperature Quaternary potential geothermal reservoirs

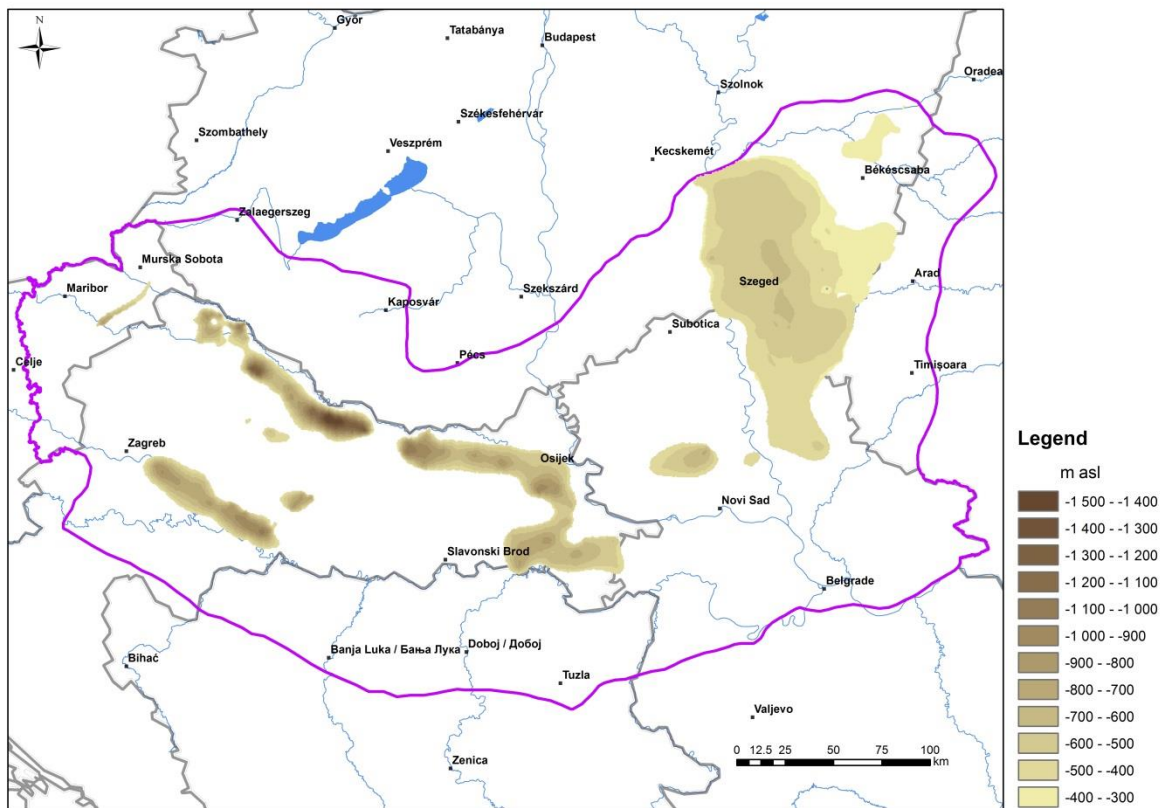


Figure 44. Bottom surface of low temperature Quaternary potential geothermal reservoirs

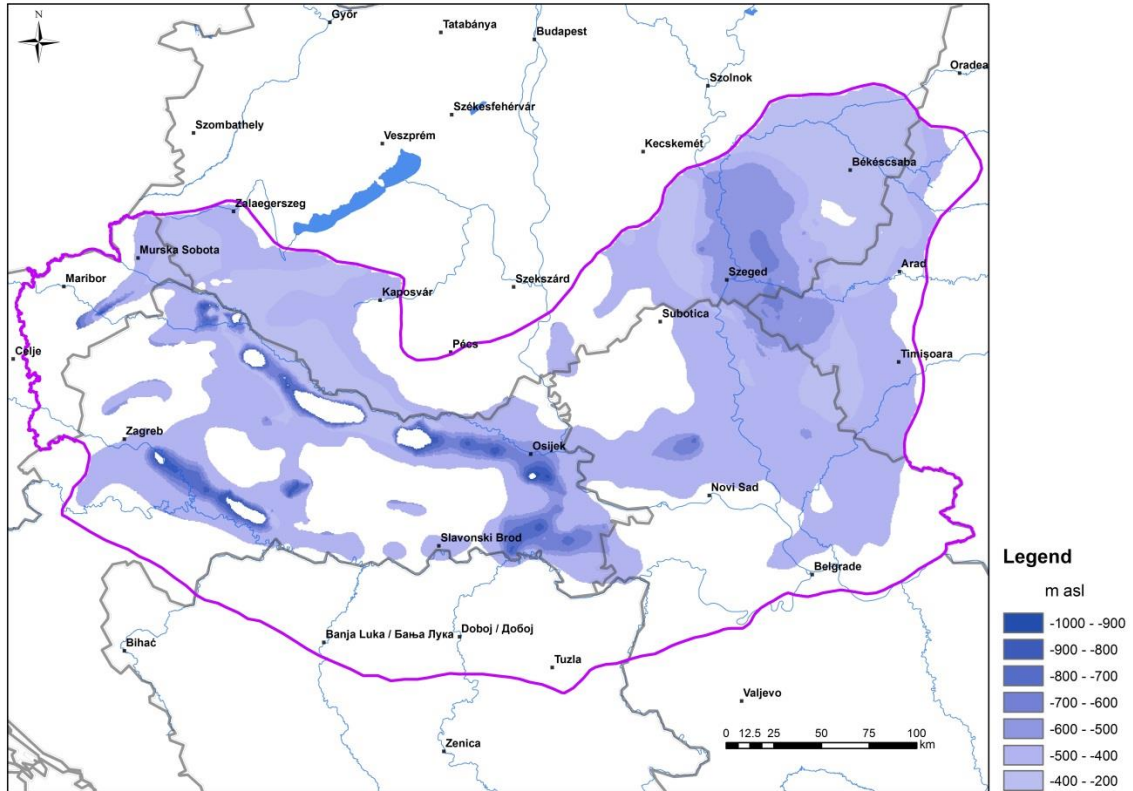


Figure 45. Top surface of the BF30-50 reservoir

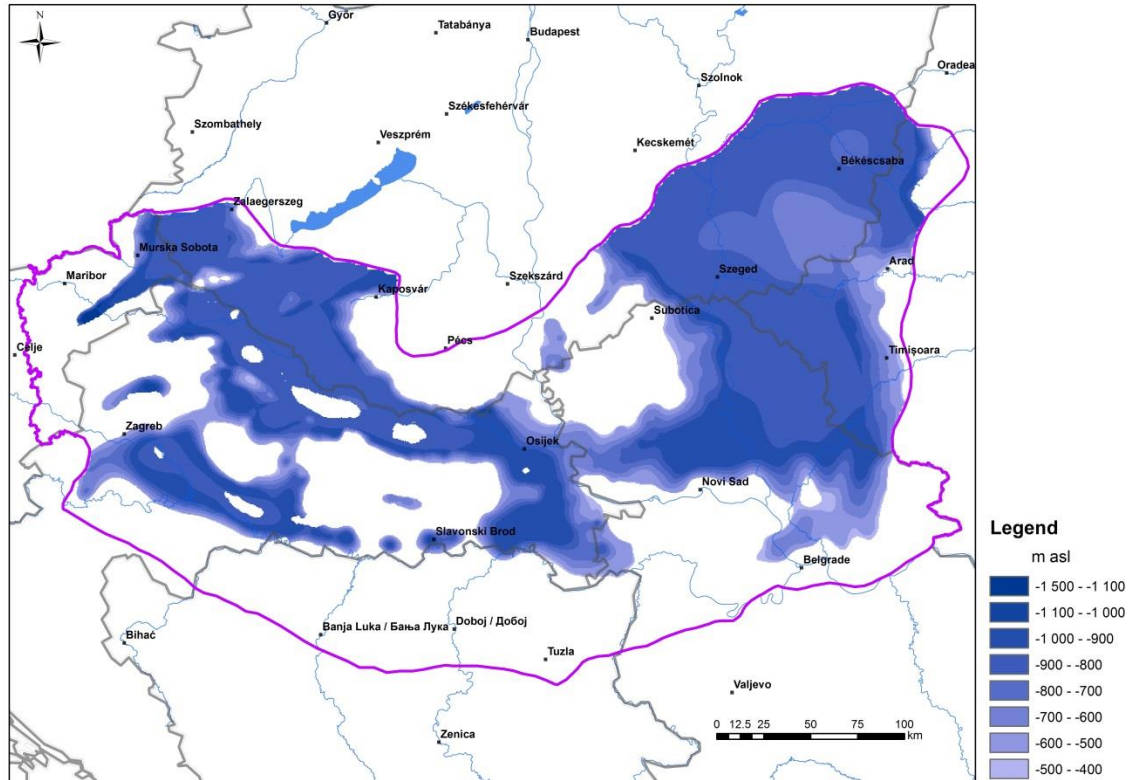


Figure 46. Bottom surface of the BF30-50 reservoir

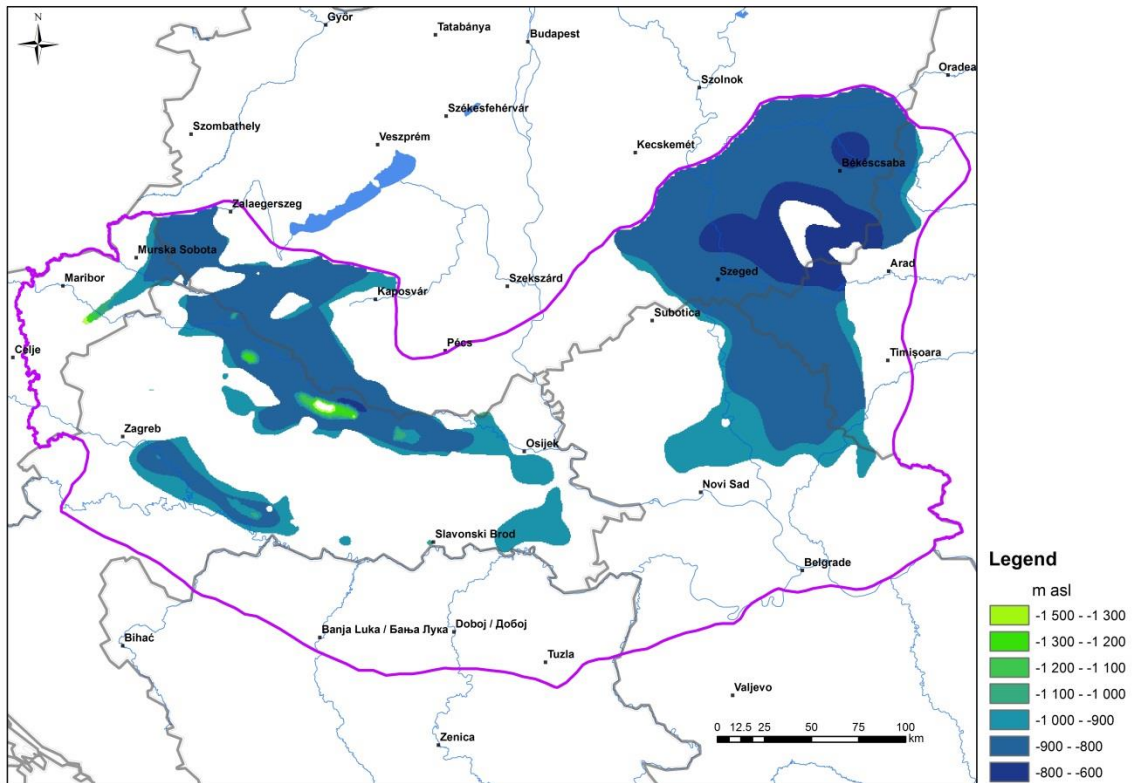


Figure 47. Top surface of the BF50-75 reservoir

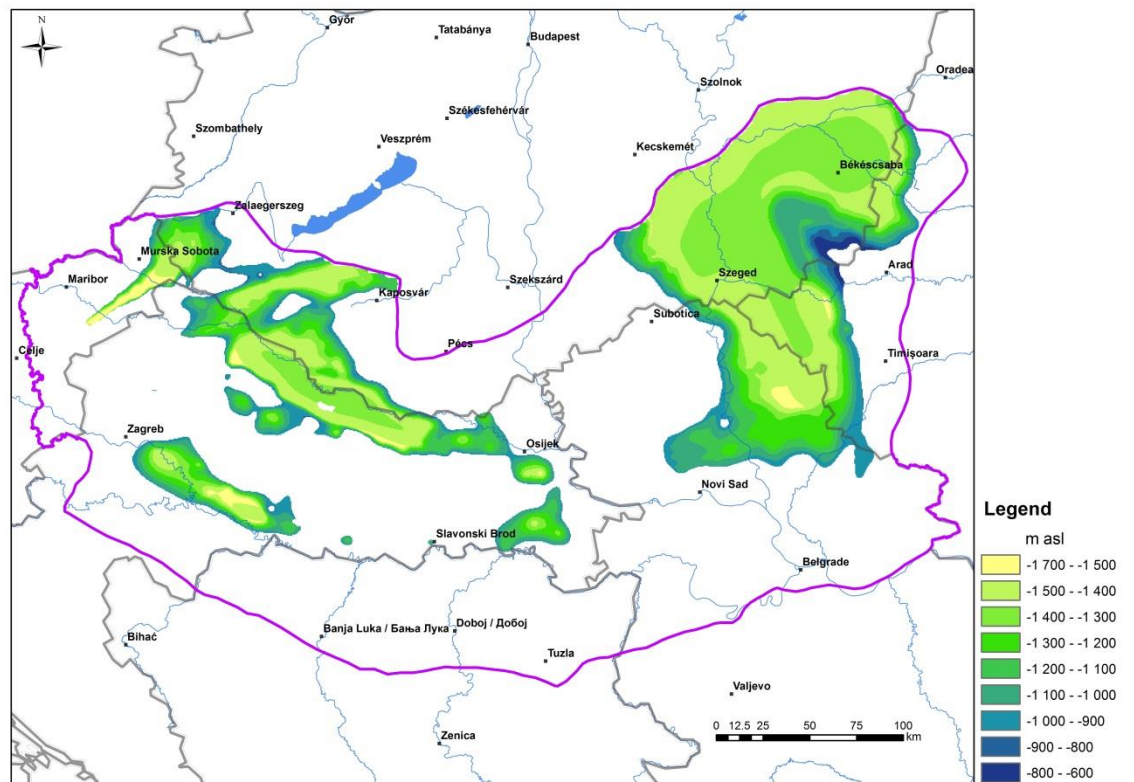


Figure 48. Bottom surface of the BF50-75 reservoir

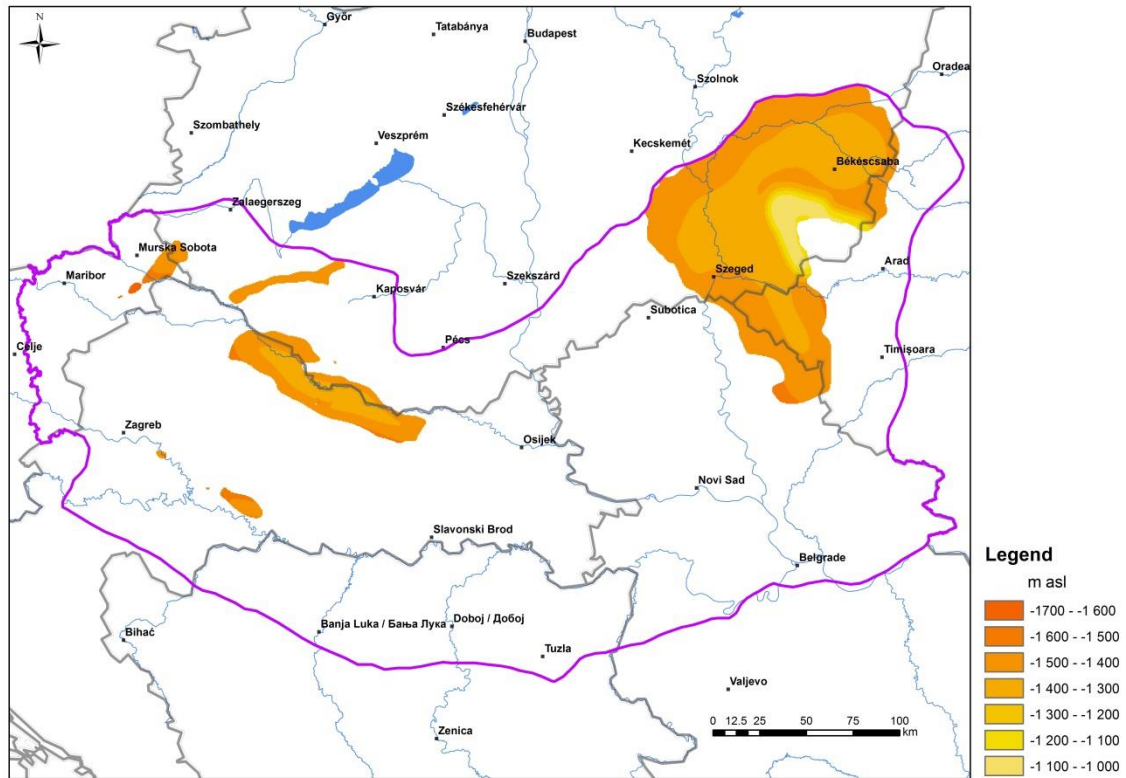


Figure 49. Top surface of the BF75-100 reservoir

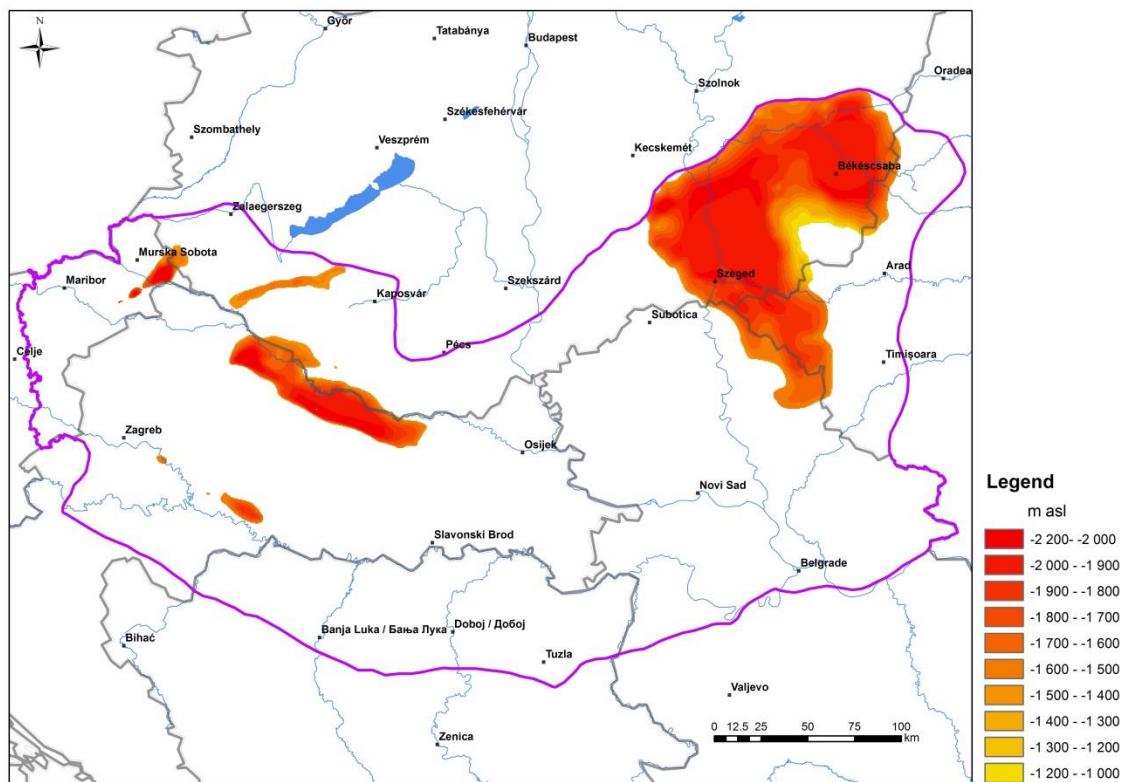


Figure 50. Bottom surface of the BF75-100 reservoir

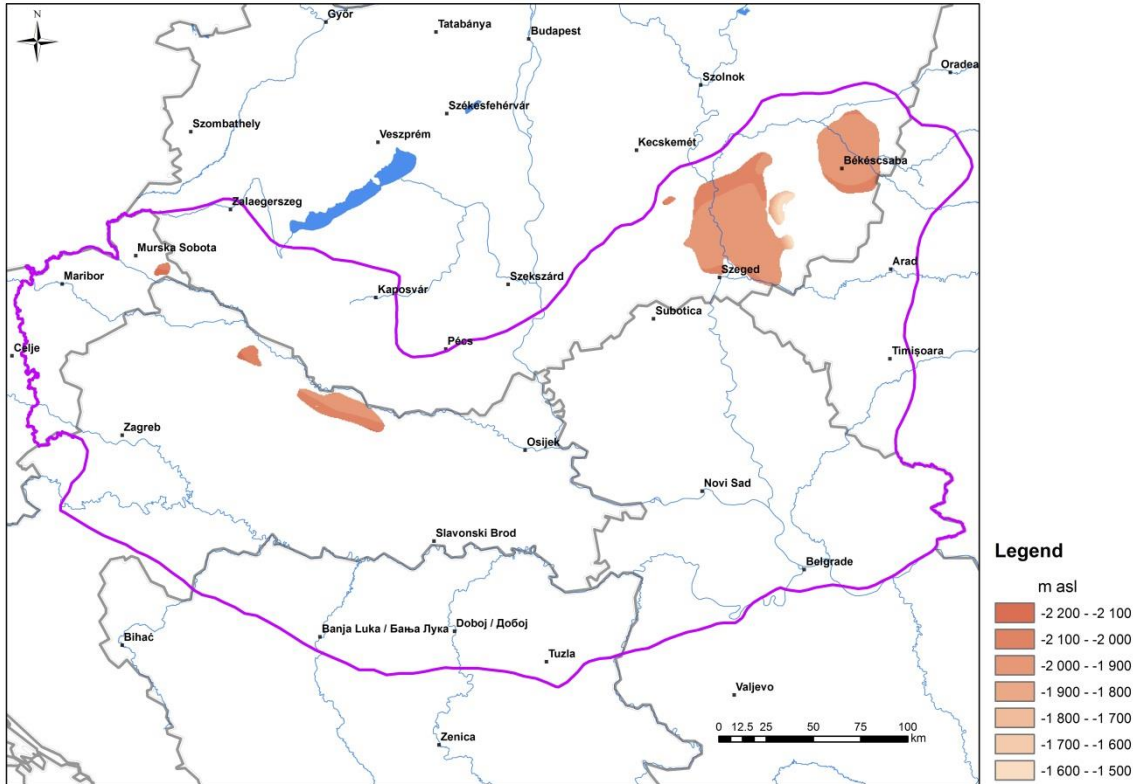


Figure 51. Top surface of the BF100-125 reservoir

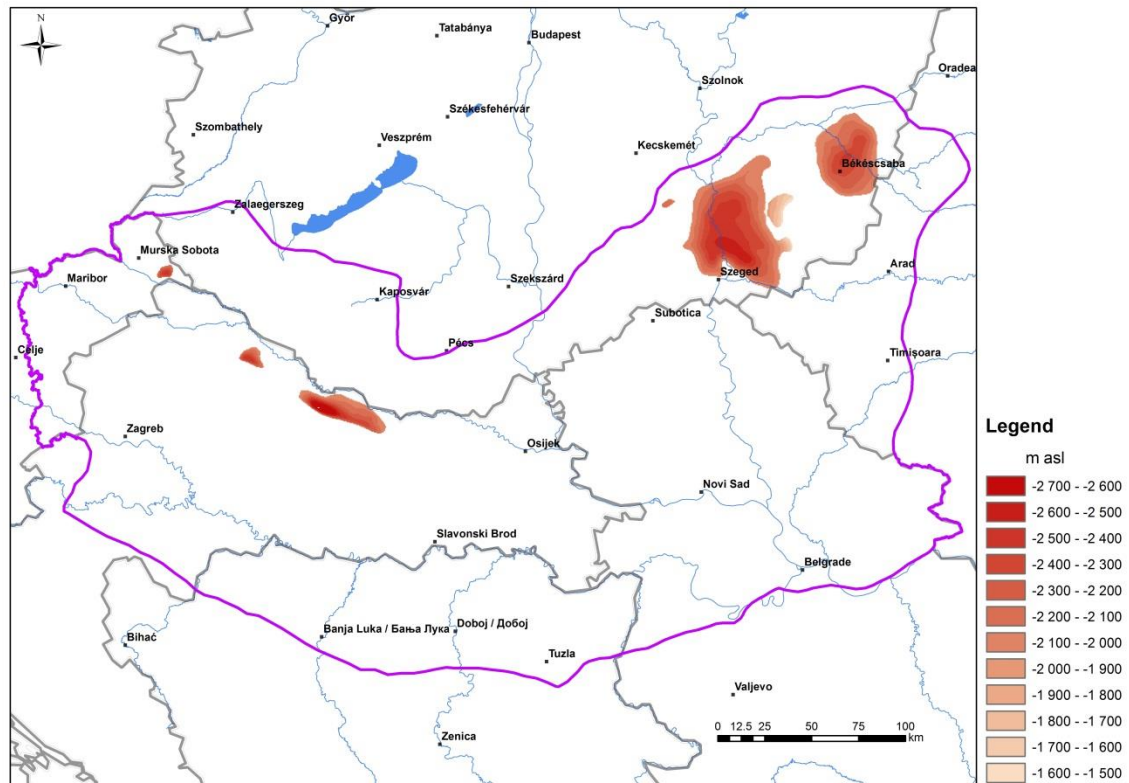


Figure 52. Bottom surface of the BF100-125 reservoir

7.4.2. Basement (BM) reservoirs

Combination of isotherm and geological surfaces is not applicable in the basement reservoirs. During outlining of basement reservoirs the relevant geological formations cannot be identified due to the scattered data in the complex geological environment. Additionally, due to the different hypothesis about tectonic evaluation of the project area and uneven geological data distribution, it was not possible to construct a common geological map showing the basement formations in the time-frame of the DARLINGe project. Therefore, we provide a general description of the potential basement reservoirs, followed by short descriptions about the basement reservoir regions of the different partner countries, based on current geological knowledge.

7.4.2.1. General description of basement reservoirs

Basement reservoirs in the Pannonian Basin are connected to those formations of pre-Cenozoic age, which are brittle and due to various processes, the secondary porosity of the rock frame could have been increased at such a level, that it is able to store a geothermal fluids suitable for economical exploitation. The brittle rocks in the basement are mostly carbonate (limestone, dolomite), crystalline (granite, granodiorite, gabbro, gneiss, mica-schist,) and subordinately volcanic (andesite, basalt) formations. Processes increasing porosity are weathering, karstification and tectonism.

During the geological evolution history, some of these rocks were sub-aerially exposed. In the course of weathering, the top surface of the outcropping rock is exposed to disintegration due to the interaction with the atmosphere. The physical weathering is the breaking down of rocks as result of temperature change, freezing of water, pressure change or growth of salt crystals. The chemical weathering is result of interaction of rock with chemicals having atmospheric or biological origin. All kinds of rock are exposed to both physical and chemical weathering, the efficiency of latter is higher at warm and wet climate. The process of chemical weathering of carbonate rocks on tropical and temperate zone results the striking features of karst, this process is called karstification. The intensity of karstification primarily depends on the duration of the process, while the rock was outcropping interacting with the atmosphere, the type of climate and the depth of karst water level, as erosional base. The longer duration, the warmer and wetter climate and the deeper karst water level will result more porous rock frame. The evaluation of time gap between the age of carbonate layer and of the overlying cap rock could give an indication on the length, therefore also on the intensity of process. During the evaluation the possible erosion of layers not presented in the geological record of a given area should be taken into consideration too (Figure 53).

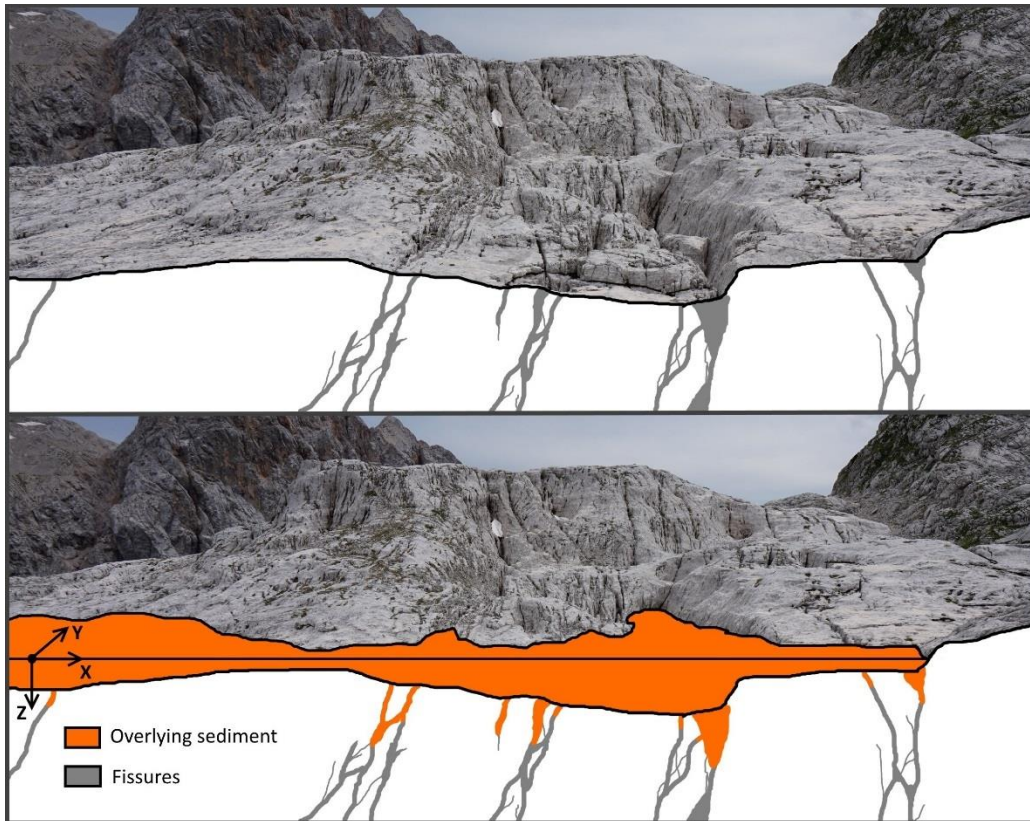


Figure 53. Recent analogue: Interpreted fissure network of a karstified limestone plateau in cross-sections before and after the arrival of overlying sediments. The sediments are filling the top part of the fissures, but the deeper part remains unplugged. The background picture was shot near Rjavo jezero (Brovn Lake) in Triglav Lakes Valley, Slovenia.

Overlying coarse-grained formations are used to preserve the increased porosity of the previously outcropped and weather surface, while overlying fine grained sediments are used to deteriorate the permeable properties of the underlying formation. The well-developed karst features are less sensitive for permeability decrease induced by fine grained sediments, because the deep part of the fissures may remain partly open (see Figure 53). Nevertheless the deep burial generally decreases previously developed fractured/karstic porosities.

Tectonism is the third process, which could create secondary porosity in formations. Sometimes it is so efficient, that at certain type of geothermal reservoirs (e.g. recent volcanic systems along active plate boundaries) this is the only one process, which creates in full extent the resource itself. Tectonic processes break the rocks along faults and fractures, which provide conduits in brittle rocks for flowing of geothermal brine. The former and recent tectonism of an area will have effect on the spatial distribution and density of a fracture network. An eventful history of tectonism will likely result numerous fractures in a several hundred million years old granite compared to a few million years old one. The present-day stress field has effect on the permeability of the fracture network, because the fractures oriented perpendicularly on maximum stress are prone to be tight, while the parallel and sub-parallel fractures are likely to be open and conductive. In case of sub-vertical and vertical open fractures, the geothermal brine can flow effectively upward causing positive geothermal anomaly, because the way of heat-flow is convective. This phenomenon reduces the geothermal gradient in the reservoir, which has effect on drilling cost, because increase in drilling depth will result less increase in resource temperature compared to conductive systems.

The above described subsurface features of basement reservoirs are presented on Figure 54.

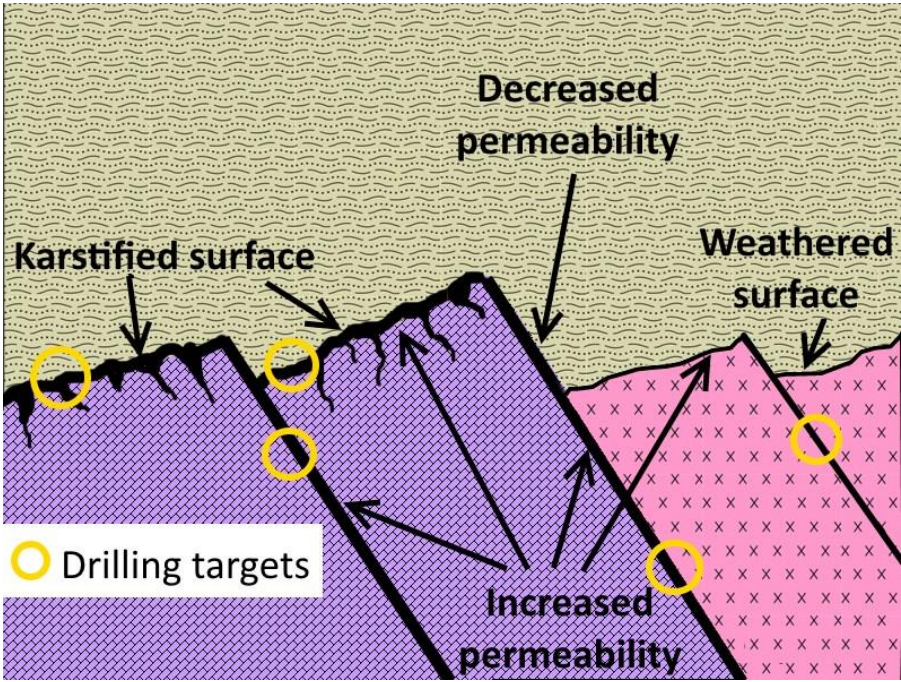


Figure 54. Simplified geological model of a basement reservoir characterized by increased porosity. The top part of crystalline rock was exposed to weathering, while the top part of limestone layer was karstified prior to the deposition of overlying sediments. The sub-vertical fractures within the basement are likely conductive, if they are not perpendicular on maximum stress. The upper part of the fractures, where it is bordered by fine-grained sediments, are likely less permeable, in those cases when faulting is approximately coeval with overlying sedimentations,. The suggested drilling targets, like faults and karstified surfaces are indicated on the figure.

Adequately known spatial distribution of zones characterized by increased permeability within basement reservoirs could provide significant help to locate target zones for geothermal drilling. In this respect the karstified surfaces of carbonate formations, and faults within the reservoir could be the most permeable feed zones for a well. The probability of success might be increased if the well aims two targets e.g. a karstified surface and a fault beneath it. The surface of young faults, which is covered by fine grained sediments doesn't seem ideal as well target. There are several processes which decrease the likelihood of having increased permeability in these zones. To demonstrate this on a surface analogue (Figure 55): On one side of the fault the karstic surface was exposed to weathering for a relatively short period compared to the plateau side, so the karstification was less intense, on the other side time for exposure was enough for eroding the loose (permeable) part of the steep fault plain



Figure 55. View on north side of Kanin Plateau between Visoki Kanin and Prestreljenik, Slovenia. The north side of Kanin Plateau is very steep as it is depicted on the elevation profile. The loose part of wall has been eroded away in the past, and the most solid (least permeable) part of the formation is outcropping now.

Taking into consideration that the large scale geothermal developments in the Pannonian Basin of the last decade are targeting basement reservoirs (heat plants in Győr HU (55 MW, built in capacity), Miskolc, HU (60 MW), or power plants: Velika Ciglena, HR (10 MW), Tura, HU (3 MW), it is expected, that increased attention will be paid for the future utilization of this type of reservoirs.

Brittle rocks, like carbonate and crystalline formations have significant extent at certain parts of the basin. There were quite long periods of the geological past, when carbonate and crystalline rocks were karstified and weathered sufficiently. The tectonic history of the basin presents numerous occasions during the Cretaceous, late Paleogene and Miocene, when significant tectonic movements broke formations along faults and fault zones. The basin is still under tectonic stress, which has been measured, evaluated and modelled (Bada et al. 2007). The present model of stress gives a good indication for the expected stress at the deep parts of the lithosphere. As the basement reservoirs to be exploited economically are well above this level, it is recommended to evaluate the stress regime site-specifically. The several decades long exploration of hydrocarbon resources in the Pannonian Basin provides numerous well data and data of surface geophysical measurements. The latter ones, especially the seismic measurements can provide significant help to visualize the surface of the pre-Tertiary basement and the tectonic structures, which are the key targets of geothermal exploration of basement reservoirs.

There are some additional features, which increase the probability of having harvestable basement reservoirs in this environment. Deep and overpressured formations start to develop beneath 2000 m, these indicate that pressure difference can contribute to fluid-flow, and thus heat-flow. Tóth and Almási (2001) interpreted the tectonic compression as the source of

overpressure in the Pannonian Basin. They described conductive tectonic lines and sedimentary windows as pathways of fluid flow, induced by large-size pressure difference from the direction of confined, compressional regime towards the unconfined, gravitational regime. Kovács et al. (2007) modelled the behaviour of fractured, crystalline basement highs, and their model suggested that these structures work like chimneys, and govern heat and fluid flow. Of course, this phenomenon can contribute to the increased heat flow, when conductive fractures and sedimentary windows are presented near the basement high, and the fluid can flow towards the upper, gravitational system. In case of total isolation by pressure seal cap rock on large scale, the flow within the basement remains very limited. There is one additional feature, which might increase the size of basement reservoirs; this is the presence of overlying porous layers. If these layers are hydraulically connected to the basement reservoirs, the volume of the resource might significantly increase in given circumstances.

In the next sub-chapters, the characteristics of pre-Tertiary basement and possible basement reservoirs will be described based on available data by countries. The descriptions provide a high-level evaluation what kind of basement reservoirs are expected by countries along the project area.

7.4.2.2. Romania

In the Romanian part of the DARLINGe Project area the pre-"Pannonian" basement of the eastern Pannonian Basin was reached by wells between -1,000 and -4,000 m depth, and up to -6,000 m, west of Socodor. It consists of three tectono-stratigraphic units, from north to south: (a) the Northern Apusenides, (b) the Transylvanides, and (c) the Median Dacides (the Supragetic Nappe of the South Carpathians, see Figure 56 and Figure 57). These units are separated by two major faults: the South Transylvanian Fault mark the transform boundary between Transylvanides and the Median Dacides, and a large reverse fault delineate the overthrust of the Transylvanides on the Northern Apusenides.

Formerly, these tectono-stratigraphic units were recognized in outcrops and subsurface of the Northern and Southern Apuseni Mountains, and their geology was in some extent proven to be common also in the area under the Pannonian Basin. For this reason, these are presented here as geological assemblages of the Apuseni Mountains (Balintoni, 1994).

(a) The Northern Apusenides, with a continental type crust, consist of two nappe systems: the Codru Nappe System (CNS) in their northern part, and Biharia Nappe System (BNS) in south, each with distinct stratigraphy and tectonics.

- In the CNS, polymetamorphic rocks associated with migmatites and granitoid bodies (U. Proterozoic, Variscan) are the oldest known in the Finiş Nappe. Thick Permian sequences, with rhyolite-basalt volcanism, followed by Triassic limestones were recognized in the Dieva-Bătrânescu and Moma nappes. Also, Triassic to Lower Jurassic limestones are known in the Vaşcău-Coleşti Nappe. In the CNS is also present a Neocomian flysch sequence followed by up to Albian terrigenous deposits (Patrulius et al. 1970-1972).

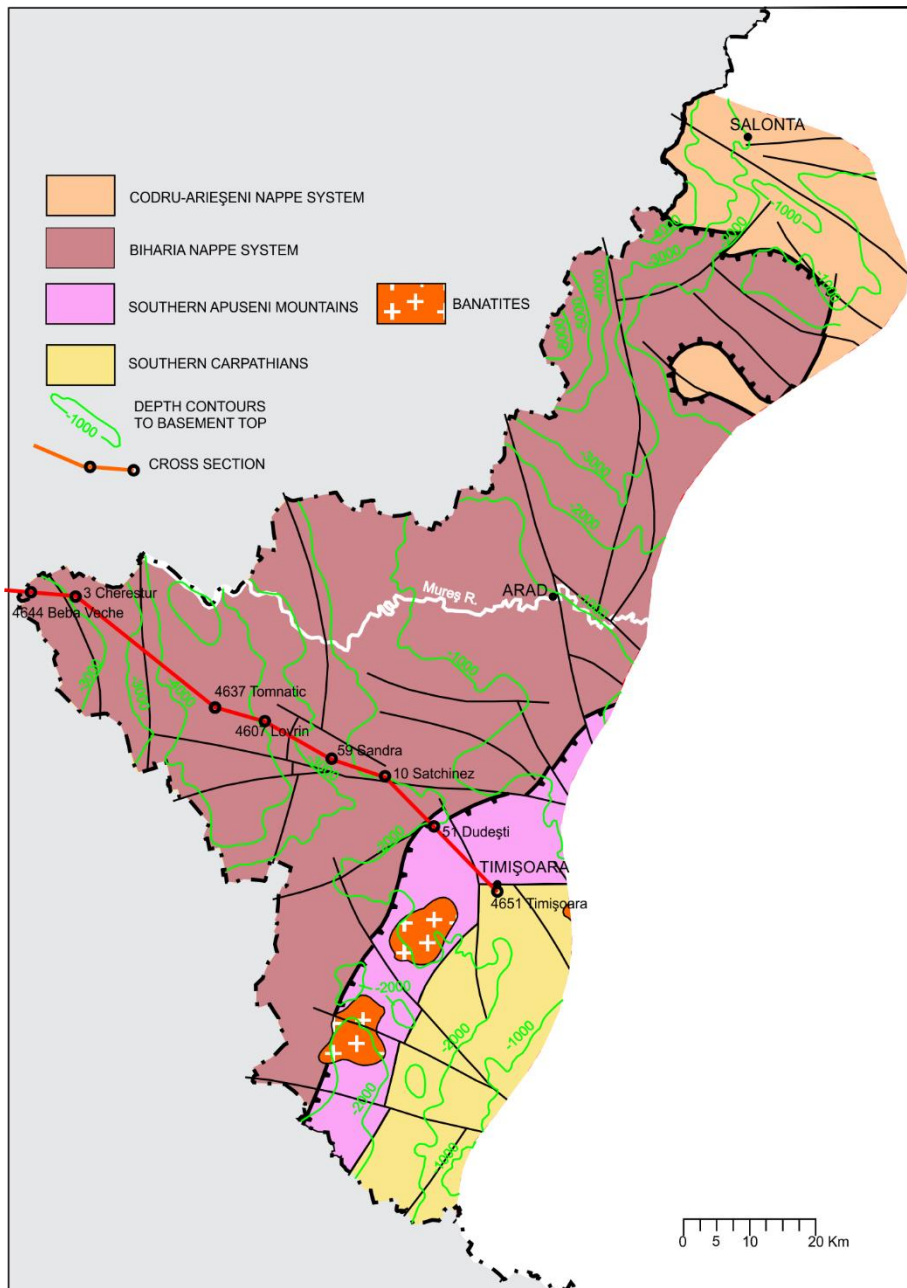


Figure 56. Tectonic units of the pre-“Pannonian” basement in the Romanian project area (after Stănică, 1990)

- In the BNS metabasites and Permian coarse-grained sediments and rhyolites are known, followed by Triassic limestones (Arieșeni Nappe). Also, the Highiș-Drocea massif is built by the epimetamorphic Păiușeni Series, intrusive granites and Permian conglomerates. At Curtici mica-schists and chlorite-quartzose schists were drilled at 2668 m. Basic metamorphites and Permian granitoids were penetrated by wells south of Arad, by Zădăreni-Semlac and Satchinez-Variaș. The metamorphosed ophiolites of the Păiușeni Series were also encountered in subsurface in the area Felneac-Frumușeni, south of Arad. Here it is also expected the presence of limestone bodies, as in the metamorphosed ophiolite complex of the Păiușeni Series in Highiș-Drocea. The contact between the Transylvanides and Northern Apusenides is sealed by Upper Jurassic-Lower Cretaceous sediments, in general limestones. A thin cover of Lower Miocene sediments lies on this geologic feature.

(b) The Transylvanides are built of ophiolites and Jurassic-Cretaceous limestones, forming a ridge at -2,000 m depth.

(c) The Median Dacides consist of Precambrian-Palaeozoic crystalline schists (Buziaş Series) of the Supragetic Nappe, covered by thin, discontinuous Mesozoic formations. Micaschists were drilled at Dumbrăvița, Bacova-Bucova-Dracsina, Giarmata, whereas paragneisses were encountered at Giroc.

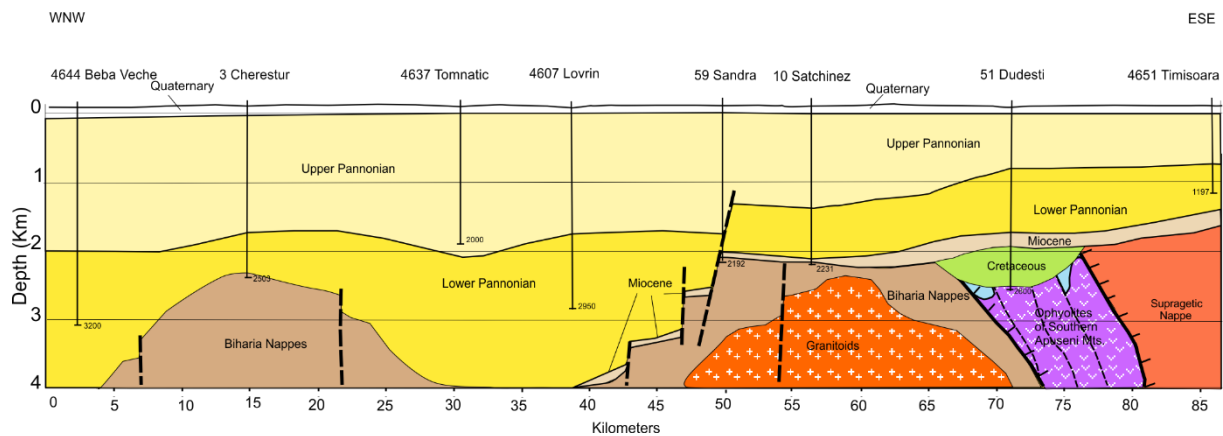


Figure 57. Cross-section Beba Veche – Timișoara, showing the pre-“Pannonian” basement and basin fill. For location see Figure 56.

Major faults are affecting all the mentioned tectono-stratigraphic units extended in the Pannonian Basin basement. Two faults (Lugoj-Zarand and Arad-Sacoșu Mare), trending NNW-SSE, delimit the transverse graben Curtici-Lugoj-Caransebeș.

Between the Nădlac-Lovrin-Beregsău Mic Fault and West Mako-East Cherestur-Teremia Mare-Ruso Selo Fault lies the Sănnicolau-Teremia Mare-Jimbolia Graben, up to 4000 m deep, which deepens northward, in Hungary. Between the two mentioned graben structures lies the Turnu-Timișoara Horst (Stănică, 1990). The deep fractures bordering raised and fallen crustal blocks are still active at present, being responsible for local seismicity in the eastern Pannonian Basin.

Potential basement aquifers

Thermal aquifers are expected to be found in karstified limestones inserted in surroundings of impermeable rocks (metamorphic and other terrigenous and volcanic rocks) wrapped around the limestone bodies. A limiting factor is the volume and extent of the permeable limestone bodies. The Triassic to Lower Jurassic limestones of Northern Apusenides type (as in Dieva-Bătrânescu, Moma, Vașcău-Colești nappes) might constitute geothermal reservoirs, if these rocks are also part of the Pannonian Basin basement (Polonic, 1996).

Early- to Mid-Miocene lithospheric extension caused the thinning of the crust and mantle, accompanied by heat generation in the eastern Pannonian Basin. The heat flow from the upper mantle under the Pannonian Basin contributes to the surface heat flow with over 50%, reaching very high values, exceeding 90mW/m² (Veliciu, 1977). This ensures a high temperature for heating water in the potential basement aquifers. Theoretically, the dense network of deep fractures allows for water flowing to deepest parts of the basement, reaching high temperature, thus resulting high grade thermal aquifers.

The crystalline rocks are continuing towards Hungary along Battonya-Pusztaföldvár basement high (Figure 58), which formed together with the Pannonian Basin. In early Mid Miocene, during

the syn-rift stage, the Makó Basin started to open because of low-angle normal faulting; this is explained by a nappe-shaped boundary within the Tisia unit of Cretaceous age. Originally, the Algyó Ridge was in a lower position than the Pusztaföldvár-Battonya Ridge, and formed the Makó Basin by slipping downward. The downward slip of the nappes caused the surface appearance of a metamorphic core complex from the Algyó Ridge during the Miocene (Tari et al. 1999). There are some syn-rift sediments of Miocene age in the intermediate and deepest parts of the basin. Based on this theory, the Triassic carbonate rocks of Villány-Bihar unit is expected at great depth underneath the crystalline rocks of Codru unit, which might be source of flow and heat at certain areas. The Battonya-Pusztaföldvár basement high has a positive geothermal gradient, but it does not indicate overpressure.

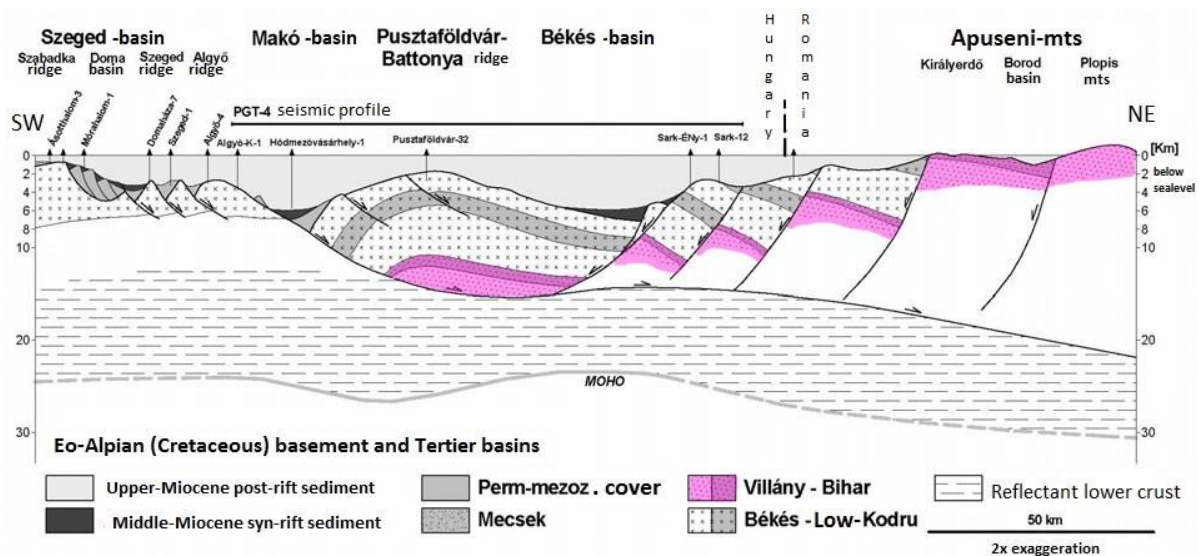


Figure 58. Structural interpretation of Battonya-Pusztaföldvár Ridge (modified after Tari et al. 1999)

On the west side of the crystalline ridge Mesozoic sediments are expected, but their presence is less likely compared to the east side. The next unit towards south is the Mures, Eastern Vardar ophiolite belt. This unit is continuing in Serbia towards the Western Vardar belt. This unit is composed of various formations, like igneous rocks of oceanic crust, and sediments of flysch. Due to the chaotic structure and the almost impermeable character of flysch sediments, this zone shows the least promising area for further exploration. Although, there is a small area, where crystalline rocks are expected on the east side of the Mures belt.

The northernmost area, where Triassic limestone are expected, seems the most prosperous zone for exploring basement reservoirs. The crystalline basement along fracture zones at vicinity of Arad and close to South Carpathians could hide basement reservoirs also.

7.4.2.3. Serbia

The pre-Cenozoic basement on Serbian part of project area consists of various rock formations, (Figure 59).

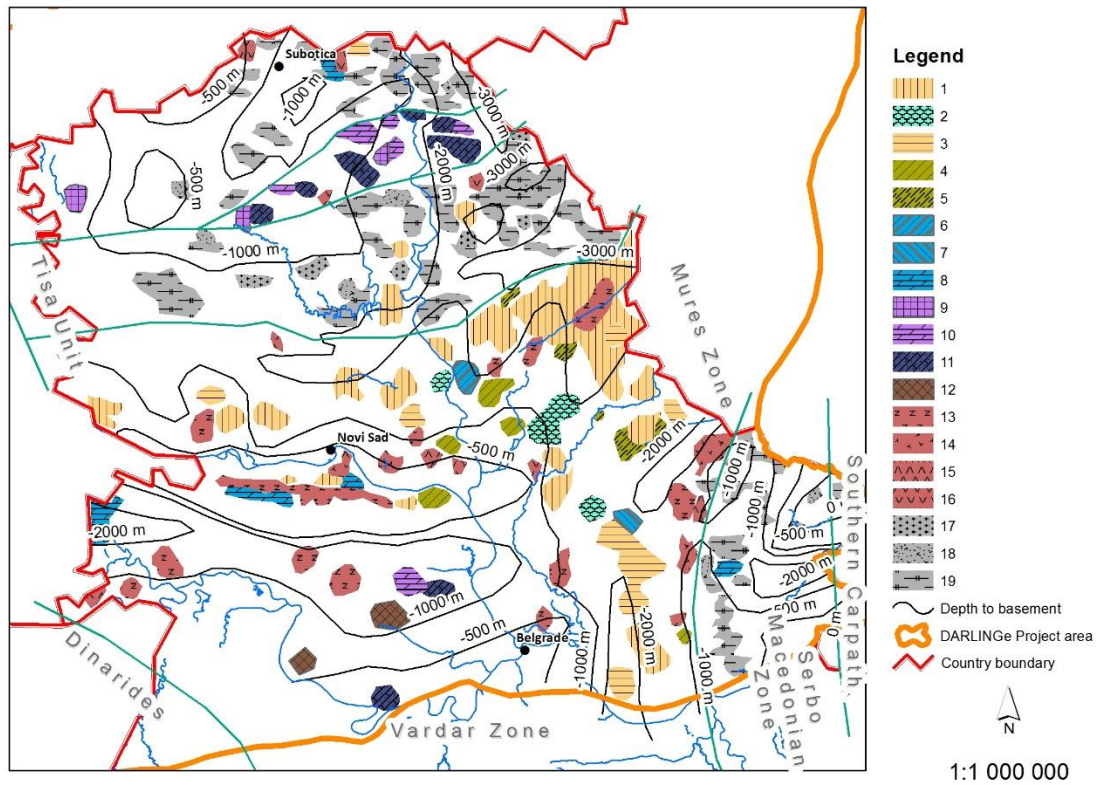


Figure 59. Geological map of the pre-Tertiary basement of the Pannonian basin in North Serbia according to well data. Legend: 1. Upper Cretaceous deep marine siliciclastic, carbonate and flysch formation, 2. Lower Cretaceous shallow marine and reefal formation, 3. Lower Cretaceous deep marine formation, 4. Upper Jurassic and Lower Cretaceous deep basin formation, 5. Jurassic and Lower Cretaceous deep marine formation, 6. Middle and upper Jurassic deep basin formation, 7. Lower Jurassic deep marine formation, 8. Middle and upper Triassic deep marine formations, 9. Upper Triassic platform carbonate, 10. Middle Triassic shallow marine formation, 11. Lower Triassic shallow marine siliciclastic carbonate, evaporite, 12. Carboniferous and Permian shallow marine formations, 13. Serpentinite, 14. Gabbro, 15. Basalt, 16. Rhyolite, 17. Granite, granodiorite, 18. Migmatite, 19. Crystalline schist in general. Source: Kemenci & Čanović, 1997.

The northern part of the area is part of the Tisia unit, the neighbouring area in south direction belongs to Vardar zone, while on the easternmost side the South Carpathian and Serbo-Macedone zone is found. The north side of Tisia unit is part of Codru nappe, where crystalline schists, sediments limestone, dolomite, evaporite were explored mainly. On Biharia nappe of Tisia unit mostly crystalline rocks (schists, granite, migmatite) were explored, at several places basin fill sediments of late Cretaceous age are found. The Mures-Vardar belt is a great mixture of different kind of rocks. This belt is composed of mainly rocks of former oceanic crust (serpentine, gabbro, basalt) and its sedimentary cover has Cretaceous age (flysch, basin fill sediments, shallow marine reefal limestone). Due to its chaotic structure, the belt has quite unpredictable character from a geological point of view. This feature and lack of carbonates and crystalline rocks decrease the likelihood of having basement reservoir in this belt. The SW side of this area, along Drina river at Macva region, is a transition zone towards the Dinarides. A proven geothermal resource exists on this area, which is under “exploitation” since decades. The resource rock is limestone of Triassic age. The South Carpathian and Serbo-Macedone zone on the east side of Vardar Maros belt mostly consists of schists and granite.

Among the unproven resources the limestone of middle and late Triassic age might be good targets on Codru nappe. The expected depth of these layers is around 1000-1600 m, so the expected outflow temperature is around 50-70 °C. The next possible targets might be the faults in crystalline rock environment. The reefal limestone of Cretaceous age located at south of Zrenjanin could be a target, if it is thick enough.

7.4.2.4. Slovenia

The pre-Cenozoic basement rocks on project area in Slovenia can be divided in two parts (Figure 60).

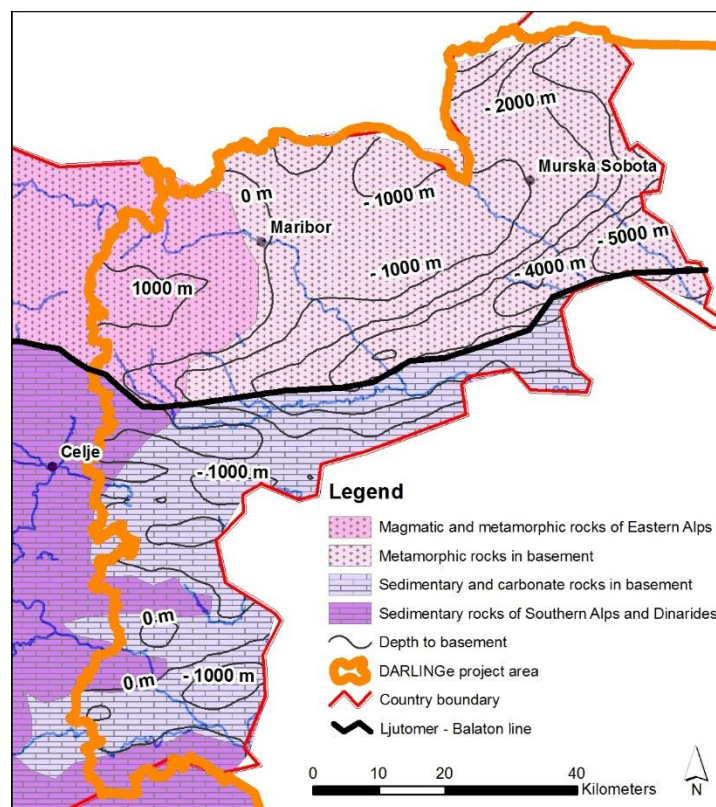


Figure 60. Simplified pre-Cenozoic basement map of east side of Slovenia, after Rajver et al. (2015)

The north part, which is located north of the Periadriatic (Ljutomer)-Balaton fault, is a crystalline-type basement. The buried Murska Sobota massif, as part of Korralpe, Wöltz, mostly consists of gneiss, schist, phyllite, marble and amphibolite formations of Paleozoic age, while in the Pohorje Mountains granodiorite of early Miocene age are known too. The Ljutomer-Balaton fault is in a 5 km deep trough, which is continuing in Hungary in east direction. The south part of basement belongs to South Karavanke unit, in which Dachstein limestone and Hauptdolomite are known between Košuta and Olševa on the surface. The rocks of Triassic and Permian age of this unit are outcropping at Boč Mountains too. An anticline structure is recognizable between Boč and Ormož, where the depth to top of basement varies between 0-3000 m. The deep part of this unit is not explored for geothermal purposes. The basement rocks are getting closer to the surface at south, which goes hand in hand with less reservoir temperature. This area belongs to Central Slovenian or High Karst unit, where thick platform carbonates of Triassic age are known.

The pre-Tertiary basement might contain geothermal resources at South Karavanke unit (Rajver et al., 2015), at fractured part of Murska Sobota massif (e.g. drilling at Benedikt, Kralj & Vršič 2007) and at Krško basin (Ivanković & Nosan 1973).

7.4.2.5. Bosnia and Hercegovina

The most of proven geothermal resources of Bosnia and Hercegovina are connected to basement reservoirs, but in the project area Tertiary formations might constitute geothermal reservoirs too. The project area is part of Sava-Vardar zone and Dinaride Ophiolite Belt (Figure 61), which is called as Eastern Thrust Belt (Figure 62).

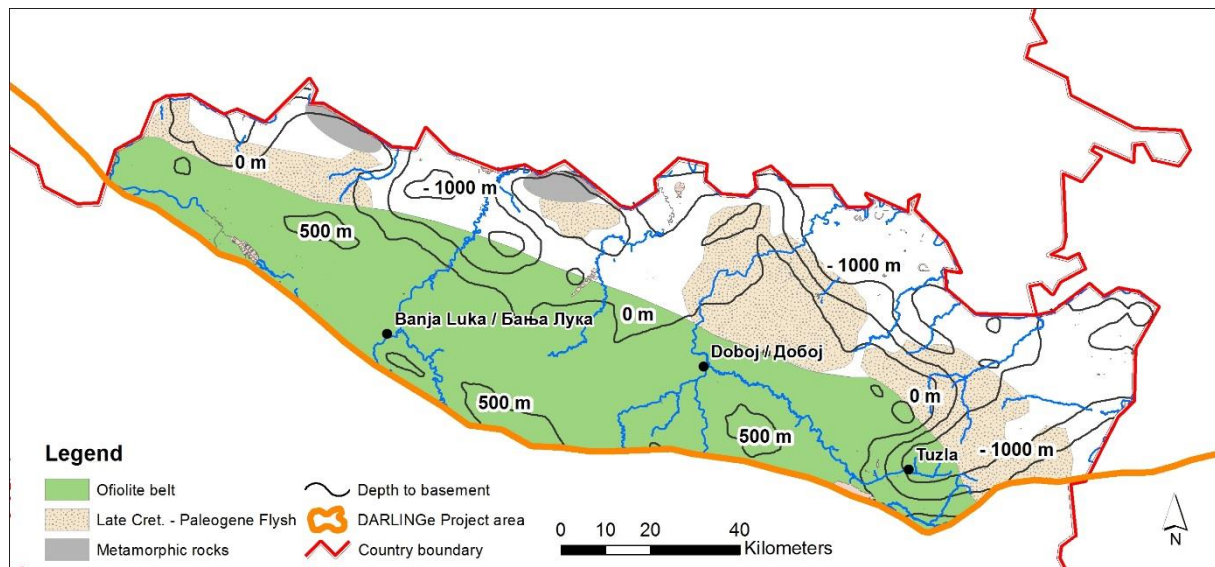


Figure 61. Pre-Tertiary basement map of Bosnia and Hercegovina

As it was described at Mures and Vardar zone in Romania and Serbia, the various compounds of poorly permeable rocks in a hardly understandable chaotic structure along this zone decrease the probability of having geothermal resources in the basement. Based on interpretation of Tari (2002) shallow marine carbonate formations are expected under the thrust belt at 6 km respectively, but the poor permeability of the ophiolite melange above it might create a barrier towards the surface (Figure 62). Another difficulty is originated from the applicability of surface geophysical measurements. In Neogene basins the seismic measurements could provide quite plausible visualization of faults and surface of the basement, but in areas where basement rocks are outcropping, the reliability of seismic measurements for locating features at 1-3 km depth is lower. One possible solution for the investigation of resources could be the overall evaluation of surface manifestation of geothermal activities. The evaluation of surface geology and tectonics coupled with hydrogeological observations and measurements could provide a hint or idea on the heat source.

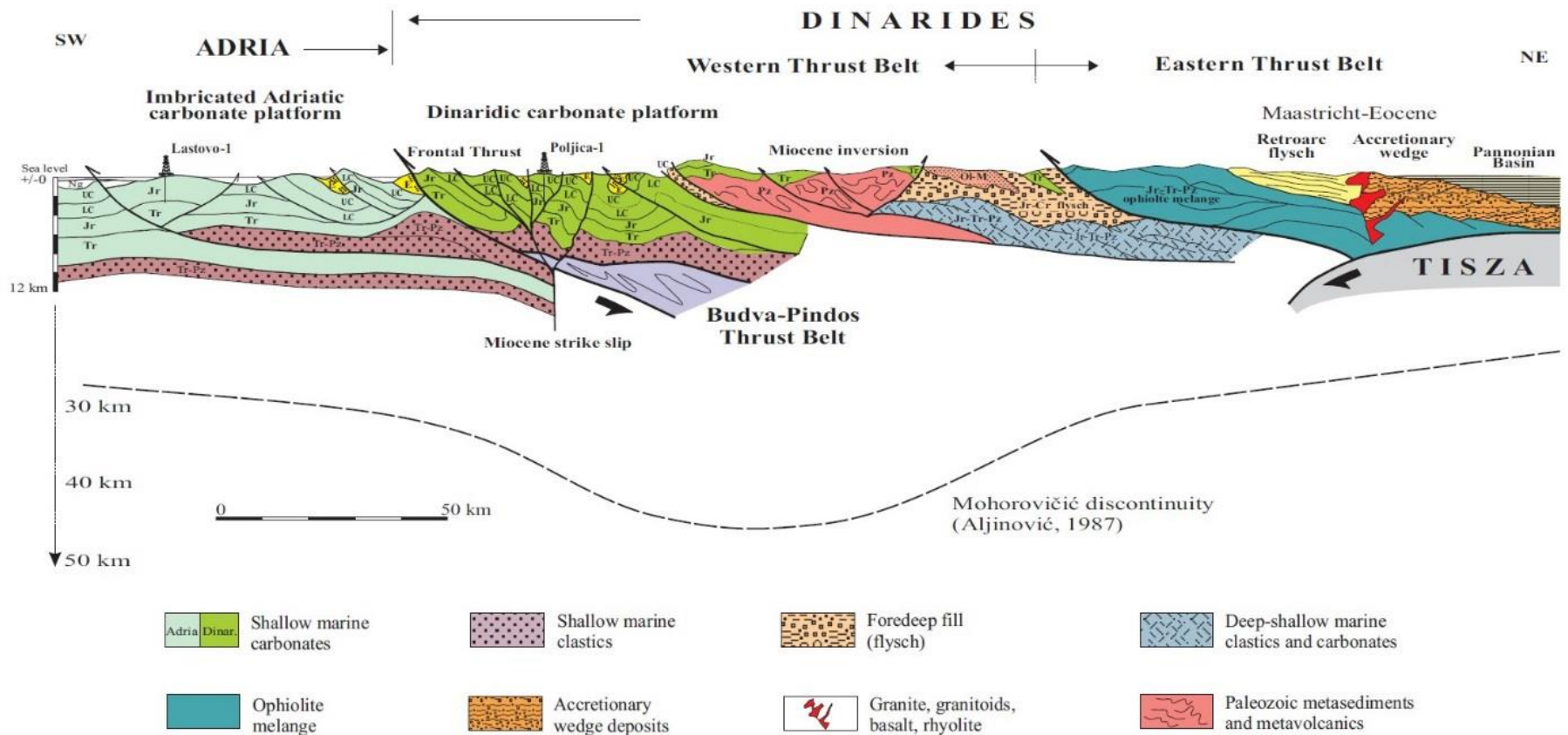


Figure 62. Geological cross section of Dinarides (Tari, 2002)

7.4.2.6. Croatia

The pre-Cenozoic basement rocks of the project area in Croatia could be grouped into 3 main types (Figure 63):

- carbonate-type formations at north (Karavanke, Ivanščica, Kalnik and Medvednica units)
- crystalline and schist formations at central and at east
- Sava zone at south.

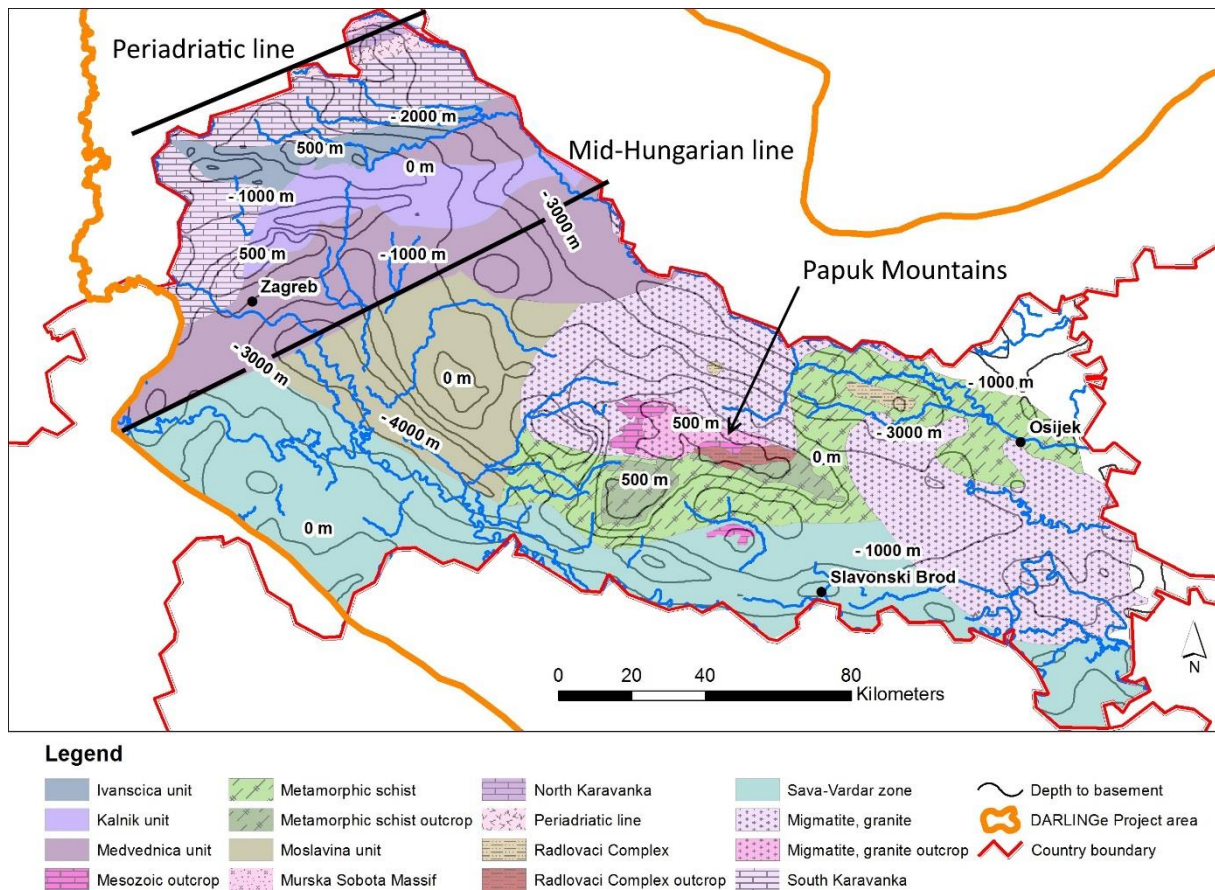


Figure 63. Pre-Tertiary basement map of Croatia. Source: Pamić & Lanphere, 1991; Haas et al. 2000.

The area at north, where presence of thick carbonate layers of Triassic age is expected, is located along and between large tectonic faults, like Periadriatic (Ljutomer) - Balaton line and Mid-Hungarian (Zagreb-Zemplín) line. The area between the two lines is where the Sava folds are located. The strike of the axes of the folds is parallel with the direction of the lines at the north and south borders. The strike of outcrops in Ivanščica, Kalnik and Medvednica is parallel with the strike of the folds respectively. The anticline position of these folds containing carbonates of Triassic age are known geothermal resources at town of Tuheljske Toplice, Stubičke Toplice, and Krapinske Toplice. The measured temperature is between 30-60 °C due to the shallow drilling depth (few hundreds of meters). The resource rocks are gradually deepening towards east in the direction of Pannonian Basin. On the geothermal field of Velika Ciglana and Lunjkovec-Kutnjak reservoir temperature was measured between 120-170 °C in the depth interval of 1700-3000 m. Also, at the capital of Croatia, Zagreb, carbonate geothermal reservoir exists where at the water depth 845 -1360 meters measured temperatures are in the range 63-78 °C. The westernmost

occurrence of geothermal reservoir on this territory is at town of Karlovac. The fractured dolomite is located between 1500-3000 meters and the expected temperature is around 130 °C. The chemistry of geothermal fluid is more benign closer to the infiltration area, while reservoirs located at greater depth and far from the infiltration area have high TDS, which induces numerous technical problems during exploitation.

The central and eastern part of the project area is mostly consisting of crystalline rocks and schist. There is one exceptional area, where outcrop of Mesozoic carbonate is known, this is the west side of Papuk Mountains, in the centre of Daruvar town thermal springs occurred. The water temperature is between 43-50 °C. At the SW foot of the mountain a thermal spring was known at town of Lipik since centuries. This manifestation (60 °C at 235 m) is presumably due to hidden fractured basement reservoirs, because the basement is deepening rapidly towards west, and the karstified limestone layer is in the vicinity as well. A proven geothermal crystalline reservoir was discovered in late 60's at town of Bizovac. The aquifer is fractured gneiss and overlying breccia of Tertiary age. The depth of the resource is around 1500-2000 m and the expected temperature is around 100 °C, the TDS is high, 25 g/l.

The Sava Zone is a hardly predictable feature. The geothermal manifestation at the village of Topusko (almost 70 °C at 150-248 m depth interval) might be a good indication of fractured aquifer of this area, and the indication at Babina Greda (121 °C at 1700-2200 m) might be another example too.

7.4.2.7. Hungary

The spatial distribution of formations of pre-Tertiary basement is depicted on Figure 64.

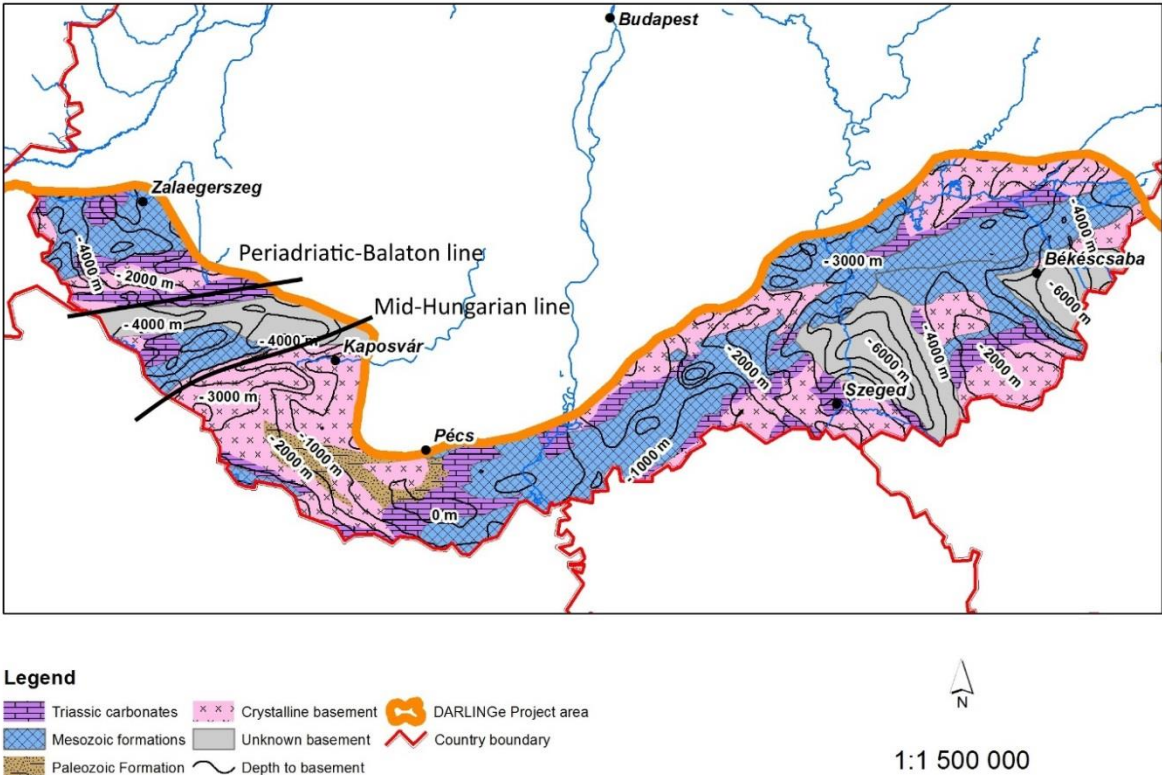


Figure 64. Pre-Tertiary basement map of Hungary (after Haas et al. 2010)

Due to large-scale tectonic movement along the Mid-Hungarian line during the Miocene, two-types of basement fragment are situated on the project area. The ALCAPA basement is located at the north side, while the Tisia basement is at the south side of the Mid-Hungarian line. These two basement fragments have been evolved differently from late Paleozoic until late Paleogene. The ALCAPA fragment is characterized by thick (>2 km) carbonate layers of middle and late Triassic age, while in Tisia fragment the carbonate layers were formed only during the middle Triassic, and its thickness is only several hundreds of meters. The areal coverage of crystalline rocks in Tisia basement is significant compared to ALCAPA. The carbonates of Triassic age are presented separately from the Mesozoic sequences on the map (Figure 64), this way the karstified, more porous part of carbonates is more visible. At certain areas the basement is so deep that drilling data is simply unavailable for the confirmation of the type of the basement rocks, at these deep troughs the basement is labelled as unknown.

On ALCAPA a side only balneological use of basement reservoirs is known at town of Zalakaros, which is a well-known spa city with a lot of facilities for recreation. The spas are producing thermal water from limestone of Triassic age at 2000 m depth along Periadriatic-Balaton line since decades. The unsuccessful initiative of MOL Plc. to test abandoned hydrocarbon wells for electricity production was completed at Iklódbördöce, which is in the North Karavanke unit. Except a thin stripe of Periadriatic magmatites, on the whole ALCAPA territory of the project area thick carbonate formations are expected at 1-4 km depth.

On Tisia basement the carbonates of Triassic age are covering significant areas, mostly with its Mesozoic covers. The carbonate reservoirs of Mesozoic age are used for balneological (Harkány, Nagybaracska) and district heating (Bóly, Szigetvár) purposes. There are further unused proven and indicative resources at the south part of Danube-Tisza interfluve (e.g. Mélykút wells: 100-105 °C at 1500-2000 m depth interval), around town of Fábíánsebestyén and Nagyszénás (180-200 °C at 3500-4000 m depth), and at Battonya-Pusztaföldvár high (at Tótkomlós-I drilling 124 °C at 1800 m depth). The crystalline rocks are less explored and less utilized compared to carbonate-type aquifers. There is only one utilization at town of Szentlőrinc along the South Mecsek line. Presumably there is more potential in this resource, e.g. crystalline part of Battonya-Pusztaföldvár high indicates increased heat-flow, or at the vicinity of town of Kiskunhalas 153 °C was measured at 2100 m depth in crystalline rock, which might be explained by contribution of convective flow.

8. Hydrogeochemical characterisation of the geothermal reservoirs

The aim of hydrochemical characterisation of geothermal reservoirs is to provide stakeholders and potential investors with relevant information, as chemistry of the geothermal fluids might have serious impacts on utilization (e.g. scaling, corrosion, etc.).

In the framework of the hydrogeochemical characterization of the reservoirs, all available archive chemical data have been collected, and analyses from almost 850 water samples have been considered in the hydrogeochemical evaluation of the project area. Out of these, 41 data are from Bosnia-Herzegovina, 40 from Croatia, 22 from Romania, 39 from Slovenia, 60 from Serbia and 646 from Hungary.

Hydrogeochemical data were grouped into three categories based on their aquifer types, namely basement, basin fill and others (Figure 65). Basement reservoirs, which are the pre-Tertiary potential thermal water aquifers of the basement formations, were represented by 123 analyses,

while 200 data were available from the other aquifers (deep Quaternary and pre-Pannonian Miocene aquifers). The data availability resulted in a very general hydrogeological description of these two aquifer types. However, the basin fill reservoirs which are built up of porous intergranular sediments of shelf front formations deposited in the Pannonian Lake could have been characterised in more details, as 492 chemical records were available, in spite the fact that data distribution was uneven.

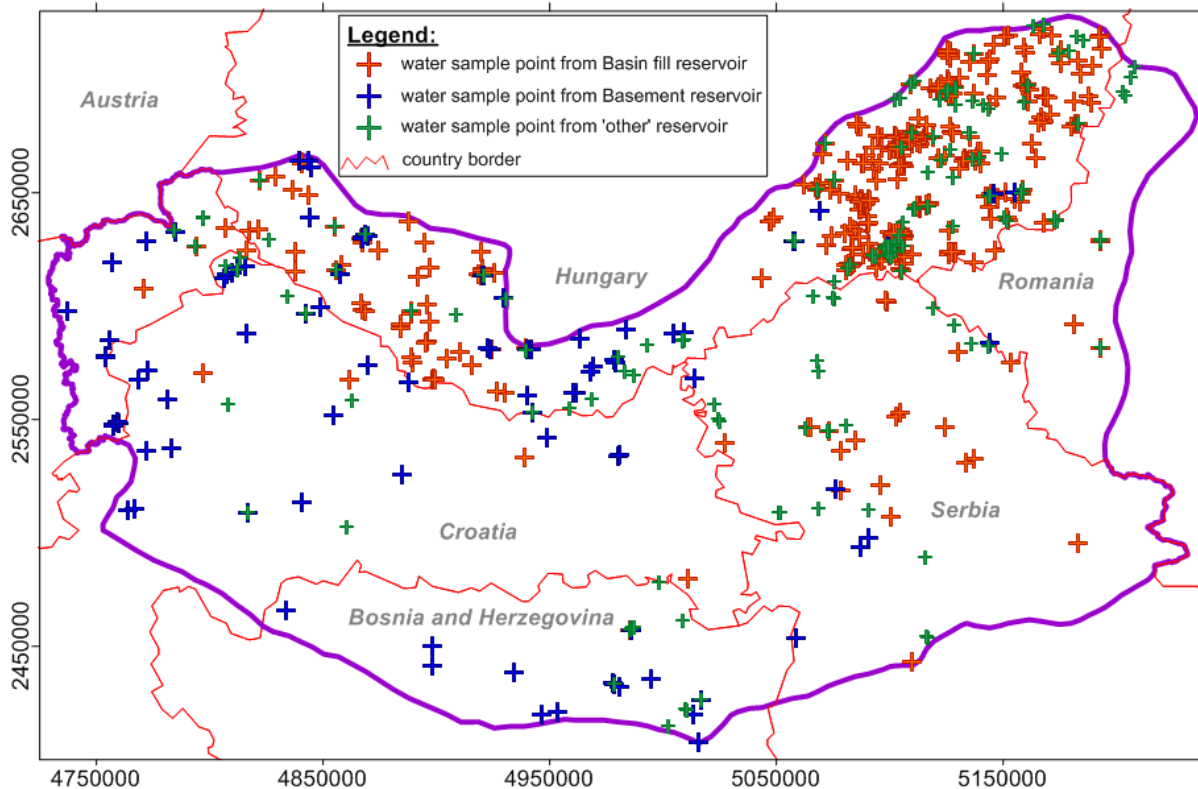


Figure 65. Location of hydro-geochemical data

8.1. Basin fill reservoirs

The hydrogeochemical characterization of the basin fill reservoirs was carried out according to the four temperature categories distinguished on the basis of the different utilization purposes (see chapter 7.1.). The main statistical parameters of major components and the total dissolved solid (TDS) are presented in Table 1..

The thermal waters with a 30 – 50 °C temperature range in the Upper Pannonian thermal aquifers are typically of Na–HCO₃ water type. At the margins of the sub-basins (eg. in south-east and south-west Hungary, Slovenia), Ca–Mg–Na–HCO₃ and Na–Ca–Mg–HCO₃ water types may also occur. The concentration distribution of some major chemical parameters and the TDS values is shown in Figure 66 and Figure 67. with Box&Whiskers diagrams. These waters have a low mineralization, with TDS values typically in the range of about 750 – 2750 mg/l.

Table 1. The main statistical values of major chemical parameters and the total dissolved solids (TDS) according to temperature categories in the basin fill reservoirs

	30-50 °C							50-75 °C						
	Na ⁺	Ca ²⁺	Mg ²⁺	Cl ⁻	SO ₄ ²⁻	HCO ₃ ⁻	TDS	Na ⁺	Ca ²⁺	Mg ²⁺	Cl ⁻	SO ₄ ²⁻	HCO ₃ ⁻	TDS
	mg/l							mg/l						
Minimum	28.5	2.1	0.2	1.0	0.1	171.0	242.3	92.0	0.1	0.6	0.4	0.1	370.0	492.0
10% percentile	181.5	4.5	1.6	3.0	0.5	460.1	751.1	206.8	4.1	1.0	6.2	1.2	555.8	807.8
Median	350	10.1	4.3	23.0	5.0	951.0	1383	431.5	6.3	2.3	50.0	5.0	1013	1604
90% percentile	708	27.2	17.5	181.2	25.6	1584.5	2757	902.8	13.5	6.7	202.2	17.8	2061	3192
Maximum	2350	219	123.8	3759	500.0	5240	8204	1270	40.0	29.0	1078	102.8	2928	4140
Number of data	150	150	150	150	139	150	143	153	153	153	153	148	153	153
	75-100 °C							100-125 °C						
	Na ⁺	Ca ²⁺	Mg ²⁺	Cl ⁻	SO ₄ ²⁻	HCO ₃ ⁻	TDS	Na ⁺	Ca ²⁺	Mg ²⁺	Cl ⁻	SO ₄ ²⁻	HCO ₃ ⁻	TDS
	mg/l							mg/l						
Minimum	140.0	0.6	0.4	3.0	0.1	427.0	633.4	395.1	1.5	0.5	10.0	3.8	1049	1488
10% percentile	330.1	4.1	1.0	12.0	4.1	775.8	1179	439.9	3.8	0.8	10.8	5.0	1213	1695
Median	730.0	6.4	2.0	39.0	6.3	1800	2603	662.6	5.7	1.3	24.1	27.0	2015	2727
90% percentile	1287	14.1	5.8	261.2	52.3	2979	4471	1586	9.1	3.0	192.6	68.2	3486	5448
Maximum	1860	48.0	19.4	1631	146.0	4570	6698	1740	15.6	3.3	387.0	76.0	4069	6045
Number of data	153	153	153	153	138	153	153	19	19	19	19	14	19	19

The thermal waters with a 50 – 75 °C temperature range in the Upper Pannonian thermal aquifers are also typically of Na-HCO₃ water type. Na-HCO₃-Cl and Na-Cl-HCO₃ water types also occur in Serbia and in the south-western part of Hungary in the 500 – 1500 m depth interval. The concentration distribution of some major chemical parameters and the TDS values is shown in Figure 66 and Figure 67 with Box&Whiskers diagrams. These waters have also low mineralization, with TDS values just slightly higher than in the temperature reservoir category, with TDS values typically in the range of about 800 – 3200 mg/l.

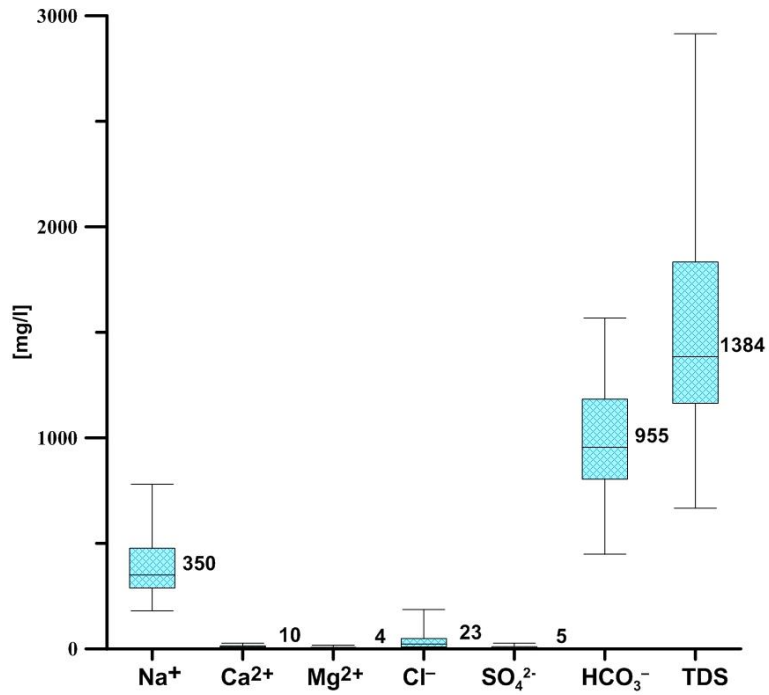


Figure 66. The concentration distribution of some major chemical parameters and the TDS values (with their median values) shown in Box&Whiskers diagrams characteristic for the thermal waters of the 30 - 50 °C temperature range of the Upper Pannonian basin fill reservoirs

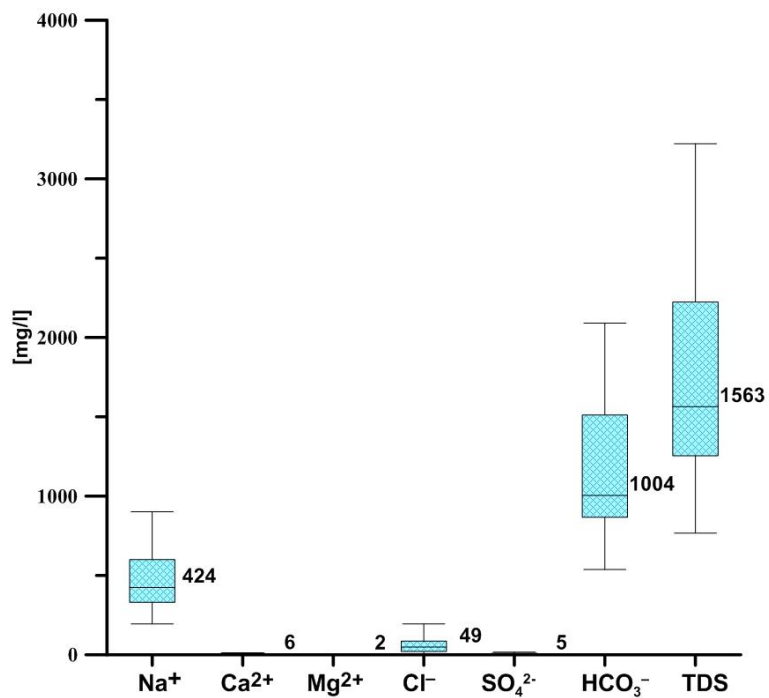


Figure 67. The concentration distribution of some major chemical parameters and the TDS values (with their median values) shown in Box&Whiskers diagrams characteristic for the thermal waters of the 50 - 75 °C temperature range of the Upper Pannonian basin fill reservoirs

The thermal waters with a 75 – 100 °C temperature range in the Upper Pannonian thermal aquifers are also typically of Na-HCO₃ water type. Na-HCO₃-Cl and Na-Cl-HCO₃ water types also occur in Serbia and in the south-eastern part of Hungary in the 1500 – 1850 depth interval. The concentration distribution of some major chemical parameters and the TDS values is shown in Figure 68 with Box&Whiskers diagrams. The TDS values of these waters are in the range of about 1200 – 4500 mg/l in accordance with larger reservoir depths and expected longer residence times.

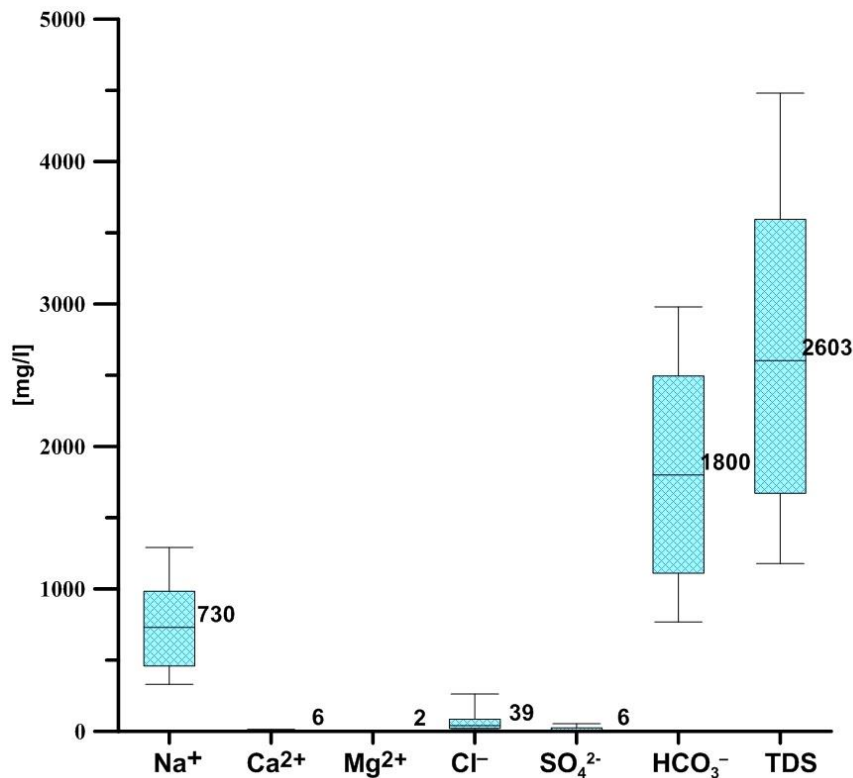


Figure 68. The concentration distribution of some major chemical parameters and the TDS values (with their median values) shown in Box&Whiskers diagrams characteristic for the thermal waters of the 75 – 100 °C temperature range of the Upper Pannonian basin fill reservoirs

The thermal waters with a 100 – 125 °C temperature range in the Upper Pannonian thermal aquifers are typically of Na-HCO₃ water type too. The concentration distribution of some major chemical parameters and the TDS values is shown in Figure 69 with Box&Whiskers diagrams. The TDS values of these waters are in the range of about 1700 – 5500 mg/l in accordance with larger reservoir depths and expected longer residence times in parallel with water-rock interactions.

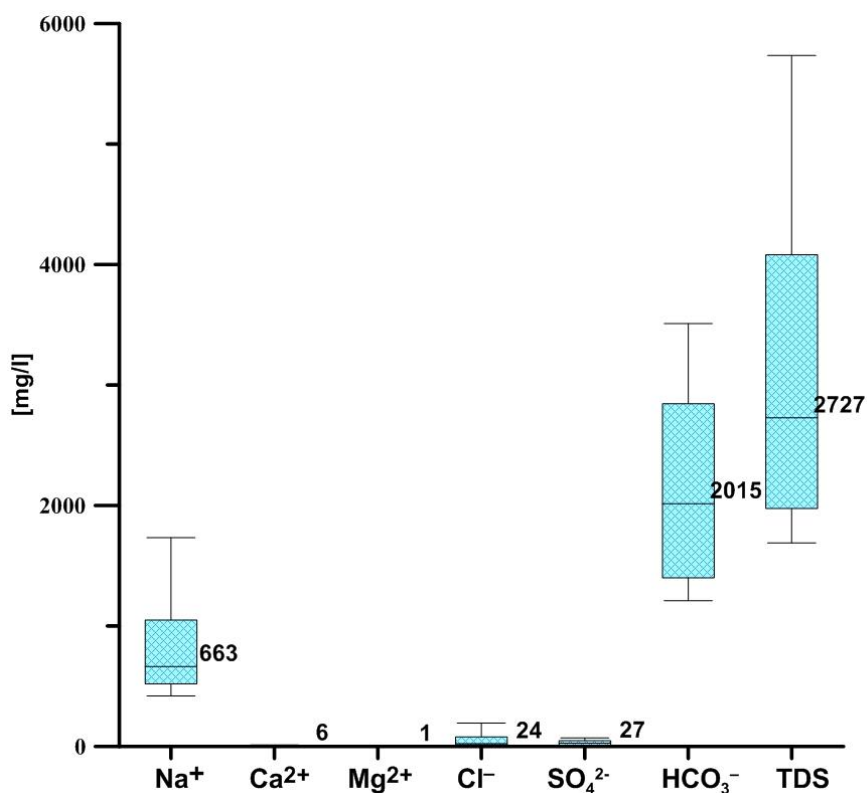


Figure 69. The concentration distribution of some major chemical parameters and the TDS values (with their median values) shown in Box&Whiskers diagrams characteristic of the thermal waters of the 100 - 125 °C temperature range of the Upper Pannonian basin fill reservoirs

8.2. Basement reservoirs

As mentioned in the introduction, the hydrogeochemical characterization of basement reservoirs was based on 120 data, which represent 83 objects. In spite of the small number of available hydro-geochemical data it can be clearly seen that both the water composition and the TDS change according to depth (Table 2. Number of hydrogeochemical water types grouped by mean depth intervals and their 10-90% percentiles and median TDS values (83 wells)). The median TDS values are less than 1000 mg/l down to about 500 meters below surface, with a slight increase in concentration up to about 3100 mg/l median TDS value in the 1500 - 2000 meters depth interval below surface. With depth the TDS values increase to a few ten thousands mg/l, with a median value above 20 000 mg/l.

The thermal waters in the upper part of the basement reservoirs, at those areas where the collected samples are from about less than 500 meters below surface, are of Ca-Mg-HCO₃, Ca-HCO₃, Na-HCO₃-Cl, Na-Cl-HCO₃ and Na-Ca-Mg-HCO₃-Cl water types. The water composition changes in accordance with the geomorphological setting of the basement, namely if it is in an uplifted or in a deeper position. In Bosnia-Herzegovina and Slovenia, where the basement is in an elevated position Ca-Mg-HCO₃ and Ca-HCO₃ water types occur, while in southern Hungary in Harkány and Nagybaracska, Na-HCO₃-Cl, Na-Cl-HCO₃ and Na-Ca-Mg-HCO₃-Cl waters are prevalent.

With an increase in depth the chloride content starts to dominate as major anion and Na-HCO₃-Cl, Na-Cl-HCO₃, Na-Cl waters are more and more common with depth. The thermal waters in the basement are of Na-Cl type from about 2500 meters depth below ground surface.

In some parts of the project area, like in the central part of Serbia, in the northern part of Bosnia-Herzegovina and in the eastern part of Croatia, high sulphate concentrations can also occur in these reservoirs, resulting in Na-Ca-HCO₃-SO₄ or Na-HCO₃-SO₄ water types. The groundwater sampled in Tetima (Bosnia-Herzegovina), in the southern part of the project area, has a very high TDS (about 320 g/l), with about 120 g/l Na⁺ and 190 g/l Cl⁻ content.

Table 2. Number of hydrogeochemical water types grouped by mean depth intervals and their 10-90% percentiles and median TDS values (83 wells)

Depth (m)	CaHCO ₃ , CaMgHCO ₃	NaCaMgHCO ₃ , NaCaHCO ₃	NaHCO ₃	NaHCO ₃ Cl, NaClHCO ₃ , NaCaMgHCO ₃ Cl	NaCaHCO ₃ SO ₄ , NaHCO ₃ SO ₄	NaCl	TDS 10-90% percentiles mg/l	TDS median mg/l
0-100	5		1	5	2		500- 1 000	900
100-500	9	1	1	2	1		500- 3 000	700
500-1000	2		2	4	1	1	1 500- 2 500	2 000
1000-1500		3	1	2		3	500-12 000	600
1500-2000		4		4	1	4	450-16 500	3 100
2000-2500			1	3		9	4 000-14 000	8 000
2500-3000						3	12 000-26 500	24 000
3000-3500						4	9 000-24 500	12 000
3500-4000						4	17 000-31 000	20 500

8.3. Other thermal aquifers

8.3.1. Pliocene and Quaternary aquifers

Thermal waters of the Pliocene, Quaternary aquifers are used for different purposes, from drinking water to balneology. Hydro-geochemical data were available only from the south-eastern part of Hungary because other partners were not invited to collect this info as their waters are colder than 30 C in such settings. The outflow water temperature of the 60 water samples analysed ranges between 30 and 42 °C, with 80% of the waters having Na-HCO₃ water type. The other 20% of the wells are in the Szeged area and their water chemistry is of Ca-Mg-Na-HCO₃, Na-Ca-Mg-HCO₃, and Ca-Na-Mg-HCO₃ type. Their TDS is relatively low, typically between 400–1400 mg/l. The 10% and 90 % percentile values of the main components are about 40–500 mg/l Na⁺, 5–40 mg/l Ca²⁺, 1–30 mg/l Mg²⁺ and 350–1350 mg/l HCO₃⁻.

8.3.2. Pre-Pannonian (older Miocene) reservoirs

The water compositions of the older Miocene reservoirs vary over a wide interval, both in their water types and in their total dissolved content. Thermal waters in the shallower part of the reservoirs (0–650 meters depth below surface) have Ca–Mg–HCO₃, Ca–Mg–Na–HCO₃, Na–Ca–Mg–HCO₃, Ca–HCO₃, Na–Ca–HCO₃ water type. The TDS at this depth is relatively low, typically between 350–1400 mg/l. The 10% and 90 % percentile values of the main components are about 10–250 mg/l Na⁺, 50–100 mg/l Ca²⁺, 10–40 mg/l Mg²⁺ and 250–900 mg/l HCO₃⁻.

From a depth of about 650 meters below the surface the sodium becomes the dominant cation and the concentration of chloride also increases. These waters are of Na-HCO₃, Na-HCO₃-Cl, Na-Cl-HCO₃ or Na-Cl water type depending how open or closed the reservoir is and very often the proximity of oil waters (add reference). Those reservoirs which have a connection with the

regional groundwater flow systems are of Na-HCO₃ type, while those which are isolated are typically of Na-Cl type. Their TDS content varies across a large range, from 500 mg/l up to 40 000 mg/l. TDS values above 20 000 mg/l occur mainly in south-east Hungary (eg. Battonya, Endrőd, Szarvas), where these reservoirs are completely or partly isolated from the regional groundwater flow systems.

Thermal waters with very high TDS can be found in the southern part of the project area, around Trnovac (Bunar-22) in Bosnia-Herzegovina. These wells are in relation with well-known Tuzla salt deposit and water of these drill holes has high TDS due to circulation of water around salt layers. These waters are brines of NaCl type and have TDS values around 300 g/l. Their Na⁺ concentration is about 100 - 120 g/l, the Cl⁻ concentration 150 - 190 g/l, with SO₄²⁻ concentrations between 1 - 13 g/l.

9. Resources assessment of geothermal reservoirs

The most important part of characterization of geothermal reservoirs is quantifying their geothermal potential, i.e. to express in a quantitative way the amount of geothermal energy to be potentially exploited from them. Different literatures identify different categories for geothermal potential. e.g. theoretical-, technical-, economic-, sustainable-, and developable potential (Rybach 2010). As the different potentials in this order are more and more realizable and require more and more detailed information, regional resource estimations usually apply the first two categories. The theoretical potential describes the physically usable energy supply (the heat in place). Due to technical, structural and administrative limitations only small fractions of the theoretical potential can actually be used. Technical potential describes the fraction of the theoretical potential that can be used under existing technical restrictions (currently available technology) (Rybach 2015).

The first limit is presented in the maximum realizable drilling depth which is between 5-7 km (Muffler & Cataldi 1978). In addition recovery factor (which means the ratio of heat recoverable versus heat in place) shows the degree of technically available part of available geothermal resources. According to practical experiences its value is rather uncertain and varies in wide ranges. Depending on the geology and permeability, it is between 0.1-0.25 in porous systems while 0.08-0.2 in fractured systems (Nádor 2016).

In the recent study the theoretical and technical potential of the geothermal reservoirs were calculated for selected sub-basins (Figure 70) with the more frequently applied volumetric method (Muffler & Cataldi 1978). The sub-basins were delineated based on geological and hydrogeological considerations.

Since in most of the cases extracting heat from the rock is possible by production of geothermal fluid, only the heat content of moveable fluid (fluid situated in the effective pore space) was considered in the calculation (further it is signed as Q_{effpor}).

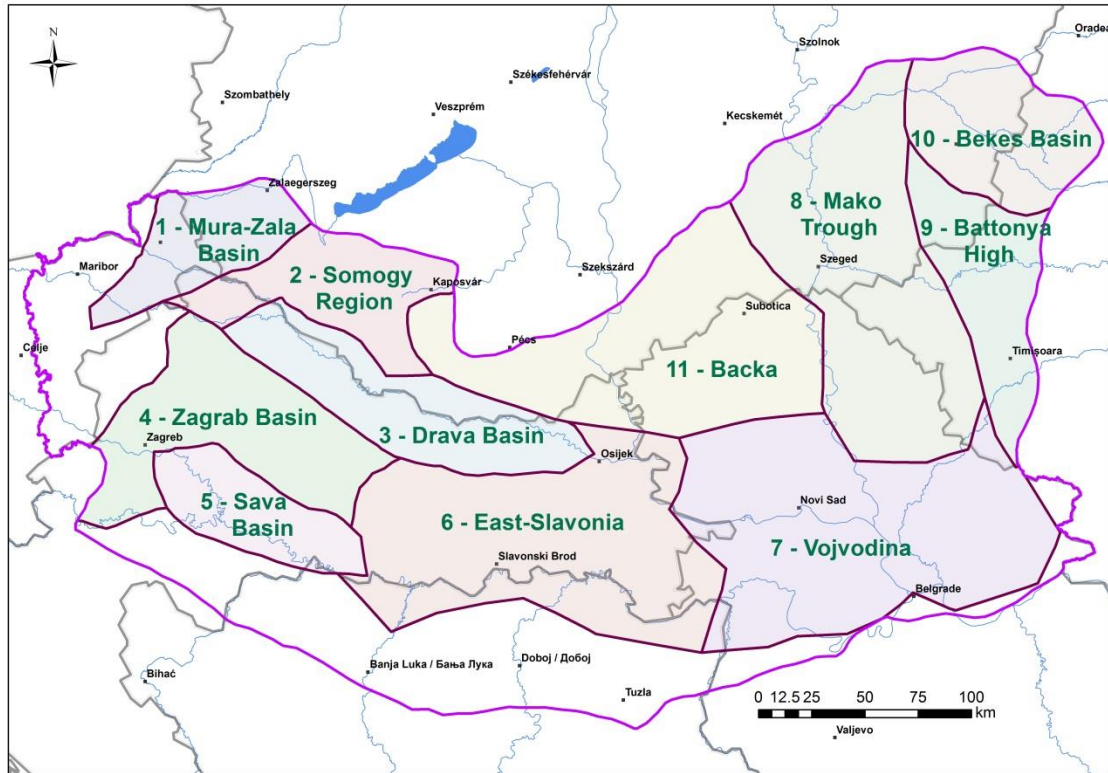


Figure 70. Regions of resources estimation

The input parameters used for estimating the heat content of movable water in the reservoirs are the followings:

- Area of the reservoirs (measured)
- Depth (measured and interpolated)
- Temperature (estimated)
- Effective porosity (estimated)

The heat content is a result of the following basic equation:

$$Q_{\text{effpor}} = C \times m \times \Delta T$$

$C = 4,187,106 \text{ J}/(1000\text{Kg} \cdot ^\circ\text{K})$ the specific heat capacity of water

m = the mass of movable water in reservoirs [1000kg]

$\Delta T = T_{\text{int ave}} - T_{\text{reference}} =$ the excess temperature over 30°C

The mass of movable water in the reservoirs can be calculated in the following:

$$m = \rho \times (1-\text{SH}) \times \Phi_t \times \Delta H \times A$$

$\rho = 1.0 \text{ [1000kg/m}^3\text{]}$ = the specific density of water

A = the area of the reservoir [m^2]

ΔH = average thickness of the reservoir slice between the top and bottom of reservoir cut out by two defined isotherms

SH = the average clay content of Upper Pannonian sediments (in the model it is 40%)

Φ_t = average total porosity of a reservoir part cut by isotherms

(where the effective porosity (Φ_{eff}) was replaced by the expression: $\Phi_{\text{eff}} = (1-\text{SH}) \times \Phi_t$)

Predictions based on the volume method are generally consistent with the results of detailed model simulations and experiences of productions when the reservoir volume and the spatial distribution of permeability are well-constrained. Significant differences arise when both the volume of a reservoir and its flow properties must be estimated (Williams 2014).

Considering uncertainty a probabilistic approach was applied with the method of Monte Carlo simulation which is well acknowledged in geothermal resource assessment (Nádor and Zilahi 2016).

The Monte Carlo simulation belongs to the stochastic simulation methods, which uses randomness to solve problems that might be deterministic in principle. Monte Carlo methods are useful for modelling phenomena with significant uncertainty in inputs, in math, evaluation of multidimensional definite integrals with complicated boundary conditions. In principle, Monte Carlo methods can be used to solve any problem having a probabilistic interpretation. The calculation relies on repeated random sampling to obtain numerical results. Summing up the Monte Carlo simulation is used as a computerized mathematical technique that allows us to account for risk in quantitative analysis and decision making.

Applying the above described principles input parameters (area of the reservoir, thickness of the reservoir, temperature, effective porosity) were determined in the following way.

The **area of the reservoirs** are considered as static value and is determined as the surface projection of the top of the reservoirs (Table 3. .).

Table 3. Area of the reservoirs related to selected sub-basins (km²)

ID and name of the region (sub-basin)	30-50 °C	50-75 °C	75-100 °C	100-125 °C	125-150 °C
1 region Mura-Zala Basin	2607	1649	333	51	
2 region Somogy region	3904	2783	400		
3 region Drava Basin	4757	4364	2342	613	55
4 region Zagrab Basin	3581	565			
5 region Sava Basin	2739	1927	223		
6 region East-Slavonia	5342	1154			
7 region Vojvodina	6280	1558			
8 region Mako Trough	11807	11814	8556	2617	
9 region Battonya High	3764	1556	537		
10 region Bekes Basin	4088	3823	3152	1199	
11 region Backa / Bačka	3476	750			

The **thickness of the reservoirs** varies from place to place. These values are determined from the top and bottom horizons of the reservoirs represented in 500 × 500 m grid files (see chapter 7.4.1. The statistical values of reservoir thickness the identified reservoirs represented in the selected sub-basins are shown in Table 4..

Table 4. Estimated average thickness of the BF reservoirs for the selected sub-basins (m).

	30-50 °C	50-75 °C	75-100 °C	100-125 °C	125-150 °C
1. region Mura-Zala Basin	395	342	224	142	
2. region Somogy region	399	329	49		
3. region Drava Basin	351	417	356	213	123
4. region Zagreb Basin	244	146			
5. region Sava Basin	328	307	145		
6. region East-Slavonia	235	181			
7. region Vojvodina	283	99			
8. region Mako Trough	368	516	396	239	
9. region Battonya High	287	295	198		
10. region Bekes Basin	438	536	435	191	
11. region Backa / Bačka	253	199			

Temperature was estimated by the conductive geothermal model (see chapter 7.3). Its value varies from place to place too, and applied as average value calculated from the conductive model. It was determined for each grid cells related to the average depth of the reservoirs (as reference depth) for each temperature intervals.

Effective porosity was derived from total porosity. Its value is the function of actual basin depth and also the function of the clay content. The clay content was handled definitely as laminar clay (The lithology consist of 100% sand and 100% clay layers, no disseminated clay in this model). Lacking detailed geological model, sediments of the shelf plain and shelf front were not separated, therefore clay content in the model varies between a wide range of 20-60 % (based on expert estimation and literature of previous regional geological and hydrogeological modelling (Nádor & Zilahi 2016, Tóth et al. 2016)) and independent from basin depth, actual depth or coordinates. The average value is estimated as 40% which is related to the entire sequence.

The **effective porosity** is calculated with Monte Carlo simulation, where three independent variables are applied. The first random variable is represented by the specific depth ($\pm 5\%$), the second one for the error of the estimated total porosity ($\pm 10\%$) and the third one is for the

estimated clay content ($\pm 20\%$). The estimated average porosity related to the different reservoirs is shown in Table 5.

Table 5. Estimated average effective porosity in the BF reservoirs for the evaluation areas in isotherm intervals in (V/V) units.

	30-50 °C	50-75 °C	75-100 °C	100-125 °C	125-150 °C
1. region Mura-Zala Basin	0.179	0.129	0.083	0.052	
2. region Somogy region	0.183	0.194	0.089		
3. region Drava Basin	0.178	0.131	0.091	0.061	0.039
4. region Zagrab Basin	0.181	0.130			
5. region Sava Basin	0.173	0.130	0.085		
6. region East-Slavonia	0.177	0.127			
7. region Vojvodina	0.183	0.137			
8. region Mako Trough	0.181	0.135	0.095	0.065	
9. region Battonya High	0.224	0.154	0.118		
10. region Bekes Basin	0.187	0.134	0.093	0.098	
11. region Backa / Bačka	0.263	0.138			

Resource estimation was performed for 11 major divided regions of the project area which was outlined based on the location of sub-basins and basement relief of the Pannonian Basin (Figure 70). Heat energy stored in the effective pore space of the BF reservoirs was calculated for each unit considering that not the entire region of the unit can act as geothermal reservoir. However, the calculated energy is related only to the delineated reservoir bodies within each region. Heat energy stored in the pores associated with high-, medium-, and low levels of confidence are based on P90, P50 and P10 of the resulting cumulative probability distribution respectively. Two types of estimation was done, calculating the total heat content of moveable fluids (

Table 6.) and calculation considering recovery factor with the conservative value of 0.1 (**Hiba! A hivatkozási forrás nem található.**7).

The detailed results of the distributions of estimated heat can be illustrated on different type of graphs. Some examples are presented for the Drava Basin in Figure 71. and Figure 72.

Table 6. Estimated heat content of effective porosity in the BF reservoirs related to selected sub-basins, confidence levels at P10, P50, P90 [PJ]

Region (sub-basin) ID and name	30-50 °C			50-75 °C			75-100 °C			100-125 °C			125-150 °C		
	P90	P50	P10	P90	P50	P10	P90	P50	P10	P90	P50	P10	P90	P50	P10
	PJ	PJ	PJ	PJ	PJ	PJ	PJ	PJ	PJ	PJ	PJ	PJ	PJ	PJ	PJ
1. region Mura-Zala Basin	5365	7399	9750	6782	9395	12329	874	1201	1579	103	143	189			
2. region Somogy region	8308	11522	15169	10937	15154	20055	235	325	427						
3. region Drava Basin	9500	13014	17228	22945	32041	42005	10265	14164	18798	1933	2691	3531	90	125	164
4. region Zagreb Basin	3119	4317	5667	892	1227	1628									
5. region Sava Basin	4820	6665	8837	6888	9510	12545	372	513	680						
6. region East-Slavonia	4870	6745	8900	2159	2979	3933									
7. region Vojvodina	7776	10683	14052	1497	2075	2751									
8. region Mako Trough	27219	37607	49658	78234	108496	143502	42474	59153	78067	9575	13278	17482			
9. region Battonya High	5562	7628	10077	6499	8924	11835	1597	2213	2930						
10. region Bekes Basin	10057	13925	18391	26802	37267	49258	17255	23648	31213	3509	4832	6410			
11. region Backa / Bačka	3637	5032	6633	1629	2267	2976									

Table 7. Estimated heat content of effective porosity considering recovery factor (0.1) in the BF reservoirs related to selected sub-basins, confidence levels at P10, P50, P90 [PJ]

Region (sub-basin) ID and name	30-50 °C			50-75 °C			75-100 °C			100-125 °C			125-150 °C		
	P90	P50	P10	P90	P50	P10	P90	P50	P10	P90	P50	P10	P90	P50	P10
	PJ	PJ	PJ	PJ	PJ	PJ	PJ	PJ	PJ	PJ	PJ	PJ	PJ	PJ	PJ
1. region Mura-Zala Basin	536.5	739.9	975.0	678.2	939.5	1232.9	87.4	120.1	157.9	10.3	14.3	18.9			
2. region Somogy region	830.8	1152. 2	1516. 9	1093. 7	1515.4	2005.5	23.5	32.5	42.7						
3. region Drava Basin	950.0	1301. 4	1722. 8	2294. 5	3204.1	4200.5	1026. 5	1416.4	1879. 8	193.3	269.1	353.1	9.0	12.5	16.4
4. region Zagreb Basin	311.9	431.7	566.7	89.2	122.7	162.8									
5. region Sava Basin	482.0	666.5	883.7	688.8	951.0	1254.5	37.2	51.3	68.0						
6. region East-Slavonia	487.0	674.5	890.0	215.9	297.9	393.3									
7. region Vojvodina	777.6	1068. 3	1405. 2	149.7	207.5	275.1									
8. region Mako Trough	2721. 9	3760. 7	4965. 8	7823. 4	10849. 6	14350. 2	4247. 4	5915.3	7806. 7	957.5	1327. 8	1748.2			
9. region Battonya High	556.2	762.8	1007. 7	649.9	892.4	1183.5	159.7	221.3	293.0						
10. region Bekes Basin	1005. 7	1392. 5	1839. 1	2680. 2	3726.7	4925.8	1725. 5	2364.8	3121. 3	350.9	483.2	641.0			
11. region Backa / Bačka	363.7	503.2	663.3	162.9	226.7	297.6									

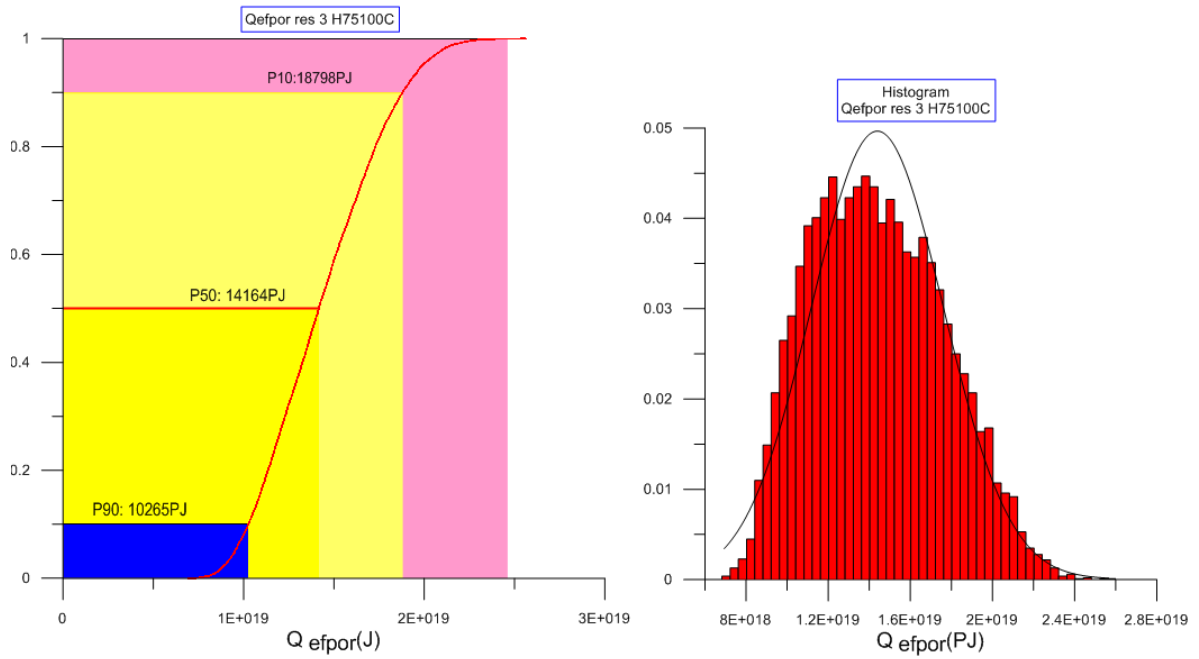


Figure 71. Distribution the estimated heat content by Monte Carlo method for Drava Basin (region 3)

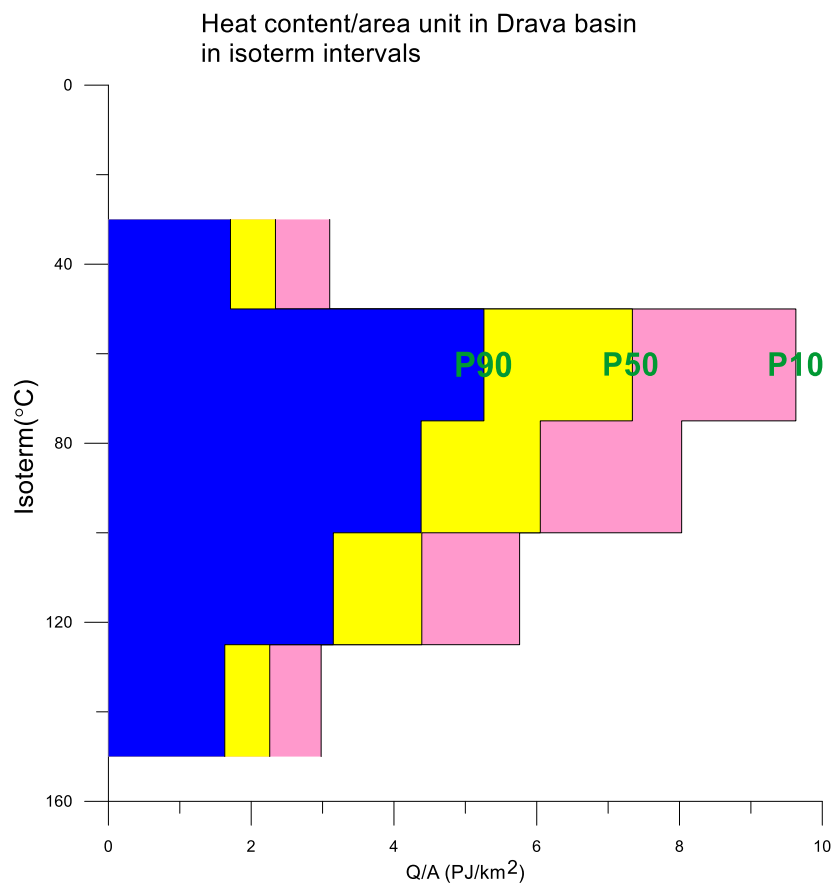


Figure 72. Heat content/km² in Drava Basin (region 3)

10. Summary and conclusions

To support the sustainable and energy-efficient use of the still untapped deep geothermal energy resources in the central and south-eastern part of the Danube Region, identifying and characterizing the main geothermal reservoirs was carried out in the frame of DARLINGE project.

On the basis of available regional geological, hydrogeological and geothermal data, two main reservoir types were identified, the thermal aquifer layers of the Pannonian shelf front and shelf plain formations (basin fill reservoir – BF), and potential thermal aquifers of the basement formations (basement reservoirs – BM). Due to the complex geological structure of the project area and irregular data distribution there was only restricted possibility to compile common geological surfaces and maps. In order to establish the delineation of geothermal reservoirs, the most important geological surfaces (the depth horizon of the pre-Cenozoic basement formations, depth horizon of the bottom of the nearshore sandy succession deposited in the Pannonian Lake – bottom bounding surface of the BF reservoirs, and depth horizon between the Pannonian Lake deposits and Quaternary terrestrial sequences – top bounding surface of the BF reservoirs) were constructed. These surfaces were applied as boundaries of the main reservoirs. Geological background of the geothermal conditions was illustrated by construction of 5 geological cross-sections that traverse the project area. They are focusing on the formations which can act as potential geothermal reservoirs.

Based on detailed evaluation of geothermal data, sub-categories were distinguished according to the available temperature in the reservoirs. Considering utilization aspects isotherm grid surfaces of 30 °C, 50 °C, 75 °C, 100 °C, 125 °C, and 150 °C were simulated by a simplified conductive geothermal model in the basin fill sediments. The spatial location of the 3D reservoir bodies were delineated by combining the geological and isotherm surfaces.

The temperature distribution was estimated by a similar conductive model on the top surface of the pre-Cenozoic basement. However, due to locally or regionally occurring convective heat-flow, these values can deviate from the real temperatures. The prosperous regions of the basement reservoirs were identified as positive anomalies from the comparison of the simulated and measured temperature values. Furthermore, a detailed description and characterisation was prepared for the potential basement reservoirs of the project region.

The hydro-chemical characters of the basin fill and the basement reservoirs were evaluated. Wide range of hydro-chemical composition can be observed in the area, but the different type of reservoirs can be characterized with typical chemical characters.

Resource estimation was carried out by applying Monte Carlo-based prediction. The variable of the simulation was the estimated heat content of the movable water in the BF reservoirs, which is the function of effective porosity, depth, clay content and temperature. Estimation was performed without and with considering recovery factor, related to 11 sub-regions. As it may be seen in the Drava Basin, the greatest heat content belongs to the reservoirs between 50-100 °C. Although the reservoir of 30-50 °C has the greatest extent, its sum heat content is similar to reservoir of 125-150 °C despite of the small extent and restricted porosity caused by greater depth of the latter one.

The above presented holistic approach and developed novel methodology provides basis for the transboundary and supra-regional thermal energy management on the south-eastern part of the Pannonian Basin and can serve as an example for other regions.

REFERENCES

- Ádám A., Vanyan L.L., Varlamov D.A., Yegorov I.V., Shilovski A.P., Shilovski P.P. 1982: Depth of crustal conducting layer and asthenosphere in the Pannonian basin determined by magnetotellurics. *Physics of the Earth and Planetary Interiors*, 28 (1982), pp. 251—260
- Almási, I. (2001): *Petroleum Hydrogeology of the Great Hungarian Plain, Eastern Pannonian Basin, Hungary*, PhD Thesis, university of Alberta, 398 p. <http://www.nlc-bnc.ca/obj/s4/f2/dsk3/ftp04/NQ60365.pdf>
- Bada, G., Horváth, F., Gerner, P., Fejes, I., 1999. Review of the present-day geodynamics of the Pannonian basin: progress and problems. *J. Geodynamics*, 27: 501–527.
- Bada, G., Horváth, F., Dövényi, P. and P. Szafián, 2007: Present-day stress field and tectonic inversion in the Pannonian basin. *Global and Planet.* 58., pp. 165-180.
- Balázs, A., Matenco, L., Magyar, I., Horváth, F., Cloetingh, S., 2016: The link between tectonics and sedimentation in back-arc basins: New genetic constraints from the analysis of the Pannonian Basin Tectonics, 35.
- Balla, Z., 1984: The Carpathian loop and the Pannonian basin: a kinematic analysis. *Geophys. Trans.*, 30(4):313-353.
- Békési E., Lenkey L., Limberger J., Porkoláb K., Balázs A., Bonté D., Vrijlandt M., Horváth F., Cloetingh S., Wees J.D. 2017: Subsurface temperature model of the Hungarian part of the Pannonian Basin. *Global and Planetary Change*, 30 September 2017
- Bräuer K, Geissler WH., Kämpf H, Niedermann S, Rman N. 2016: Helium and carbon isotope signatures of gas exhalations in the westernmost part of the Pannonian Basin (SE Austria/NE Slovenia): Evidence for active lithospheric mantle degassing. *Chemical Geology*; 422: 60-70.
- Csontos, L., Nagymarosy, A., Horváth, F. and Kovác, M. 1992: Tertiary evolution of the Intra Carpathian area: a model. *Tectonophysics*, 208:221-241
- Csontos, L. 1995: Tertiary tectonic evolution of the Intra- Carpathian area: a review. *Acta Vulcanologica* 7, pp. 1–13.
- Čičić, S., Miošić, N. 1986: Geothermal energy of Bosnia and Herzegovina, *Geoinženjering, Sarajevo*, pp. 1-205.
- Dövényi, P., Horváth, F. 1988: A review of temperature, thermal conductivity, and heat flow data from the Pannonian basin. In: Royden, L.H., Horváth, F. Eds.): *The Pannonian Basin: a study in basin evolution*, AAPG Memoir 45, 195–235
- Fodor, L., Csontos, L., Bada, G., Györfi, I. and L. Benkovic, 1999: Tertiary tectonic evolution of the Pannonian Basin system and neighbouring orogens: a new synthesis of paleostress data. In: Durand et al. (1999) pp. 295-334.
- Froitzheim, N., Plašienka, D., Schuster, R. 2008: Alpine tectonics of the Alps and Western Carpathians. In book: *The geology of Central Europe*. Publisher: Geological Society (London) Editors: Tom McCann

- Gavriliuc, R., Rosca, M., Polizu, R., Cucuțeanu, D. 2016: Geothermal energy use, country update for Romania. Abstracts, European Geothermal Congress 2016, Strasbourg, France, 19-24 September, 2016
- Gerner, P., Bada, G., Dövényi, P., Müller, B., Oncescu, B., Cloetingh, S. and F. Horváth, 1999: Recent tectonic stress and crustal deformation in and around the Pannonian basin: data and models. In: Durand et al. (1999) pp. 269-294.
- Grenerczy, Gy., Sella, G. F., Stein, S. and Kenyeres, A. 2005: Tectonic implications of the GPS velocity field in the northern Adriatic region. *Geophysical Research Letters* 32, L16311,
- Haas J., Mioč, P., Pamić J., Tomljenović, B., Árkai, P., Bérczi-Makk, A., Koroknai, B., Kovács, S. & Rálišch- Felgenhauer, E., 2000: Continuation of the Periadriatic lineament, Alpine and NW Dinaridic units into the Pannonian basin — *Int. J. Earth Sciences* 89, 377–389.
- Haas, J. (ed.) 2001: *Geology of Hungary* — Budapest, Eötvös University Press, 317 p.
- Haas, J., Kövér, Sz., Fodor, L.: Map of pre-Cenozoic basement units of the Pannonian basin and surroundings – National Atlas of Hungary, In press
- Hámor, G., Pogácsás, Gy., Jámor, Á. 2001: Paleogeographic/structural evolutionary stages and the related volcanism of the Carpathian-Pannonian region. *Acta. Geol. Hung.*, 44, 193-222p.
- Handy M., R. Ustaszewski, K., Kissling, E. 2014: Reconstructing the Alps–Carpathians–Dinarides as a to understanding switches in subduction polarity, keyslab gaps and surface motion *Int J Earth Sci (Geol Rundsch)* DOI 10.1007/s00531-014-1060-3 Published online
- Horváth, F., Dövényi, P., Szalay, Á., L.H. Royden 1988: Subsidence, thermal and maturation history of the Great Hungarian Plain. In: Royden and Horváth (1988), pp. 355-372.
- Horváth, F. and Cloetingh, 1996: Stress-induced late stage subsidence anomalies in the Pannonian basin. *Tectonophysics* 266:287-300.
- Horváth, F., Bada, G., Szafián, P., Tari, G., Ádám, A., Cloetingh, S., 2006: Formation and deformation of the Pannonian basin: Constraints from observational data. In: Gee, D.G., Stephenson, R.A. (Eds.), *European Lithosphere Dynamics*, Geol. Soc., London, Mem. 32, pp. 191–206.
- Horváth, F. 2007: A Pannon-medence geodinamikája. Akadémiai doktori értekezés 239 p.
- Horváth, F., Pap, N., Reményi, P., Tóth, T. (editors) 2012: *Geothermal Resource Assessment of the Drava Basin. Hungary - Croatia IPA Cross-border Cooperation Programme*, project number HUHR/0901/2.1.3./0006, IDResearch Kft. / Publikon Publishers
- Horváth, F., Musitz, B., Balázs, A., Végh, A., Uhrin, A., Nádor, A., Koroknai, B., Pap, N., Tóth, T., Wórum, G., 2015: Evolution of the Pannonian basin and its geothermal resources. *Geothermics* 53., 328-352.
- Hrvatović, H., Pamić, J. 2015. Principal thrust-nappe structures of the Dinarides, *Acta Geologica Hungarica* 01/2005; 48(2):133-151 DOI:10.1556/AGeol.48.2005.2.4
- Hurter, S. and Haenel, R. (Eds.) 2002: *Atlas of Geothermal Resources in Europe*. Office for Official Publications of the European Communities, Luxembourg.
- Ivanković, J., Nosan, A. Hidrogeologija Čateških toplic = Hydrogeology of Čatež Spa area (in Slovene). 1973. *Geologija* 16, 353-361.

- Juhász Gy. 1992: A pannóniai s.l. formációk térképezése az Alföldön: elterjedés, fácies és üledékes környezet (Pannonian s.l. lithostratigraphic units in the Great Hungarian Plain: distribution, facies and sedimentary environment). – *Földtani Közlöny* **122/2–4**, 133–165. (in Hungarian with English abstract)
- Lenkey L., Dövényi P., Horváth F., and Cloetingh S. A. P.L. 2002: Geothermics of the Pannonian basin and its bearing on the neotectonics. EGU Stephan Mueller Special Publication Series, 3, 29–40, 2002
- Lenkey L., Raab D., Goetzl G., Lapanje A., Nador A., Rajver D., Rotár-Szalkai Á., Svasta J., Zekiri F. 2017: Lithospheric scale 3D thermal model of the Alpine–Pannonian transition zone. *Acta Geod Geophys* 2017 52:161–182., DOI 10.1007/s40328-017-0194-8
- Magyar, I., Geary, D.H., Müller, P. 1999: Paleogeographic evolution of the Late Miocene Lake Pannon in Central Europe. – *Palaeogeogr. Palaeoclimatol. Palaeoecol.* **147**, 151–167.
- Magyar I. 2010: A Pannon-medence ősföldrajza és környezeti viszonyai a késő miocénben. (Palaeogeography and environmental conditions of the Pannonian basin in the Late Miocene). GEO-Litera Szeged, 134 p (in Hungarian)
- Magyari, Á., Chikán, G., Scharek, P., Babinszki, E., Kercksmár Zs. 2011. Basement horizon map of the Quaternary sediments in Hungary — Manuscript, Geological Institute of Hungary
- Maros, Gy., Albert, G., Barczikayné Szeiler, R., Fodor, L., Gyalog, L., Jocha-Edelényi, E., Kercksmár, Zs., Magyari, Á., Maigut, V., Nádor, A., Orosz, L., Palotás, K., Selmeczi, I., Uhrin, A., Viktor, Zs., Atzenhofer, B., Berka, R., Bottig, M., Brüstle, A., Hörfarer, C., Schubert, G., Weilbold, J., Baráth, I., Fordinál, K., Kronome, B., Maglay, J., Nagy, A., Jelen, B., Lapanje, A., Rifelj, H., Rižnar, I., Trajanova, M. 2012: Summary report of geological models — TRANSENERGY, Transboundary Geothermal Energy Resources of Slovenia. <http://transenergy-eu.geologie.ac.at/>
- Márton, E., Fodor, L., 1995: Combination of paleomagnetic and stress data: a case study from North Hungary. — *Tectonophysics* 242, 99–114. Amsterdam.
- Márton, E., 2001: Tectonic implications of Tertiary paleomagnetic results from the PANCARDI area (Hungarian contribution). *Acta Geol. Hung.*, 44:135-144.
- Márton, E., & Fodor, L. 2003: Tertiary paleomagnetic results and structural analysis from the Transdanubian Range (Hungary): Rotational disintegration of the AlCaPa unit, *Tectonophysics*, 363(3–4), 201–224.
- Márton, E., Tischler, M., Csontos, L., Fügenschuh, B., and Schmid, S., 2007: The contact zone between the AlCaPa and Tisza-Dacia mega-tectonic units of Northern Romania in the light of new paleomagnetic data, *Swiss J. Geosci.*, 100, 109–124.
- Matenco, L., Radivojević, D. 2012: On the formation and evolution of the Pannonian Basin: Constraints derived from the structure of the junction area between the Carpathians and Dinarides — *Tectonics*, Vol.31. TC6007, DOI: 10.1029/2012TC003206
- McKenzie, D. 1978: Some remarks on the development of sedimentary basins. *Earth and Planet. Sci. Lett.*, 40:25-32.
- Kovács I., Falus Gy., Stuart G., Hidas K., Szabó Cs., Flower M.F.J., Hegedűs E., Posgay K., Zilahi-Sebess L. 2012: Seismic anisotropy and deformation patterns in upper mantle xenoliths from the central Carpathian–Pannonian region: Asthenospheric flow as a driving force for Cenozoic extension and extrusion? *Tectonophysics*, Vol. 514–517, pp. 168-179

- Matenco, L. C., and D. Radivojević, 2012: On the formation and evolution of the Pannonian Basin: Constraints derived from the structure of the junction area between the Carpathians and Dinarides, *Tectonics*, v. 31, TC6007.
- Miošić, N. 2010: Research and the utilization of hydrogeothermal resources of Bosnia and Herzegovina, *Herald of mining and geology*, 14, Mostar.
- Miošić, N., Samardžić, N., Hrvatović, H., 2013: Geothermal potentials and current status of their use and development, Bosnia-Herzegovina – Abstracts, European Geothermal Congress 2013, Pisa, Italy, 3-7 June 2013
- Muffler, P. & Cataldi, R. 1978: Methods for regional assessment of geothermal resources. — *Geothermics* 7, pp. 53–89.
- Nádor A. 2014: Danube Region geothermal report. Ministry of Foreign Affairs and Trade of Hungary.
- Nádor, A., Rotár-Szalkai, Á., Prestor, J., Tóth, Gy., Goetzl, G., Lapanje, A., Rman, N., Szócs, T., Černák, R., Schubert, G., Svasta, J., 2013: Transboundary geothermal energy resources of Slovenia, Austria, Hungary and Slovakia (TRANSENERGY) – contributions to integrated resource management policies and regional development. Abstracts, European Geothermal Conference, June 3-7, Pisa, Italy, ISBN 978-2-8052-0226-1
- Nádor, A., Kujbus, A., Tóth, A.N., 2016: Geothermal energy use, country update for Hungary. Abstracts, European Geothermal Congress 2016, Strasbourg, France, 19-24 September, 2016.
- Nádor A., Zilahi-Sebess L. 2016: Entering geothermal energy into the UNFC-2009 classification system: case studies of direct-use projects from Hungary. European Geothermal Congress, Strasbourg, France, 19-24 Sept. 2016 (extended abstract).
- Nádor A. 2016: A geotermikus energiavagyon nemzetközi osztályozási és jelentési rendszerei és a hazai adaptáció első lépései. *Földtani Közlöny*, 146/2, pp. 123–134.
- Nádor A., Zilahi-Sebess L., Szócs T. (in press): Geotermikus adottságok, hévizek. In: Haas, J, Brezsnýánszky, K. (eds): Magyarország Nemzeti Atlasza, Földtan.
- Nuhović, S., Djokić, I., 2013: Geothermal energy use, country update for Serbia - Abstracts, European Geothermal Congress 2013, Pisa, Italy, 3-7 June 2013
- Oudech, S., Djokić, I., Radomir, S., 2016: Geothermal energy use, country update for Serbia. Abstracts, European Geothermal Congress 2016, Strasbourg, France, 19-24 September, 2016
- Palcsu, L, Vető, I, Futó, I, Vodila, G, Papp, L, Major, Z., 2014: In-reservoir mixing of mantle derived CO₂ and metasedimentary CH₄-N₂ fluids - Noble gas and stable isotope study of two multistacked fields (Pannonian Basin System, W-Hungary). *Marine and Petroleum Geology*; 54: 216-227.
- Pamić J., Tomljenović, B., 1998: Basic geologic data from the Croatian part of the Zagorje-Mid Transdanubian zone. – *Acta Geologica Hungarica*, Budapest, 41. 389-400.
- Rajver, D., Prerstor, J., Lapanje, A., Rman, N., 2013: Geothermal energy use, country update for Slovenia Abstracts, European Geothermal Congress 2013, Pisa, Italy, 3-7 June 2013
- Rajver, D., Lapanje, A., Rman, N., Prestor J. 2016: Geothermal Energy Use, Country Update for Slovenia. European Geothermal Congress 2016 Strasbourg, France, 19-24 Sept 2016

Rman, N., Gal, N., Marcin, D., Weibold, J., Schubert, J., Lapanje, A., Rajver, D., Benková, K., Nádor, A., 2015: Potentials of transboundary thermal water resources in the western part of the Pannonian basin. *Geothermics* 55, 88-98

Rman, N., Ádám L., Bobovečki I., Brkić Ž., Farnoaga R., Gal N., Jolović B., Koren K., Kuhta M., Lapanje A., Larva O., Marković T., Medgyes T., Mérész E., Milenić D., Rotár-Szalkai Á., Samardžić N., Szanyi J., Szócs T., Šolaja D., Šošarić F., Toholj N., Vijdea A.M., Vranjes A., 2018: D.5.2.1 Summary report on the current status of thermal water users. DARLINGe project report. <http://www.interreg-danube.eu/approved-projects/darlinge>

Rosca, M., Bendea, C., Cucueteanu, D., 2013: Geothermal energy use, country update for Romania -Abstracts, European Geothermal Congress 2013, Pisa, Italy, 3-7 June 2013

Rotár-Szalkai, Á., Nádor, A., Szócs, T., Maros, Gy., Goetzl, G., Zekiri, F., 2017: Outline and joint characterization of Transboundary geothermal reservoirs at the western part of the Pannonian basin. *Geothermics*, 70. (2017), 1-16.

Royden L. & Keen C. 1980: Rifting processes and thermal evolution of the continental margin of eastern Canada determined from subsidence curves. – *Earth & Planetary Science Letters*, 51, 343-361.

Royden, L. H., 1988: Late Cenozoic Tectonics of the Pannonian Basin System. –In: Royden, L.H. & Horváth, F. (Eds.): *The Pannonian Basin. A Study in Basin evolution*. AAPG Memoir, 45, pp. 27–48.

Royden, L.H. & Horváth, F., 1988: *The Pannonian basin. A study in basin evolution*. Am. Assoc. Pet. Geol. Memoir, 45.

Rybach, L. 2010: “The Future of Geothermal Energy” and Its Challenges, Proceedings of the World Geothermal Congress 2010 Bali, Indonesia, 25–29 April 2010, available at: <http://www.geothermal-energy.org/pdf/IGAstandard/WGC/2010/3109.pdf>

Rybach, L.: Classification of geothermal resources by potential, *Geoth. Energ. Sci.*, 3, 13-17, <https://doi.org/10.5194/gtes-3-13-2015>, 2015.

Samardžić N. and Hrvatović H., 2016: Geothermal Energy Use - Country Update Report for Bosnia and Herzegovina. European Geothermal Congress 2016, Strasbourg, France, 19-24 Sept 2016

Schmid S. M., Bernoulli D., Fügenschuh B., Matenco L., Schefer S., Schuster R., Tischler M. & Ustaszewski K., 2008: The Alpine-Carpathian-Dinaridic orogenic system: correlation and evolution of tectonic units *Swiss J. Geosci.* Birkhäuser Verlag, Basel, 2008 DOI 10.1007/s00015-008-1247-3

Sclater, J. G., Royden, L., Horváth, F., Burchfiel, B. C., Semken, S. And L. Stegena, 1980: The formation of the intra-Carpathian basins as determined from subsidence data. – *Earth & Planetary Scientific Letters*, 51, 139-162p.

Szanyi, J., Kovács, B., Scharek, P., 2009: Geothermal energy in Hungary: potentials and barriers. *European Geologist* 27, 15–19

Szanyi, J., Kovács, B., 2010: Utilization of geothermal systems in South-East Hungary. *Geothermics* 39, 357–364. <http://dx.doi.org/10.1016/j.geothermics.2010.09.004>

Szócs T., Rman N., Süveges M., Palcsu L., Tóth G., Lapanje A., 2013: The application of isotope and chemical analyses in managing transboundary groundwater resources. *Applied Geochemistry* 32: pp. 95-107.

Szócs T., Frapé S., Gwynne R., Palcsu L., 2017: Chlorine stable isotope and helium isotope studies contributing to the understanding of the hydrogeochemical characteristics of old groundwater. *Procedia Earth and Planetary Science* pp. 877-880. DOI information: 10.1016/j.proeps.2017.01.004

Szócs, T., Tóth, Gy., Nádor, A., Rman, N., Prestor, J., Lapanje, A., Rotár-Szalkai Á., Černák, R., Schubert, G., 2015: Long-term impact of transboundary cooperation on groundwater management. *European Geologist* 40, 29-33.

Tari G., Báldi T. & Báldi-Beke M., 1993: Paleogene retroarc flexural basin beneath the Neogene Pannonian Basin: a geodynamic model — *Tectonophysics* 226, 433–455.

Tóth, Gy., Rman, N., Rotár-Szalkai, Á., Kerékgyártó, T., Szócs, T., Lapanje, A., Černák, R., Remsík, A., Schubert, G., Nádor, A., 2016: Transboundary fresh and thermal groundwater flows in the west part of the Pannonian Basin. - *Renewable and Sustainable Energy Reviews*, 57, 439-454.

Tóth, J., Almási I., 2001: Interpretation of observed fluid potential patterns in a deep sedimentary basin under tectonic compression: Hungarian great plain Pannonian Basin. *Geofluids* 1:11–36. <http://dx.doi.org/10.1046/j.1468-8123.2001.11004.x>.

Tóth, J., 2009: *Gravitational Systems of Groundwater Flow – Theory, Evaluation, Utilization*. University Press, Cambridge, UK, 67-69.

Williams C. F. 2007: Updated Methods For Estimating Recovery Factors For Geothermal Resources. *Proceedings, Thirty-Second Workshop on Geothermal Reservoir Engineering* Stanford University, Stanford, California, January 22-24, 2007.

Williams C. F. 2014: Evaluating the Volume Method in the Assessment of Identified Geothermal Resources. *GRC Transactions*, Vol. 38, 2014., pp. 967-974.

Zilahi-Sebess L. 2013: Geothermal Potential Estimation. Extended abstract, 16th HU and 5th HR-HU Geomathematical Congress, Mórahalom, 30 May – 01 June, 2013

Živković, S., Kolbah, S., Škrlec, M., 2016: Croatia Country Update. *European Geothermal Congress 2016*, Strasbourg, France, 19-24 Sept 2016